Nationaal Lucht- en Ruimtevaartlaboratorium

National Aerospace Laboratory NLR

NLR-CR-2000-147

An enhanced method for the calculation of third party risk around large airports

with application to Schiphol

A.J. Pikaar, C.J.M. de Jong and J. Weijts

This investigation has been carried out under a contract awarded by the Netherlands Department of Civil Aviation (RLD), contract number DGRLD 1999.2.007.

Division:	Air Transport
Issued:	April 2000
Classification of title:	unclassified

Summary

In 1992 NLR developed a method for the calculation of third party risk levels around airports. The method is applied in many airport risk studies. With the experience gained over the years in application of the method, and due to the availability of improved historical data, the risk models were updated in 1999.

This report consists of two parts. In the first part the update to the risk model is described. The second part presents calculations made with the improved method.

The following improvements and amendments are discussed in this report:

1. The probability of an accident to happen per aircraft movement, *i.e.* the accident rate, is determined again based on more recent and accurate data. The rates are over 50% lower than was estimated in the original model. This is partly a result of actual improvement of air traffic safety, and partly of better adaptation to the Schiphol situation;
2. Accident rates are determined separately for three aircraft generations and for six flight phases: take-off veer-off, take-off overrun, take-off overshoot, landing undershoot, landing veer-off, and landing overrun. The accident rates for second and third generation aircraft are found statistically equal for the flight phases take-off overshoot and take-off veer-off. These accident rates are compounded;
3. The distribution of the accident locations over the area around the airport is also determined again using a larger data set;
4. Different distributions are determined for four of the six flight phases: take-off overrun, take-off overshoot, landing undershoot, and landing overrun. A distribution of veer-off accidents is not yet available;
5. The distributions for take-off overshoots and for landing undershoots consist of a route dependent part and a runway dependent (route independent) part. All accident locations on the extended centreline are declared route dependent, all other locations are runway dependent. The distribution of operational traffic is used to model the lateral distribution of route dependent aircraft accident locations;
6. The dimensions of the consequence areas are determined again after thorough inspection of the data point’s debris areas. The terrain type did not appear to contribute much to the size of the consequence area. The consequence areas are 45 to 65% smaller than they were in the original model;
7. The lethality is re-evaluated and is found slightly smaller than it was in the original model.

Calculations made with the improved model show that both individual risk levels and societal risk values are considerably lower than predicted with the original model.

The updated model discussed in this report replaces the former model of 1992. However, this report does not replace the report describing the former model (reference [1]). This report only describes the changes and amendments and is to be used together with reference [1].

Contents

Abbreviations **6**

Definitions **7**

Introduction **9**

2 Accident Rate Model **11**
2.1 Data selection 11
2.1.1 Airport selection 11
2.1.2 Accident selection 12
2.1.3 Aircraft movements 13
2.2 Determination of accident rates 14

3 Accident Location Model **17**
3.1 Data 17
3.1.1 Selection 17
3.1.2 Analysis 18
3.2 Distribution functions 22
3.2.1 Basic functions 22
3.2.2 Choice of distributions 23
3.3 Parameters 24
3.3.1 Parameter estimation 25
3.3.2 Distribution of operational traffic 25
3.3.3 Weight factor 27
3.3.4 Resulting parameters 27

4 Accident consequence model **29**
4.1 Dimension of consequence area 29
4.2 Lethality 30

5 Model comparison **33**
5.1 Former models 33
5.1.1 IMER model 33
5.1.2 TNLI model 33
5.2 Model comparison 34
5.2.1 Accident rates 34
5.2.2 Accident locations 37
5.2.3 Accident consequences 39

6 Scenario description **41**
6.1 Dimension of the study area 41

6.2 Model parameters 41
6.2.1 Accident Rates 41
6.2.2 Consequence area and lethality 42
6.3 Route structure and runway thresholds 43
6.4 Traffic data 43
6.5 Population density data 44
6.6 Building density data 44

7 Results 47
7.1 Measures of risk 47
7.1.1 Individual Risk 47
7.1.2 House counts and summed weighted risk 47
7.1.3 Societal Risk 47
7.2 Calculated results 47
7.2.1 Individual Risk 47
7.2.2 Societal risk 48
7.2.3 House counts and summed weighted risk 48

8 Verification and validation 56
8.1 Verification of input 56
8.2 Validation of risk 57
8.2.1 Visual inspection 57
8.2.2 Total risk volume 59
8.2.3 Expectation of number of third party victims 59
8.3 Upper limits 61

9 Concluding remarks 66

10 References 67

Appendix A Aircraft generation 69

Appendix B Airport list 74

Appendix C Aircraft accident list 75

Appendix D Lethality 83

Appendix E Route structure of the scenarios S4S1-1990 and S5P-2010 86

Appendix F Aircraft movements 96

Appendix G Distribution of traffic over the routes 100

(104 pages in total)

Abbreviations

ACN	Address Co-ordinates Netherlands
ADREP	Accident Data Report (ICAO)
ALPA	Air Line Pilot's Association
AMER	Supplemental Environmental Impact Analysis (Dutch)
ATIS	Automatic Terminal Information Service
BCAR	British Civil Airworthiness Requirements
CA	Crash Area
CAA-UK	U.K. Civil Aviation Authority
CBS	Statistics Netherlands (Dutch)
EFIS	Electronic Flight Instrumentation System
EGPWS	Enhanced Ground Proximity Warning System
FANOMOS	Flight Track and Noise Monitoring System
FAR	Federal Aviation Regulation
GGR	Summed Weighted Risk (Dutch)
GPS	Global Positioning System
GPWS	Ground Proximity Warning System
ICAO	International Civil Aviation Organization
ILS	Instrument Landing System
IMER	Integrated Environmental Impact Statement (Dutch)
IMU	Interim Model Update
JAA	Joint Aviation Authorities
JAR	Joint Airworthiness Requirements
MD	Survey Department (Dutch)
MTOW	Maximum Take-Off Weight
NLR	National Aerospace Laboratory (Dutch)
NM	Nautical Mile
NTSB	National Transportation Safety Board
OAG	Official Airline Guide
ONL	Development National Airport (Dutch)
PTT	Post, Telegraph, Telephone
RDC	rectangular Dutch co-ordinate system (Dutch)
RLD	Directorate-General of Civil Aviation (Dutch)
SID	Standard Instrument Departure
TAR	Terminal Area Surveillance Radar
TCAS	Traffic Alert and Collision Avoidance System
TNLI	Future Dutch Aviation Infrastructure (Dutch)
VOLMET	Meteorological information for aircraft in flight

Definitions

Accident type	Classification of accident based upon two criteria: take-off or landing, and position of accident location relative to the runway.
Aircraft accident	Every unwanted contact of an aircraft with the ground outside the runway.
Aircraft generation	Classification of aircraft type based upon the technological advances applied within the aircraft. This specifically applies to the design of the cockpit and its instrumentation.
Aircraft movement	Either a take-off or a landing.
Consequence area	The area in which the effects of a particular aircraft accident are potentially fatal.
GGR	Sum of the individual risk values at the location of all houses within a defined area.
Individual risk	The probability per year that a person permanently residing at a particular location in the area around the airport is killed as a direct consequence of an aircraft accident.
Lethality	The probability of not surviving an aircraft accident when residing in the consequence area.
Societal risk	the probability per year of more than N third party victims due to an aircraft accident somewhere in the area around the airport.
Study area	A defined part of the geographical area outside the perimeter of the airport, which is considered to be subject to increased risk of aircraft accidents due to the presence of the airport.
Third party	Inhabitant of the area around an airport.

This page intentionally left blank

1 Introduction

Airports cause concentrations of air traffic over the area around the airport. This increases the local probability of aircraft accidents and hence the risk to the population in the vicinity of the airport. Due to the strong growth in air traffic volumes, airports need to increase their capacity, which often involves considerable infra-structural development such as the constructing of new runways. The Environmental Impact Statement, required in the course of these developments, usually must also address third party risk. This in return necessitates the availability of adequate models.

Third party risk analysis models consist of three elements: an accident probability model, an accident location probability model and an accident consequence model. The results of these sub-models are combined to calculate individual risk levels (local probability of death), and societal risk (probability of death of a group of more than N people).

Since third party risk plays an increasingly important role in Environmental Impact Statement procedures, the methods used to assess third party risk are evolving at a quick pace. NLR has developed their first model to calculate third party risk around airports in 1992 (see reference [1]) and applied it to many airports since then. While several smaller improvements to the model were made since 1992, a major update of the model was undertaken in 1999 and has resulted in the Interim Model Update-model (IMU model) described here.

The improvements and extensions of the method consist of both adaptation of model parameters and conceptual changes of the external risk models. These were made possible by the availability of much improved historical data on aircraft operations and accidents, and by the extensive experience gained in the application of the method in a variety of risk assessment projects for several airports.

The enhanced method is used to evaluate third party risk around Amsterdam Airport Schiphol. The results have been used to support government decision-making on 17 December 1999 on whether to accommodate further growth of air-traffic in the Netherlands at Amsterdam Airport Schiphol. Two scenarios are considered: one representing the use of airport Schiphol in the year 1990, and one to predict the situation in the year 2010.

This report describes the results of the interim model update. It is not by itself meant as manual for a third party risk evaluation model. In that respect it should be considered next to the report describing the original method (reference [1]).

This report consists of two parts: the modelling aspects of the enhanced method are discussed in the chapters 2 to 5 (appendices A to D), and the calculations made for Schiphol airport are described in the chapters 6 to 8 (appendices E to G). The improvements and extensions for each of the 3 models within the method are described in chapter 2 to 4. Chapter 5 compares the enhanced quantitative risk assessment method with the original method. The chapters 6 and 7 present the input and the calculated results evaluated with the improved method for the two scenarios. Chapter 8 describes the validation and verification steps undertaken to check the validity and correctness of the enhanced method. Concluding remarks are made in chapter 9. Finally, references are presented in chapter 10.

2 Accident Rate Model

The accident rate model provides probabilities for an aircraft crash. The probabilities differ between aircraft generation and flight phase. The rates in this report are based on historical data and are tailored (by data selection) to represent the circumstances of Amsterdam Airport Schiphol.

2.1 Data selection

When predicting occurrences of events based on historical data it is important that the used data set is both large and specific enough. In general, world wide accident data are not representative (or specific) for the situation that can be expected at Amsterdam Airport Schiphol. A selection of data from the available world wide data is required. Reference [3] indicates a number of factors that contribute to the safety of an airport. Airports that are similar to Schiphol in terms of these factors, are selected in the data set. The selection should leave a basis large enough to make useful statistical predictions.

First a selection of comparable airports is made, then a set of aircraft accidents is selected. An aircraft accident that occurred in the past, which is not likely to occur in the vicinity of Schiphol, is removed from the data selection to make the selection more Schiphol specific. Aircraft accidents which occurred on the runway in use, are removed from the selection of aircraft accidents, because they do not contribute to external risk around an airport.

2.1.1 Airport selection

The criteria used to select comparable airports are:
1. Terminal Approach Radar (TAR) should be present at the airport;
2. at least 70% of the approaches should be precision approaches;
3. the operators of at least 90% of the flights should operate from JAA-countries or from North America;
4. Automatic Terminal Information System, ATIS, and Meteorological information for aircraft in flight, VOLMET, should be present at the airport;
5. no obstacles higher than 2000 ft within 6 NM, and no obstacles higher than 6000 ft within 25 NM; and
6. the airport should at least have accommodated 150,000 commercial movements in any single year within the period 1980 - 1997.

In addition, an expert judgement on the selected airports is applied to exclude airports that are for other reasons (climatic, operational) not comparable to Schiphol.

Criteria 1, 2, 4 and 5 are based on a study described in reference [3]. Criterion 2 is based on the fact that about 90% of the approaches at Schiphol is a precision approach. The limit is set to 70% to allow enough airports to be selected. It appeared that 89% of the approaches at the selected airports were precision approaches. Criterion 3 ensures that the mix of operators at the airport is comparable to that at Schiphol. The operator is an important factor in the level of safety. Criterion 6 is to exclude small airports that, due to their size, are not comparable to Schiphol.

Application of the above six criteria on NLR's airport database (consisting of over 5000 airports world wide) resulted in a set of 41 airports. It is felt that Denver International Airport, which complies with the six criteria, is not comparable to Schiphol due to its very specific climate in combination with its altitude. Denver airport is characterised by sudden weather changes accompanied by strong changes in wind. The list of airports comprises 40 airports. These airports are listed in appendix B.

As a result of criterion 3, all selected airports are either in Europe or in North America. It can be argued that some Australian airports are also comparable to Schiphol and should be included in the set. For reasons of consistency, all six criteria are maintained, and therefore none of the Australian airports is selected[1].

2.1.2 Accident selection

The sources of accident data are: Airclaims, ICAO ADREP, NTSB, KIMURA, Breiling and ALPA. These sources contain factual information (date, location, aircraft type, operator, et cetera) and narratives of all known accidents since well before 1980. There are 850 aircraft accidents in the sources related to the 40 airports (no double counts). A selection of these accidents is made on basis of the narratives provided with the accident data, supplemented with accidents reports and other sources. The criteria used for the selection are as follows:

1. the accident happened in the period 1980 - 1997;
2. helicopter accidents are excluded;
3. accidents with military aircraft are excluded;
4. accidents that occurred during a test flight or an air show are excluded;
5. the maximum take-off mass of the aircraft is 5700 kg or more;
6. the accident happened in one of the flight phases: take-off, initial climb, initial approach, final approach, landing or go-around; and
7. accidents caused by sabotage, terrorism or military actions are excluded.

[1] There are 3 Australian airports comparable to Schiphol. No accident occurred on the Australian airports between 1980 and 1997. Based on the extra number of movements in this period, it can be concluded that the ratios would be 2.4% (generation 2) to 4.2% (generations 1 and 3) lower.

Criteria 2, 3, 4, 6 and 7 are again based on the study described in reference [3]. No accidents before 1980 are considered because accident data are less detailed documented and movement data are unavailable or incomplete over that period[2]. Light aircraft (under 5700 kg) are excluded, because their contribution in the traffic at Schiphol is negligible.

The selection resulted in a list of 75 accidents (see appendix C).

2.1.3 Aircraft movements

Movement data are obtained from the Official Airline Guide database. This database contains data on the scheduled movements of aircraft heavier than 5700 kg performed on all commercial airports world wide. The database contains departure airport, destination airport, operator, aircraft type, date, and service type (*e.g.* regular, charter, combi, or cargo).

Figure 2-1 shows the total number of movements per year that were performed on the 40 selected airports. The number of movements show a yearly increase, except for the period 1989 - 1993 which is attributed to the Gulf War. A division is made into generations of aircraft (see appendix A). The use of third generation aircraft has increased, whereas the use of first and second generation aircraft is gradually diminishing. This is mainly caused by fleet renewal and by noise abatement measurements.

The validity of the Official Airline Guide (OAG) database is checked by comparing the number of movements given in the database for Schiphol with those given in the Statistical Annual Reviews of Amsterdam Airport Schiphol. The results are presented in figure 2-2. Although the OAG database does not contain non-scheduled flights, the difference with the annual reviews is on average less than 0.3% which is negligible. It is noted that the number of non-scheduled flights at Schiphol is very low.

It was not always possible to obtain detailed aircraft information from the OAG database. This information is necessary to categorise the aircraft into generations. In cases the information in the OAG database was insufficient, individual fleet data were used to distinguish between aircraft generations.

[2] Despite of the inadequate data, the period 1976-1980 was included in the IMER model. This was necessary to achieve enough data.

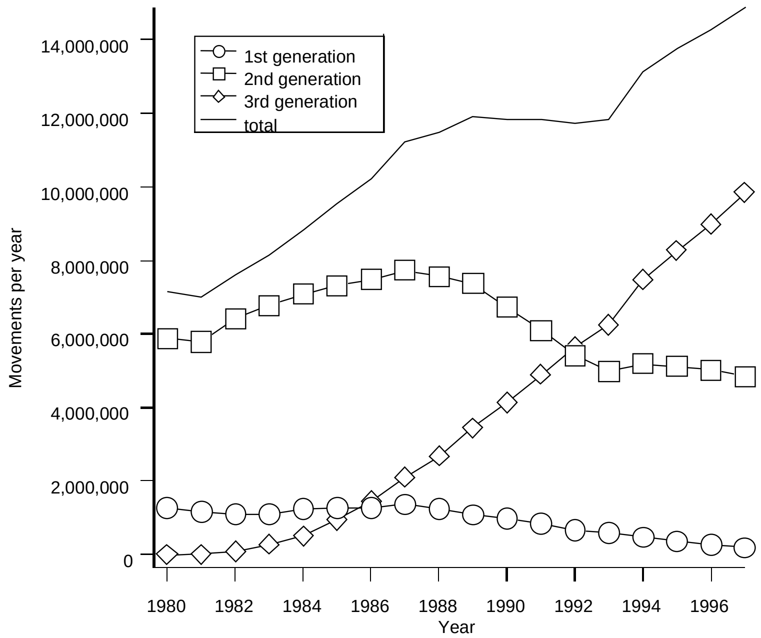

Figure 2-1: Number of aircraft movements per generation per year for the selected set of airports.

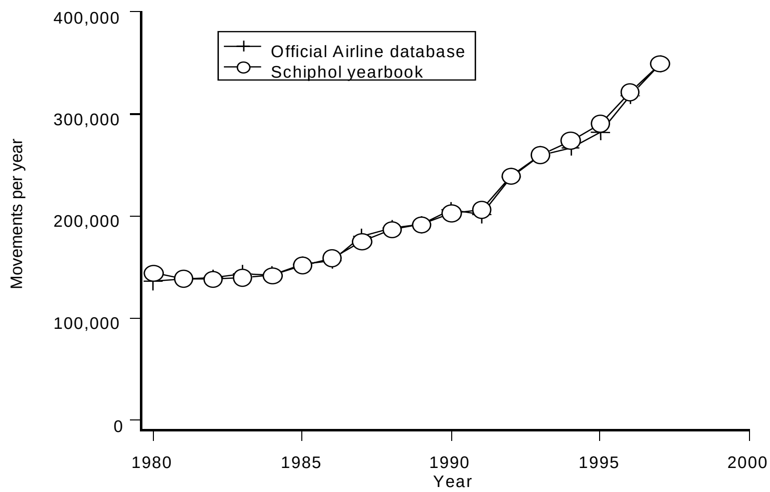

Figure 2-2: Comparison of yearly aircraft movements according to the Airline database and to the Schiphol annual review.

2.2 Determination of accident rates

The number of accidents for each of the three generations and for the six accident types take-off overrun, landing overrun, take-off overshoot, landing undershoot, take-off veer-off, and landing veer-off are given in the following table. The number of movements for each aircraft generation is also shown. The specification of the aircraft generations is covered in appendix A.

Table 2-1: Number of accidents per generation and per accident type.

	Generation 1 (7,965,111 movements)	**Generation 2** (55,136,273 movements)	**Generation 3** (32,206,672 movements)
take-off overrun	3	6	2
landing overrun	2	11	2
take-off overshoot	1	3	1
landing undershoot	6	8	4
take-off veer-off	3	2	1
landing veer-off	7	10	3

Only two accident types, take-off veer-off and take-off overshoot, have an accident rate of which the difference is statistically not significant. In all the other cases the difference is statistical significant. To determine statistical significance (95% confidence interval) of the difference in accident rates the Chi-square (McNemar) is used.

The accident ratios together with their confidence intervals are given in table 2-2 and graphically represented in figure 2-3.

Table 2-2: Accident rates and 95% confidence limits per accident type and generation.

Accident type	**Generation**	**Rate** (per million flights)	**Lower band** (95% confidence)	**Upper band** (95% confidence)
Landing overrun	1	0.251	0.0304	0.907
	2	0.200	0.0996	0.357
	3	0.062	0.0075	0.224
Landing undershoot	1	0.753	0.276	1.640
	2	0.145	0.063	0.286
	3	0.124	0.034	0.318
Landing veer-off	1	0.879	0.353	1.811
	2	0.181	0.087	0.334
	3	0.093	0.019	0.272
Take-off overrun	1	0.377	0.078	1.101
	2	0.109	0.040	0.237
	3	0.062	0.008	0.224
Take-off overshoot	1	0.126	0.003	0.700
	2 & 3	0.046	0.013	0.117
Take-off veer-off	1	0.377	0.078	1.101
	2 & 3	0.034	0.007	0.100

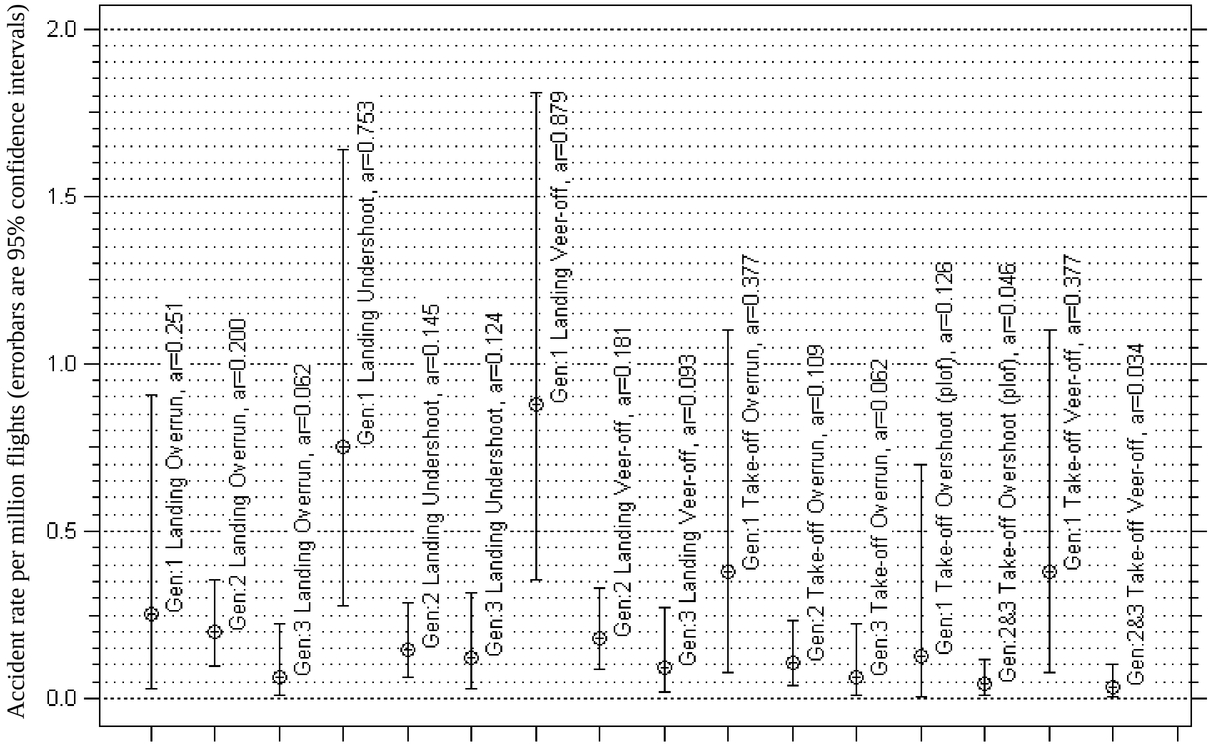

Figure 2-3: Representation of the accident rates and their confidence intervals.

3 Accident Location Model

The accident location model gives the distribution of accident locations, under the assumption that an aircraft accident occurs. The distribution of locations is assumed to depend on the flight phase.

3.1 Data

The data set used for the accident location model is built up from the following sources:

- ADREP 678 points
- ALPA 807 points
- Airclaims 32 points
- NTSB 59 points
- CAA-UK 26 points

The sources differ in accuracy and completeness. Furthermore, data are presented in different ways, *e.g.* in different co-ordinate systems. In the current data set, only the Cartesian co-ordinate system is used. The system can be defined relative to the approach-end or to the departure-end of the runway, the choice of which depends on the accident type.

Some data points were excluded from the data set, because there were doubts about the correctness of the location of the accident.

3.1.1 Selection

Some accidents are reported in more than one source. These double counts were excluded from the combined sources by sorting on accident date, airport, and aircraft type successively.

The data set was divided into five categories: overshoot, take-off overrun, undershoot, landing overrun and veer-off. The division is made by two persons after evaluation of the narrative given for each accident. Data points that could not be assigned to one of the categories were excluded.

The following table shows the result of the division into categories.

Table 3-1: Number of data points per source and per category.

	Overshoot	Take-off overrun	Undershoot	Landing overrun	Veer-off	*Exclude*	**Total**
ADREP	67	35	109	67	74	*326*	678
ALPA	29	61	296	164	211	*46*	807
Airclaims	5	--	21	2	--	*4*	32
NTSB	5	3	9	4	11	*27*	59
CAA	--	4	--	18	--	*4*	26
Total	106	103	435	255	296	*407*	**1602**

3.1.2 Analysis

Scatter plots of the accident data per category can be found in the following figures. The *x*-axis represents the extended centreline.

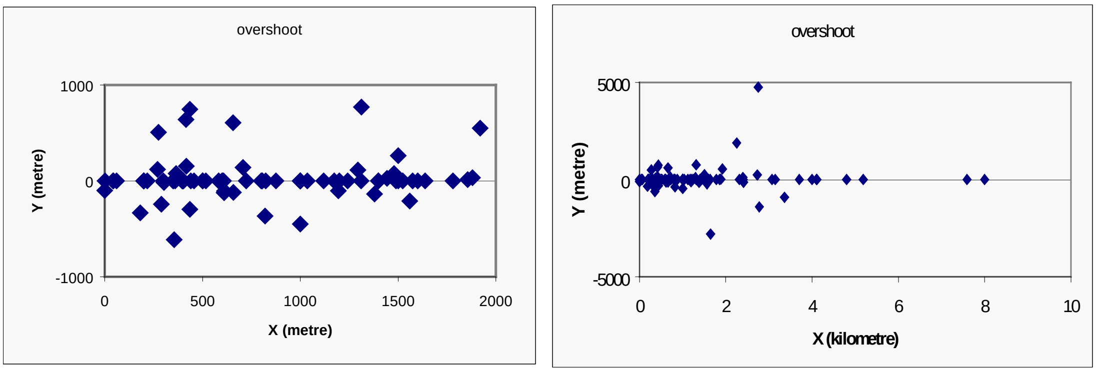

Figure 3-1: Scatter plots of overshoot data points (left: zoomed in).

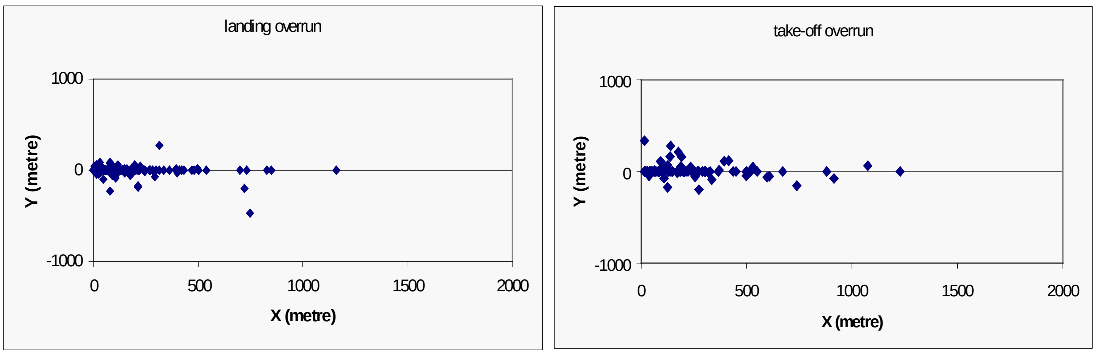

Figure 3-2: Scatter plots of overrun data points (left: landing, right: take-off).

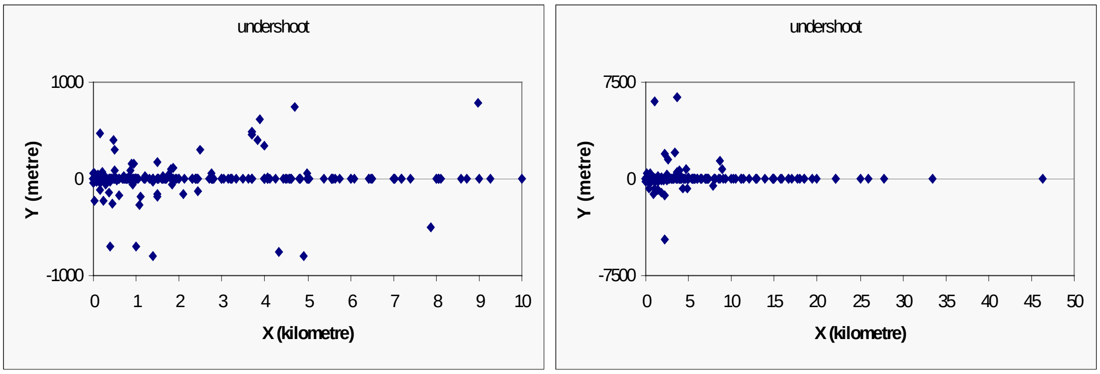

Figure 3-3: Scatter plots of undershoot data points (left: zoomed in).

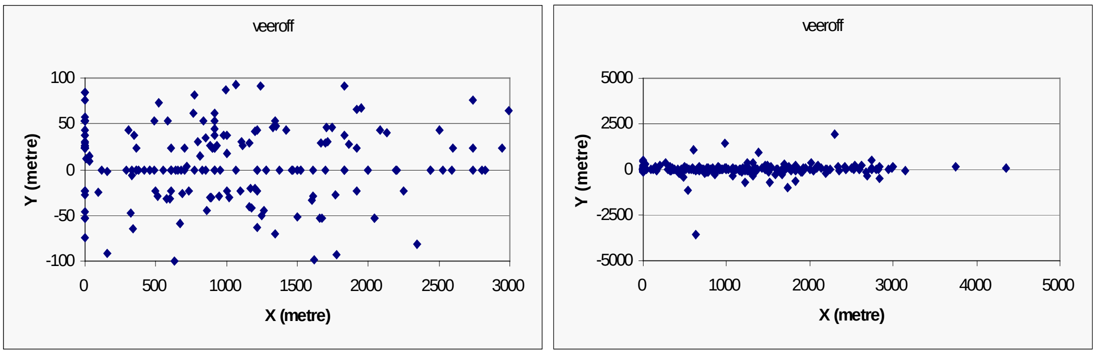

Figure 3-4: Scatter plots of veer-off data points (left: zoomed in).

Points on the extended centreline

Each of the five subsets contain a significant number of points on the extended centreline, *i.e.*, with *y*-co-ordinate equal to 0. A few possible explanations come to mind:

1. Accidents really do frequently occur on the extended centreline;
2. The value *y*=0 is used by accident investigators when accidents occur close to, but not necessarily on the extended centreline;
3. The accident location is given in only one co-ordinate, being the distance to the airport, and the value *y*=0 is inadvertently assigned when transforming to the two-dimensional co-ordinate system.

There may be more reasons that explain the phenomenon.

Only for a small number of accidents it can be show that the accident location was exactly on the extended centreline. More often it seems that the actual accident location is close to the centreline, for instance when the accident aircraft did not show any defects. Especially for accident locations at great distances from the airport it is most likely that the transformation from one to two dimensional representation of the location is the cause for the value *y*=0.

The table below indicates the number of points reported on the extended centreline for each accident type. Based on accurate location data (source: CAA), close to 40% of the overrun accidents can be assumed to be located exactly on the extended centreline. The percentages in the data are considerably higher.

Table 3-2: Number of points on the extended centreline for each accident category, and percentage of the total number in the category.

	Number on centreline	Percentage of total
Overshoot	68	65
Take-off overrun	72	70
Undershoot	353	81
Landing overrun	203	80
Veer-off	54	18

The large number of points on the extended centreline is not new. It is handled in the past using a Dirac function for the lateral distribution of locations. However, this introduces undesirable side-effects. First, due to the use of nominal routes, the distribution of accident locations on large distances from the runway is narrower than the actual operational distribution of traffic. Furthermore, the Dirac function gives continuity problems when bending the probability field around a curved route.

Lack of route information

In most cases, the intended route of an aircraft can not be deduced from the accident data. The following assumptions are made:

- Unless otherwise stated, the intended route is for a landing equal to the extended centreline (x=s and y=t) when x < 12 km and $|y|$ < 6 km;
- Unless otherwise stated, the intended route is for a take-off equal to the extended centreline when x < 6 km.

These assumptions seem reasonable, as departures and approaches are usually performed using SIDs (standard instrument departure) and ILS (instrument landing system). In addition, take-off accidents that occurred further from the runway than 6 kilometres may also be given relative to the extended centreline. In case of an emergency, the pilot will generally try to keep the aircraft level.

Longitudinal - lateral distribution dependency

It is previously assumed that the lateral distribution of locations depends on the longitudinal co-ordinate *x*:

$$f(x, y) = f(y; x) \cdot f(x).$$

Alternatively, the distributions in both directions could be assumed to be independent

$$f(x, y) = f(y) \cdot f(x).$$

In order to make a well-decided choice, we considered the correlation between the distances *x* and |*y*| (see table 3-3). Based on these correlations we consider the distributions to be dependent. The lateral distribution is assumed to be linear dependent on the co-ordinate *x*.

Table 3-3: Correlation between x and |y|.

	x against |*y*|
Landing undershoot	0.2421
Landing overrun	0.4251
Take-off overrun	-0.2872
Take-off overshoot	0.2764

Veer-off accidents

Part of the veer-off accidents have an *y*-co-ordinate lower than 23 metre, which is in contradiction to the definition of the accident type. An extra selection of data is necessary for this reason. Distributions of veer-off accidents are not yet deduced.

Veer-off accidents are, by definition, related to two runway points. Simply modelling the points relative to only one of the runway points can cause interference with other accident types. A veer-off accident that occurred near the end of a long runway, for instance, should be treated on a short runway as an overrun accident. For this reason, veer-off accident locations should be scaled to the runway length. Unfortunately, the length of the runway is often unknown.

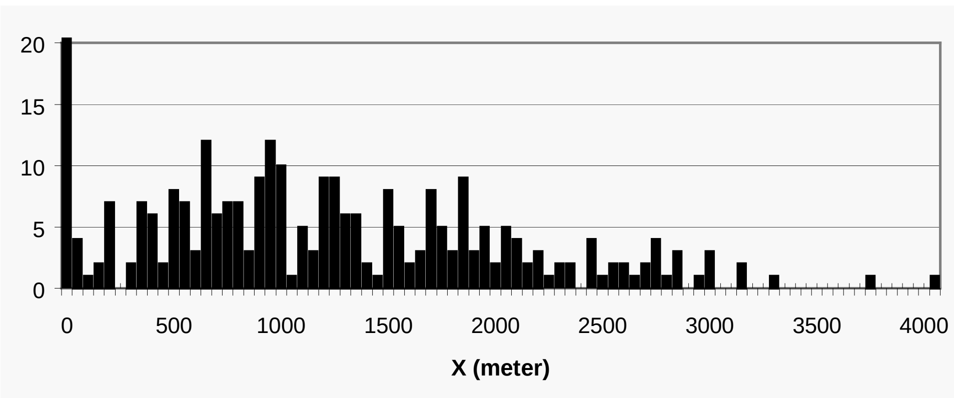

Figure 3-5: Frequency of x-values for veer-off accidents.

The distribution of veer-off accident locations along the runway is uniform. From a practical point of view it will be assumed that the distribution is indeed uniform.

3.2 Distribution functions

The functions used to model the distribution of accident locations in the interim model update are essentially the same as used in the original model. Due to the use of new data, the function parameters will change. More important, the interim model uses another perspective on route-dependency.

3.2.1 Basic functions

Three standard distribution functions are used: the Weibull function, the generalised Laplace function and the normal or Gauss function.

Weibull function

The Weibull function is used to model the longitudinal distribution of locations. This function is defined for $x \geq 0$ and $\eta, \beta > 0$ as:

$$f_{Weibull}(\eta, \beta; x) = \frac{\beta}{\eta}\left(\frac{x}{\eta}\right)^{\beta-1} e^{-\left(x/\eta\right)^{\beta}}.$$

The parameter η is called the scale parameter. The parameter β is the shape parameter; for $\beta > 1$ the Weibull function is of an asymmetric clock shape and for $\beta \leq 1$ the function is exponential. The Weibull function is used in a wide range of applications to model the longitudinal distribution.

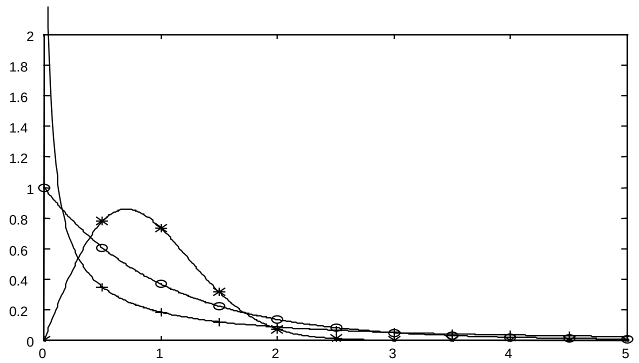

Figure 3-6: Weibull function for η=1 and (+) β=½; (O) β=1; (*) β=2.

Generalised Laplace function

The lateral distribution of points is modelled using the generalised Laplace function. This function is defined for all *y* and for *a, b* > 0 as:

$$f_{gen\ \ Laplace}(b,a;y)=\frac{1}{2ab\Gamma(b)}e^{-\left|y/a\right|^{1/b}},$$

with *a* the scale parameter and *b* the shape parameter. When $a=\sqrt{2}\cdot\sigma$ and $b=½$, the generalised Laplace is equal to the Gauss function below. For larger values of *b* the tails of the generalised Laplace function are heavier than those of the Gauss function.

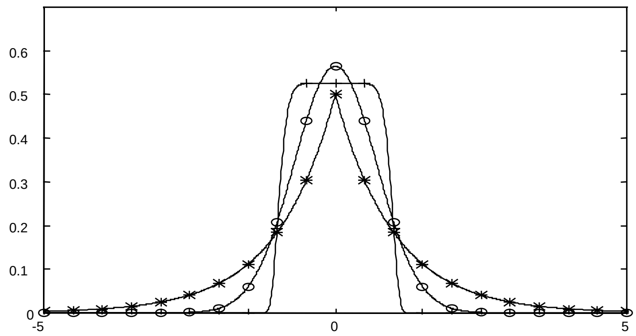

Figure 3-7: Generalised Laplace function for a=1 and (+) b=0,1; (O) b=½; (*) b=1.

Gauss function

The formal representation of the Gauss function is given here as:

$$f_{Gauss}(\sigma;y)=\frac{1}{\sigma\sqrt{2\pi}}e^{-\frac{1}{2}\left(\frac{y}{\sigma}\right)^2}.$$

This function is used for the lateral distribution of locations on the extended centreline.

3.2.2 Choice of distributions

Distribution functions are chosen for each of the accident types. The function parameters are chosen such that the distribution best fit the data for the given accident type. Statistical tests are used to decide if the resulting distributions are acceptable or not.

This paragraph discusses the choice of distribution functions. The next chapter discusses the derivation of parameters.

Overrun distributions

From a flight mechanical point of view there is no difference in landing overruns and take-off overruns. In both cases the pilot will try to stop the plane using normal means as brakes and thrust-reversers. NTSB data shows that the exit speeds for both flight phases are equal, *i.e.* an equal distribution in kinetic energy at the thresholds. Take-off and landing overruns are therefore modelled using the same distribution functions (although with different parameters).

A pilot engaged in an overrun accident will try to stop the plane as quickly as possible. The urge to steer the plane will only exist to avoid obstacles. The accident location of overruns is therefore situated close to the extended centreline. The large number of locations reported exactly on the extended centreline is due to the fact that the accident investigator observed the aircraft to lie within the width of the runway, but not necessarily on the extended centreline.

The distribution function for overruns is of the form:

$$f_{overrun}(s,t) = f_{Weibull}(\eta,\beta;s)\cdot\left\{p\cdot f_{Gauss}(\sigma_0;t) \;+\; (1-p)\cdot f_{gen.\,Laplace}(b,a_0+a_1 s;t)\right\}.$$

Undershoots en overshoots

Undershoots and overshoots are also modelled with equal functions. These functions are split into a route dependent and a runway dependent (route independent) part. The runway dependent part is added to account for aircraft that crash during an emergency manoeuvre in which the aircraft has no intended route known beforehand.

The functions used to model undershoot and overshoot distributions are:

$$f_{under\,/\,overshoot}(s,t) = p\cdot f_{route\;dependent}(s,t) + (1-p)\cdot f_{runway\;dependent}(s,t).$$

The route dependent part is modelled as

$$f_{route\;dependent}(s,t) = f_{Weibull}(\eta,\beta;s)\cdot f_{Gauss}(\sigma_0+\sigma_1 s;t)\;,$$

and the runway dependent part as

$$f_{runway\;dependent}(s,t) = f_{Weibull}(\eta,\beta;s)\cdot f_{gen.\,Laplace}(b,a_0+a_1 s;t).$$

The parameters of both Weibull functions will be based on separate data sets and will be different.

The division into route dependent and runway dependent is not straightforward. The accident database itself normally does not provide information that relates an accident uniquely to a runway or to a route. Due to the short available time within the interim model update, a division is made on pragmatic grounds. All accidents reported on the extended centreline are considered to be route dependent and all other accidents are runway dependent.

3.3 Parameters

Most of the parameters are estimated from the location data. Some parameters cannot be deduced from the accident data and these follow from operational traffic data.

3.3.1 Parameter estimation

The parameters of the distribution functions are estimated from the accident location data using the maximum likelihood method. The function

$$L(\theta) = \sum_{i=1}^{n} \log(f(s_i, t_i; \theta))$$

is maximised for the parameter vector θ. The solution $\hat{\theta}$ for which the function $L(\hat{\theta})$ obtains its maximum value represents the most likely distribution given the data set (s_i, t_i).

Whether the solution of the maximum likelihood method is acceptable or not is to be determined with a goodness of fit test. We used the Kolmogorov-Smirnov one-sample test. This test essentially determines the largest distance D_{KS} between the data set and the proposed distribution. The proposed distribution is acceptable if the distance D_{KS} is less than a given critical distance D_C. The critical distance depends on the sample size and can be found in standard statistical literature.

3.3.2 Distribution of operational traffic

By NLR choice all route dependent accidents lie on the extended centreline. It is not possible to derive a lateral distribution from the accident location data set. Alternatively, the lateral distribution of route dependent accident locations is derived from the operational distribution of the traffic. It is assumed that the traffic is normally distributed with a flight phase dependent standard deviation.

The standard deviation of the operational traffic close to the runway will be smaller than further away from the airport. A linear relation between the standard deviation and the distance to the runway is assumed.

Deviation at threshold

The operational traffic will already deviate from the extended centreline while crossing the thresholds. The standard deviation at this point is determined from JAR-rules. JAR-AWO 131, paragraph 1.4c, prescribes the maximum probability of exceeding a minimum distance to the runway boundary [3].

For an average aircraft (Boeing 737), where the distance between the two main gears is approximately 6 metres, the JAR-rule is infringed when the centre of the aircraft is 18 metres (21-6/2) away from the runways centreline. This may occur not more than once per million aircraft movements on average. Assuming that the traffic is normally distributed around the

[3] Lateral touchdown with the outboard landing gear greater than 21 m from the runway centreline, assuming a 45 m runway: on average 10^{-6}.

centreline, the deviation at the threshold must be smaller than 18/4.89 = 3.68 metres. The standard deviation at the threshold used in the model is 3.5 metres. This means that about 99 of the 100 aircraft fly within half the width of the runway ($6\sigma = 21$ metres) which is very plausible.

Deviation for landing

The ICAO report “Manual on the Use of the Collision Risk Model (CRM) for ILS Operations” (Doc 9274-AN/904) provides standard deviations for the lateral distribution of aircraft flightpaths during ILS CAT II approaches. The data used in the ICAO report come from German (137 points), Dutch (930), American (295) and British (160) airfields. Given the high amount of observations in the Netherlands, the results are believed to be very much applicable to Schiphol.

Figure 3-8 illustrates the standard deviations for ILS CAT II approaches performed with flight director as given in table II-3-6 of the ICAO report. The standard deviation at threshold is also depicted. A regression line is drawn based on these observations. The line has a slope of $4.9 \cdot 10^{-3}$ which means that the standard deviation for the lateral distribution increases 4.9 metres per kilometre. The standard deviation for landing is $\sigma_{\text{landing}} = 3.5 + 4.9 \cdot 10^{-3}\, s$.

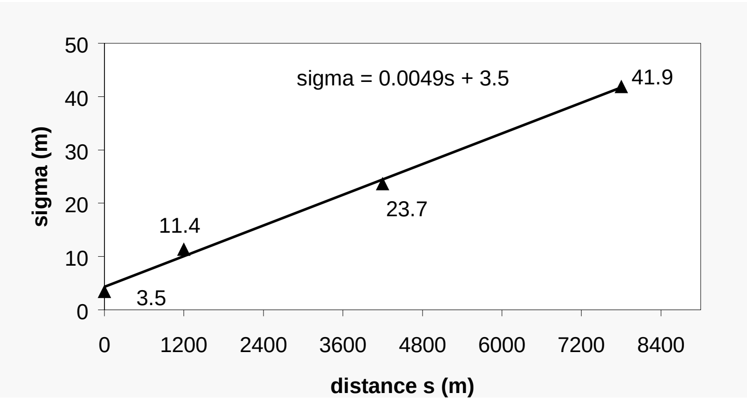

Figure 3-8: Standard deviation at four points along the route (source: ICAO) and least squares linear fit.

Deviation for take-off

The lateral deviation for take-off is determined by means of actual Schiphol data from the FANOMOS flight tracking system. The width of the area within which 95% of the traffic is observed is measured both at the threshold and at a distance of 6 kilometres from the start of the runway. Under the assumption that the traffic is normally distributed, these measured widths should (approximately) correspond to 4 times the standard deviation. The calculation of the increase in deviation is straightforward.

Table 3-4: Calculation of the increase in deviation along the route.

Route	Width 95%-area (m)		Increase in deviation ($\Delta\sigma$)	$\Delta\sigma/s$ ($\cdot 10^{-3}$)
	at threshold	at 6 km		
01L BER	148	740	148.0	54.8
01L LEK	185	704	129.8	48.1
01L LOP	185	778	148.3	54.9
01L PAM	185	630	111.3	41.2
01L RFS	259	815	139.0	51.5
01L SPY	185	407	55.5	20.6
01L TXL	87	739	163.0	60.4
01L VLA	130	913	195.8	72.5
19L AND	163	776	153.3	58.9
19L ARN	204	1306	275.5	106.0
19L BER	167	729	140.5	54.0
19L LEK	245	857	153.0	58.8
19L LOP	327	1265	234.5	90.2

The length of runway 01L is 3300 metres, the length of runway 19L is 3400 metres. The mean value of the increase in deviation per metre route ($\Delta\sigma/s$) is $59.4\cdot 10^{-3}$. The standard deviation for take-off is $\sigma_{\text{take-off}} = 3.5 + 59.4\cdot 10^{-3}\, s$.

3.3.3 Weight factor

The lateral distribution consists of two parts: one representing the locations on the extended centreline and one representing all other locations. The factor determining the weight of each part follows from:

$$p\int_0^\infty f_{Weibull}(\eta,\beta;s)ds + (1-p)\int_0^\infty f_{Weibull}(\eta,\beta;s)\cdot f_{gen.Laplace}(b,a_0+a_1 s;t=0)ds = \frac{n_{y=0}}{n_{total}}$$

or in normal words: the chance that the accident location is on the extended centreline equals the fraction of points in the data set that lie on the extended centreline. The value p indicates the fraction of the distribution that lies on the extended centreline. The above equation is approximately equal to:

$$p + (1-p)\frac{1}{2a_0 b\Gamma(b)} = \frac{n_{y=0}}{n_{total}} \Leftrightarrow p = \frac{{}^{n_{y=0}}\!/_{n_{total}}\, 2a_0 b\Gamma(b) - 1}{2a_0 b\Gamma(b) - 1}.$$

The weight factor can be calculated from this equality.

3.3.4 Resulting parameters

The following tables present the parameters of the distributions

Table 3-5: Parameters of the overshoot distribution (n_{total}=106; $n_{y=0}$=68).

distribution		**function**	**parameters**	D_{KS}	D_c
Longitudinal	y=0	Weibull	η ; β	0.0887	0.1649
	y≠0	Weibull	η ; β	0.0884	0.2206
Lateral	y=0	Gauss	σ_0 ; σ_1		
	y≠0	gen. Laplace	a_0 ; a_1 ; b	0.0786	0.2206
Weight factor			p		

Table 3-6: Parameters of the take-off overrun distribution (n_{total}=103; $n_{y=0}$=72).

distribution		**function**	**parameters**	D_{KS}	D_c
Longitudinal		Weibull	η ; β	0.0563	0.1340
Lateral	y=0	Gauss	σ_0		
	y≠0	gen. Laplace	a_0 ; a_1 ; b	0.0918	0.2458
Weight factor			p		

Table 3-7: Parameters of the undershoot distribution (n_{total}=435; $n_{y=0}$=353).

distribution		**function**	**parameters**	D_{KS}	D_c
Longitudinal	y=0	Weibull	η ; β	0.0494	0.0724
	y≠0	Weibull	η ; β	0.0471	0.1502
Lateral	y=0	Gauss	σ_0 ; σ_1		
	y≠0	gen. Laplace	a_0 ; a_1 ; b	0.0449	0.1422
Weight factor			p		

Table 3-8: Parameters of the landing overrun distribution (n_{total}=255; $n_{y=0}$=203).

distribution		**function**	**parameters**	D_{KS}	D_c
Longitudinal		Weibull	η ; β	0.0572	0.0852
Lateral	y=0	Gauss	σ_0		
	y≠0	gen. Laplace	a_0 ; a_1 ; b	0.0978	0.1807
Weight factor			p		

4 Accident consequence model

The accident consequence model defines the consequences of an aircraft accident at a particular location in debris area size and in lethality. For external risk assessments it is necessary to quantify these consequences. Together with the population density information, they determine the number of people involved in the accident.

Determination of the dimension of the consequence area and of the lethality are based on the same database: the ‘debris area database’. The information in the database is composed mainly from NTSB accident reports, completed with information from the internet, ICAO summaries and other sources. The database consists of a total of 182 data points. Not all data points were suitable for the determination of the consequences. Depending on the available information, the data points were used for both, only one or none of the consequence parameters.

4.1 Dimension of consequence area

The size of the consequence area is estimated from 71 data points. Each data point was first investigated by one person and then examined by two. The following information was sought for each point:

- Size of the debris area;
- Size of the plane;
- Terrain type of debris area;
- Accident category.

The size of the debris area is estimated from the distribution of the larger pieces of the aircraft. Small aircraft parts are not considered. If available, the size of the debris area was estimated from a photograph or drawing of the accident location. When no graphical representation of the scene was available, the text of the report was examined for apparent indications of the size of the consequence area. In several cases, the consequence area was calculated by multiplying the plane’s wingspan with the reported skid distance. Reported crash area sizes were always checked and corrected if necessary.

It is not always possible to determine a reasonable area size. In some cases the documentation of the accident was insufficient to reconstruct the dimensions of the area. This is especially so when no picture or drawing of the accident location was available. Also in cases where the aircraft disintegrated, for instance after a mid-air collision or after an explosion, it was almost never possible to determine the size of the debris area, because no large piece of debris could be identified. These data points are excluded.

A relation can be assumed between the dimensions of an aircraft and its crash area. Large aircraft will impact upon a large area. The size of the plane can be expressed in different ways, *e.g.* by the weight of the aircraft, or by its wetted area. In this report the maximum take-off weight (MTOW) is used as measure of the aircraft's size. This measure, unlike the actual weight and the wetted area, is generally mentioned in accident reports and is easy to use in the calculations.

Distinction was made in the IMER consequence model between several types of terrain. In accordance with this model, the data points were divided into the four categories built-up terrain, open terrain, forest and water. Crash areas in water were unrealistically large and therefore not considered in the remaining of this report. The number of data points for built-up terrain was insufficient for statistical use and were not considered separately.

All data points are categorised in one of seven accident categories:
1. Overshoot;
2. Undershoot;
3. Veer-off during take-off;
4. Veer-off during landing;
5. En route;
6. Mid-air; or
7. Other accidents (such as explosions).

The categories were not used in the remaining of this report.

The set of data points is depicted in figure 4-1. A linear fit through the points is also shown. The regression line has a constrained intercept of the vertical axis at a crash area size of zero. Although an unconstrained regression line would result in a marginally better correlation co-efficient r^2, the intercept at zero is chosen. This results in the easiest fit, whereby a crash area for any MTOW can be found. This results in a crash area equal to 83 m^2/ton MTOW.

4.2 Lethality

Lethality is the probability of receiving fatal injuries when residing in the consequence area of an aircraft crash. It is determined as the ratio of the number of third party fatalities and the total number of people present in the consequence areas.

Although the sources are clear about the number of fatalities, they normally do not provide the number of people who were within the consequence area at the time of the crash. A reliable estimation of the number of people within the consequence area of each crash is necessary to make a good estimate of the fatality ratio.

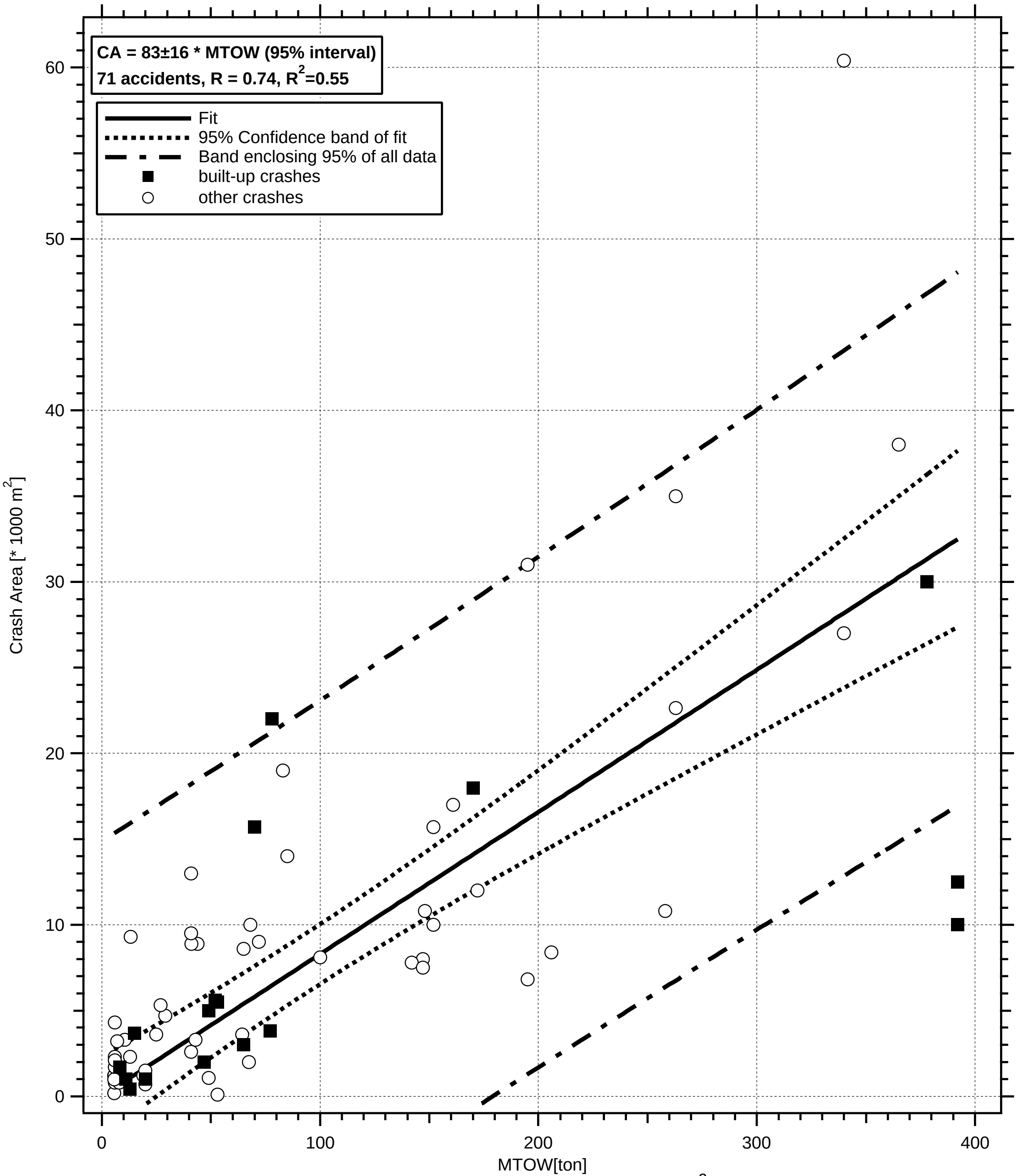

Figure 4-1: Data points and fit of crash area size (in 1000 m^2) against MTOW (in tons).

In this report an estimation of the population in the consequence areas is made based on engineering judgements. This is only possible if sufficient information is provided in the documentation of an accident. Useful information is for instance: the number of destroyed or damaged buildings, the local time of the crash, the number of fatally, seriously and slightly injured people, et cetera. In the accident reports, these facts are gathered in the chapter “other damage”.

A number of 132 data points were considered in the debris area database. An estimated population in the consequence areas could be determined for a total of 115 data points. Of the 115 data points the unpopulated consequence areas (84 data points) provide no information on the lethality and are ignored. Consequently, the lethality is based on 31 data points (see appendix D).

Given both the fatality numbers and the population for a set of accidents, there are two obvious ways to determine the lethality. One can:

1. divide the sum of third party fatalities of all accidents by the sum of estimated population in the consequence areas, or
2. calculate the (mathematical) mean value of the fatality ratios.

Contrary to the second method, the first method weighs the fatality ratios. In the determination of the lethality aircraft accidents involving a relatively large population are weighed more than accidents involving only a few people. It is found that the former group of accidents is better documented than the latter. Therefore, it is assumed that the higher the population in the consequence area, the more accurate the estimate for the fatality ratio becomes. The calculation of the lethality could possibly be improved if the fatality ratios could be weighed by their own relative accuracy. Due to insufficient time, no attempt was made to determine the accuracy of the fatality ratios.

The lethality is determined using the first method and is calculated to be 0.278. It is noted that three data points together are responsible for more than 50% of the lethality.

An upper limit to lethality can be determined by assuming that all persons in the consequence area are either killed or injured. In reality there may have been more people in the area, but certainly not less. The fatality ratio will be lower when there were unharmed people in the area. The ADREP database provides numbers of fatalities and seriously and slightly injured people. Since all these people are certain to be present in the consequence area, an upper bound of 0.612 is obtained for the lethality based on the ADREP data.

A lower limit to lethality can be made by estimating the maximum possible population in each consequence area. Such an estimate is not determined and is therefore not given in this report.

5 Model comparison

This chapter compares the results of the model updates as discussed in the previous chapters to former models.

5.1 Former models

The IMU model described in this report is compared to the original IMER model and to the TNLI model. Both models will be discussed shortly in the next two paragraphs.

5.1.1 IMER model

The first model to carry out external risk analysis was developed by the NLR in 1992 and is referred to as the IMER model. The IMER model was developed under the Integrated Environmental Impact Statement (IMER).

The accident rates of the IMER model are shown in table 5-1. The consequence parameters are given in table 5-2.

Table 5-1: Accident rates of the IMER model.

	1990	2003	2015
Landing	$0.70 \cdot 10^{-6}$	$0.65 \cdot 10^{-6}$	$0.61 \cdot 10^{-6}$
Take-off	$0.435 \cdot 10^{-6}$	$0.435 \cdot 10^{-6}$	$0.435 \cdot 10^{-6}$

Table 5-2: Consequence parameters of the IMER model.

	CA/ton MTOW	lethality
Open terrain	250 m^2	0.3
Built-up terrain	200 m^2	0.3
Forrest/water	150 m^2	0.3

5.1.2 TNLI model

In 1998 new estimates of the accident rate and the consequence area were made for the Future Dutch Aviation Infrastructure (TNLI). Due to time limitations imposed by TNLI, no elaborate analysis was performed to arrive at these estimates The estimates should therefore be considered rough approximations. The estimated values will be referred to as the TNLI values.

It was estimated that the accident rates for Schiphol for the year 1997 were roughly 50% lower than the IMER value for the year 1990. This difference is attributed partly to more accurate modelling based on better data than was available in 1990, and partly to the development of safety on Schiphol. The new aspect of the TNLI rates was that the actual influence of the aircraft generations was taken into account. The classification of an aircraft into generation 1, 2 or 3 is discussed in appendix A. Fleet changes between 1990 and 1997 are expected to account for about 35% of the improved real safety per aircraft movement at Schiphol [2]. Figure 5-1 shows the distribution of the Schiphol fleet in generations of aircraft for the years 1990 to 1997, according to the Official Airline Guide (OAG) Timetable database.

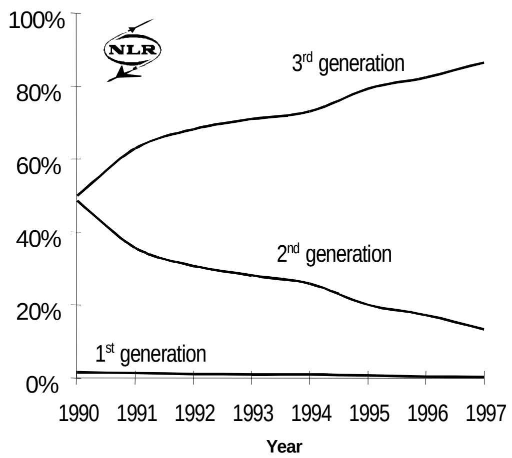

	1st	2nd	3rd
1990	1.5	48.6	49.9
1991	1.4	35.7	63.0
1992	1.1	30.8	68.2
1993	0.9	28.1	71.0
1994	1.0	25.9	73.1
1995	0.7	20.0	79.3
1996	0.4	17.2	82.4
1997	0.3	13.3	86.4

Figure 5-1: Percentage of the contributions of first, second and third generation aircraft in the fleet of Schiphol in the period from 1990 to 1997(source: OAG Timetable database).

The consequence parameters of the TNLI model are shown in table 5-3.

Table 5-3: Consequence parameters of the TNLI model.

	CA/ton MTOW	lethality
Open terrain	160 m^2	0.3
Built-up terrain	130 m^2	0.3
Forrest/water	130 m^2	0.3

5.2 Model comparison

5.2.1 Accident rates

The accident rate in the IMU model depends on the distribution of aircraft generations in the fleet. The percentages of generation of aircraft for the years 1990, 1997, 1998 and 2010 are shown in table 5-4. This information is taken from the Statistical Annual Reviews of Amsterdam Airport Schiphol, which are published by Schiphol Group. The percentages for 2010 are derived from the fleet composition of 2010 obtained from KLM Royal Dutch Airlines.

Table 5-4: Percentages of generation of aircraft for the relevant years according to the IMU model (source: fleet composition Schiphol Group and KLM).

	Generation 1 [%]	Generation 2 [%]	Generation 3 [%]
1990	13.3	40.4	46.3
1997	1.2	13.1	85.7
1998	0.7	11.0	88.3
2010	-	0.9	99.1

The percentage in table 5-4 differ from those in figure 5-1. The TNLI estimates of the accident rates are based on the OAG Timetables database, which results in an underestimation of especially the percentage of generation 1 aircraft of the 1990 fleet.

Table 5-5 presents the accident rates (veer-off accidents are not taken into account) of the IMER, TNLI and IMU models for the years 1990, 1997, 1998 and 2010. It shows that the total IMU accident rate $((AR_{take\text{-}off} + AR_{landing})/2)$ for 1990 is 52% lower than the total IMER accident rate for that year. The total IMU accident rate for 2010 is reduced with 45% compared to the total the IMU rate for 1990. The total IMU rate for 1997 is 38% smaller than the total IMU rate for 1990.

Table 5-5: Accident rates per million flights (no veer-off) for four relevant years according to the IMER model, the TNLI model and the IMU model.

	IMER			**TNLI**			**IMU**		
	take-off	landing	total	take-off	landing	total	take-off	landing	total
1990	0.435	0.700	0.568	0.370	0.595	0.483	0.180	0.359	0.270
1997	0.435	0.673	0.554	0.218	0.350	0.284	0.119	0.216	0.168
1998	0.435	0.669	0.552	0.218	0.350	0.284	0.116	0.209	0.162
2010	0.435	0.627	0.531	0.218	0.350	0.284	0.108	0.187	0.148

The fact that the IMU accident rates are much lower than the IMER rates is mainly caused by the distinction in aircraft generations made in the IMU model. This distinction was not made in the IMER model. As a result of this, a relatively large amount of first and second generation aircraft, as observed in the average fleet related to the selected airports, contribute to the higher accident rate in the IMER model. Furthermore, the trend in the IMER accident rate was not sufficient to account for the relatively fast replacement in the Schiphol fleet of first and second generation aircraft by third generation aircraft. The IMU rates are more in line with the risks of the actual fleet. Another reason why the IMU rates are distinctly lower than the IMER rates is that the fraction of business jet in the IMU model, due to airport selection criterion 3, is very small. Business jets are involved in 50% of the accidents.

To explain the difference between the TNLI estimates for 1990 and the IMU values for 1990, the following observations are made:

1. In the TNLI estimate hull loss rate data was used, because this was readily available. In the IMU analysis individual accidents were selected. In some cases, hull loss accidents were not considered an accident in the IMU analysis. For example, an aircraft collapsing through its landing gear can be declared a hull loss, but will not likely result in an (third party risk) accident. Note also that older aircraft are declared a hull loss more quickly than newer aircraft. In general, accident ratios based on hull loss are higher than ratios based on accidents relevant to third party risk analysis;
2. The TNLI estimates include cruise accidents and accidents on the runway;
3. The TNLI accident rates are estimated from world-wide data, whereas the IMU rates are based on accidents related to a selection of airports comparable to Schiphol regarding safety.

The differences in safety between the generations of aircraft are based on world wide data. First generation aircraft are probably more common in regions where the general safety level is less than in the Western World, and are operated by less safe operators. Therefore, it can be expected that the differences in safety between generations of aircraft at Schiphol is smaller than the TNLI data shows. In IMU the differences in safety between generation of aircraft are based on data from a selected set of airports.

The Timetables database, used to make figure 5-1, is not always accurate. In some cases the reported aircraft type is not specific enough to decide of which generation the aircraft was. A third generation aircraft can erroneously be considered to be of the first or second generation[4]. The database is also not complete. Many ad-hoc operations are not reported in the database. Incidentally, the number of ad-hoc operations at Schiphol is very small. Because of the time pressure during the TNLI study, a proper check of the results could not be carried out. The results of IMU have pointed out that the effect of using the Timetables database as such has resulted in an overestimation of the accident rates of the TNLI estimates.

Figure 5-2 shows the total accident rates per million flights of the IMER, TNLI and IMU model (excluding veer-offs), while figure 5-3 shows the normalised total accident rates of these three models.

[4] The deficiency of inaccuracy of the OAG database was bypassed in the IMU model by considering the actual fleet of each operator in each year. Using this extra information, the aircraft with unspecific aircraft type in the database could be classified into generations.

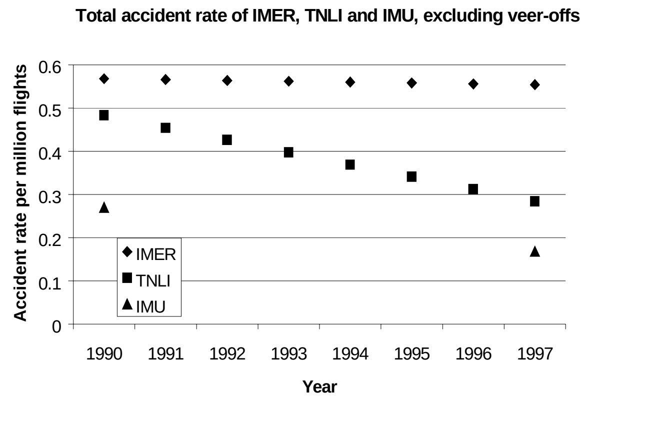

	IMER	TNLI	IMU
1990	0.568	0.483	0.270
1991	0.566	0.454	-
1992	0.564	0.426	-
1993	0.562	0.397	-
1994	0.560	0.369	-
1995	0.558	0.341	-
1996	0.556	0.312	-
1997	0.554	0.284	0.168

Figure 5-2: Total accident rates per million flights of the IMER model, the TNLI model and the IMU model (excluding veer-offs).

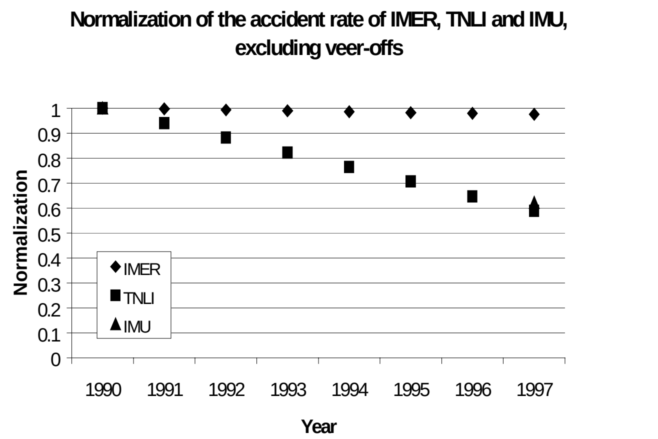

	IMER	TNLI	IMU
1990	1	1	1
1991	0.997	0.940	-
1992	0.993	0.882	-
1993	0.990	0.822	-
1994	0.986	0.764	-
1995	0.983	0.706	-
1996	0.979	0.646	-
1997	0.976	0.588[5]	0.622

Figure 5-3: Normalised total accident rates (1990=1) of the IMER model, the TNLI model and the IMU model (excluding veer-offs).

5.2.2 Accident locations

The IMU location model can only be compared to the IMER location model. No separate location model and no separate location parameters were developed during the TNLI estimations.

It is noted that changes in the accident location model do not increase or decrease the overall probability of an aircraft accident, but merely provides another distribution of the total risk. It is possible, however, that societal risk increases (or decreases) due to changes in the location model when the redistribution of accident probability results in higher (or lower) probabilities in densely populated areas.

[5] The reduction in the accident ratio of TNLI between 1990 and 1997 is 41% instead of 35% as stated in section 5.1.2. This is caused by reducing the IMER ratio for 1990 with 15% instead of reducing the TNLI ratio for 1997 (50% of IMER ratio for 1990) with 35%.

A number of differences can be identified between both location models.

Route dependence

The IMU model distributes only part of the accident probability for undershoots and overshoots around a route, where the IMER model distributes the entire probability for undershoots and overshoots around the routes. An apparent advantage of the IMU approach is that risk contours look smoother and less distorted than in the IMER approach. The IMER contours sometimes show improbable bulges and indentations (see figure 5-4), caused by the transformation of accident probability distribution around a route.

Dirac function

The discontinuous Dirac function in the IMER model is replaced by a continuous Gauss distribution function. This resolves problems that occur when transforming the distribution function around the routes. The consequences to the calculated risk levels are minimal.

Operational traffic distribution

It is recognised that air traffic has a larger distribution at some distance from the airport, than close to the airport. This was not incorporated in the IMER model in a satisfactory manner.; the Dirac function, implemented as a step function of fixed width, did not reflect an increasing deviation from the route at increasing distance from the airport. The Gauss function in the IMU model that replaces the Dirac function has distance dependent parameters, and does show an increasing traffic distribution at increasing distances from the airport. The effect of incorporating operational traffic distribution is especially noticeable for departure routes at larger distances from the airport: the routes are still recognisable, but are shorter and wider.

New parameter estimation

The accident probability distribution in the IMU model is based on different data than in the IMER model. Although the underlying functions used to model the distribution are basically the same in both models, the function parameters differ, and therefore the distributions are different. In general, the distribution in the IMU model is narrower, resulting in higher risks close to the routes and lower risks further from the routes.

Figure 5-4 compares the probability distributions of both models. It shows the contours of a particular value for a departure route (01L LEKKO) and for an arrival route (24 VIS). In addition, the routes themselves are illustrated. The contour of the IMU model is smoother and narrower than the contour of the IMER model. The use of both a route dependent part and a route independent part in the IMU model is clearly noticeable. Also the incorporation of operational traffic distribution in the IMU model can be recognised.

5.2.3 Accident consequences

The dimensions of the crash areas per ton MTOW according to the IMER model, the TNLI parameters and the IMU model are repeated in table 5-6. The judgements made in the TNLI study predicted that the crash areas would be approximately 35% smaller than deduced in the IMER model. This TNLI estimation of reduction in crash area per ton MTOW is based on more data. Determination of the crash areas per ton MTOW for the IMU model is based on more information of the crash area, and so, more accurate evaluations were made of the size of a crash area. The reduction of the dimensions of the crash areas per ton MTOW according to the IMU model is roughly 60% to 65% smaller than deduced in the IMER model.

Table 5-6: Crash area dimensions per ton MTOW according to the IMER model, the TNLI parameters and the IMU model.

	IMER model	**TNLI parameters**	**IMU model**
Open terrain	250 m^2	160 m^2	83 m^2
Build-up terrain	200 m^2	130 m^2	83 m^2
Forrest or Water	150 m^2	130 m^2	83 m^2

An estimate of an increase or reduction in lethality was not made in the TNLI study, because of lack of time and the need for a proper research. Lethality is reduced from 0.3 in the IMER model (and TNLI parameters) to 0.278 in the IMU model. This is a reduction of less than 10%.

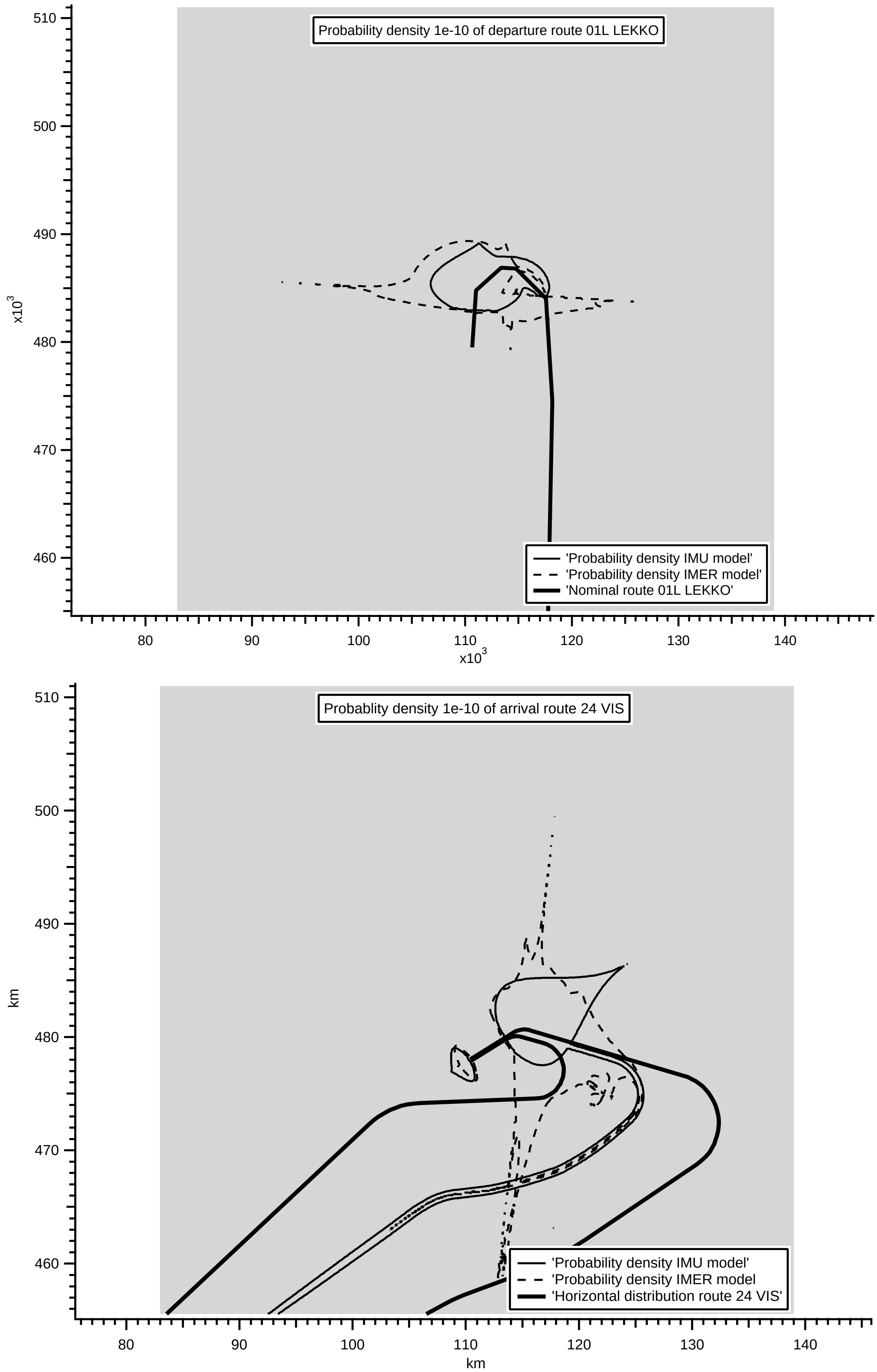

Figure 5-4: Comparison of the probability distributions of the IMU model and the IMER model; above the departure route 01L LEKKO and below the arrival route 24.

6 Scenario description

The model as described in the first part of this report is used to evaluate third party risk for two scenarios. One of the scenarios, denoted as S4S1-1990 (calculation number 00012103), represents the traffic at Schiphol in the year 1990 with its four-runway layout. This scenario is used for reference. The other scenario, denoted as S5P-2010 (calculation numbers 00012101 and 00012102), expresses the five-runway situation in the year 2010, which is the mid-term planning horizon.

This section describes the input that is used for the evaluations. The results follow in the next section. The input can be divided into the following:
1. dimension of the study area;
2. model parameters;
3. route structure and runway thresholds;
4. traffic data;
5. population density data; and
6. building density data.

6.1 Dimension of the study area

The risk calculations around the airport are limited to a defined area, called the study area or domain. The study area around Schiphol is 56 by 56 kilometres large, with the airport in the centre. The co-ordinates of two angular points of the area are given in the rectangular Dutch co-ordinate system RDC in table 6-1.

Table 6-1: RDC co-ordinates of the study area.

Angular point	X (m)	Y (m)
lower left corner	83,000	455,000
upper right corner	139,000	511,000

6.2 Model parameters

Relevant model parameters are the accident rates, the size of the consequence area and the lethality.

6.2.1 Accident Rates

As described in chapter 2, accident rates are based on the distribution of the aircraft generations in the traffic of a scenario. Appendix F shows the determination of the percentages of generation of aircraft in the 1990 and 2010 scenario.

Table 6-2: Distribution of traffic over aircraft generations for the S4S1-1990 and the S5P-2010 scenarios according to the IMU model.

Scenario	Generation (%)		
	1	2	3
S4S1-1990	13.3	40.4	46.3
S5P-2010	-	0.9	99.1

In combination with table 2-2, the accident rates for the relevant accident types can be determined by multiplying the accident rate from table 2.2 with the percentage of generation of aircraft. The result is shown in the table below.

Table 6-3: Construction of accident rates for the S4S1-1990 and S5P-2010 scenarios from aircraft generations.

Accident type	S4S1-1990: generation				S5P-2010: generation			
	1	2	3	total	1	2	3	total
Take-off overrun	0.050	0.044	0.029	**0.123**	-	0.001	0.061	**0.062**
Take-off overshoot	0.017	0.019	0.021	**0.057**	-	0.000	0.046	**0.046**
Landing overrun	0.033	0.081	0.029	**0.143**	-	0.002	0.061	**0.063**
Landing undershoot	0.100	0.059	0.057	**0.216**	-	0.001	0.123	**0.124**

6.2.2 Consequence area and lethality

The consequence area of an individual crash is impossible to predict; it depends on a large number of parameters, such as the terrain features, the attitude of the aircraft, its speed, load, fuel content, the weather, et cetera. Statistically, however, there is a fairly direct proportionality between the area of an impact site, and the size of the aircraft. The MTOW is found a good estimator for the size of the aircraft. For statistical analysis, a simple circular crash area is assumed, with its area linearly dependent on the MTOW of the crashing aircraft.

Appendix F shows the average MTOW of the traffic in the S5P-2010 scenario. The average MTOW of the S4S1-1990 scenario is taken from the Statistical Annual Review of 1990. The following average MTOW values, and corresponding crash areas were found. Recall that the size of the consequence area is 83 m^2 per ton MTOW. The lethality is a fixed number for all scenarios, and is given here for reasons of completeness.

Table 6-4: Consequence parameters for the S4S1-1990 and S5P-2010 scenarios.

Scenario	MTOW (ton)	Crash Area (m^2)	Crash radius (m)	Lethality
S4S1-1990	88	7304	48.22	0.278
S5P-2010	100.8	8366	51.61	0.278

6.3 Route structure and runway thresholds

The routes used in the calculations represent as closely as possible the nominal air route structure, with exception of the landing routes for the 2010 scenario. A nominal route of these landings is based on the horizontal spread of the landing route. The route structure is depicted in a number of figures in appendix E. The routes for the 1990 risk calculations were provided by RLD.

The position of the runways are presented in the risk calculations by runway thresholds. In general, the thresholds will match the physical ends of a runway. However, it is possible that a threshold is located more to the centre of the runway. The runway thresholds as used in the calculations are presented in table 6-5.

Table 6-5: Runway threshold co-ordinates.

Runway			X (m)	Y (m)	X (m)	Y (m)
01L	19R		110,672	479,512	110,887	482,804
01L	19R	2010, threshold 01L moved 450 m	110,701	479,961	110,887	482,804
01L	19R	2010, threshold 19R moved 630 m	110,672	479,512	110,846	482,175
01R	19L		113,392	478,268	113,613	481,660
06	24	1990	110,656	478,102	113,417	479,798
06	24	2010	110,443	477,971	113,417	479,798
06	24	2010, threshold 06 moved 250 m	110,656	478,102	113,417	479,798
09	27		111,303	481,159	114,751	481,322
18	36	only 2010	109,005	486,302	108,757	482,510

6.4 Traffic data

Air traffic data consists of the number of movements per route over a period of one year. Movement numbers for the S5P-2010 scenario were provided by KLM. Movement numbers for the recalculation of the S4S1-1990 scenario were used from the 1990 scenario as calculated on behalf of the AMER S5P for the 1990 situation.

Table 6-6 shows the number of movements for each of the runways in use for the S4S1-1990 and the S5P-2010 scenario. Appendix G shows the number of movements of both scenarios for each individual route. The total number of movements used in the S4S1-1990 calculation is 207,010 and the total number of movements used in the S5P-2010 calculation is 600,497.

To calculate societal risk, traffic data of day and night is used. Daytime is considered to be from 7.00 till 19.00 hours, night-time is considered to be from 19.00 till 7.00 hours.

Table 6-6: Traffic numbers per runway for the S4S1-1990 and the S5P-2010 scenarios.

	S4S1-1990		S5P-2010	
Runway	**Take-off**	**Landing**	**Take-off**	**Landing**
01L	36,765	0	69,190	25,944
01R	0	7,194	0	74,893
06	202	41,219	0	74,825
09	7,723	0	4,052	219
18	0	0	0	66,064
19L	5,763	0	38,035	0
19R	0	30,610	2,321	40,519
24	52,030	2,008	75,523	2,741
27	1,094	22,402	5,110	15,081
36	0	0	105,980	0
Total	**103,577**	**103,433**	**300,211**	**300,286**

6.5 Population density data

The population data, as used in the S5P-2010 calculations in this report, was provided to NLR by the Survey Department (MD). A separate day and night population database was provided by the MD. The population data of the MD is derived from the building density file of the MD, including information about location of companies. The MD has considered the number of people present in a study area of 83 x 84 km to be constant during the day and during the night. With the help of Statistics Netherlands (CBS) information, the MD has estimated the number of people present in hospitals, schools, companies, et cetera during the day. Knowing this, an average factor of people present within a house during the day is determined. The same method is applied to the population density database of the night.

In analogy with the ADECS population density files, the population within the airport perimeter as it existed in 1990 is removed from the population density files of the MD. The same is done with the population within the airport perimeter as it will exist in 2010. Figure 6-1 represents the population density at day-time for the 2010 situation. It is the MD 1998 file, with population at the location of the fifth runway removed.

6.6 Building density data

The building density data used in the calculations in this report was provided to NLR by MD. The building data is derived from a combination of an Address Co-ordinate file of the Netherlands (ACN) and the plot code of a PTT-file. The plot code can be used to distinguish between houses and companies. Information of the location of companies is derived from the database of LISA. Objects with more than 3 employees are considered to be used as an office and are marked as such in the building file. From this building density file NLR has derived a building density file which only contains information about the number of houses at a certain location. Only information about locations of houses is chosen to be able to compare the building density file of the MD with the building density file of ADECS.

This building density file of the MD is used for the calculation of houses within the individual risk contours and the determination of GGR. For the S5P-2010 scenario the houses at the location of the fifth runway are removed, conform the airport perimeter as it will be in 2010. For the S4S1-1990 reference situation the ADECS 1990 building density file is used. This file only contains information about the location of houses within the study area. Figure 6-2 represents the building density of the 2010 situation with five-runway lay-out .

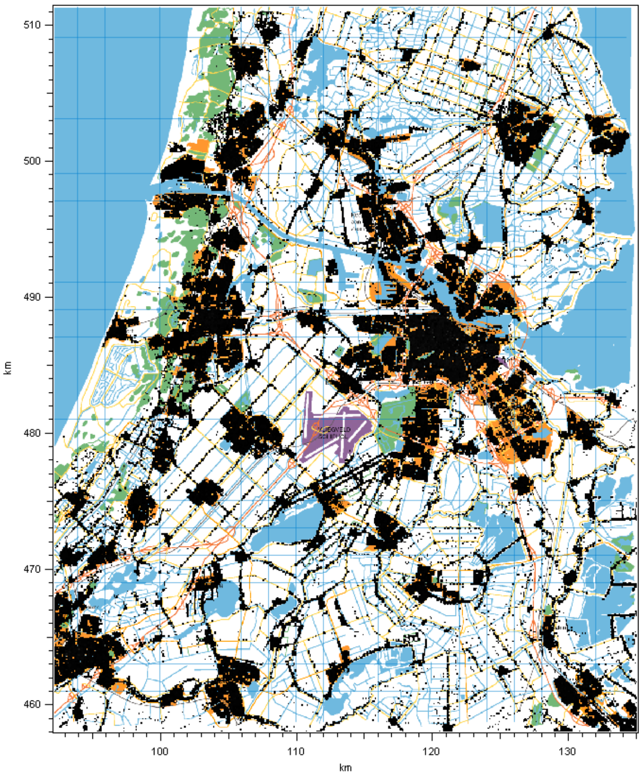

Figure 6-1: Population density for day-time of the 2010 situation; MD 1998 file with correction for the fifth runway.

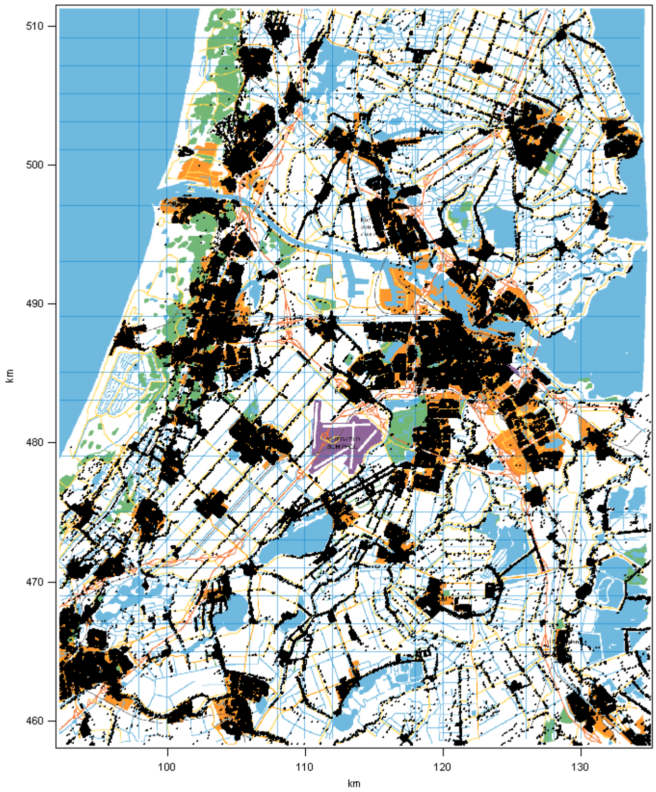

Figure 6-2: Building density of the 2010 situation; MD 1998 with correction for the fifth runway.

7 Results

7.1 Measures of risk

7.1.1 Individual Risk

Individual Risk is the probability (per year) that a person permanently residing at a particular location in the area around the airport is killed as a direct consequence of an aircraft accident. After local individual risks have been calculated for the entire area around an airport, risk contours can be generated and plotted on a geographical map. Risk levels indicated by the contours in this report are $5{\cdot}10^{-5}$, $1{\cdot}10^{-5}$, $1{\cdot}10^{-6}$ and $1{\cdot}10^{-7}$. The highest risk levels ($5{\cdot}10^{-5}$) occur close to the runway thresholds and are present in a relatively small area only. The lower risk levels occur at larger distances from the runways and from the routes followed by arriving and departing traffic. The runways which are used by the majority of traffic show larger individual risk contours than those which are used less often.

7.1.2 House counts and summed weighted risk

The individual risk contours can be used as a basis for derived risk indicators. Since high individual risk levels are only a problem if they coincide with population concentrations, a relation between local risk levels and population density information is useful. An example is the count of number of houses or persons within a risk contour, *i.e.* counting the number of houses exposed to a risk level exceeding a particular individual risk value. By performing these calculations for different scenarios an objective comparison can be made.

The Summed Weighted Risk (GGR) is by definition equal to the sum of the individual risk values of all houses within the domain.

7.1.3 Societal Risk

Societal Risk is the probability per year of more than N third party victims due to an aircraft accident somewhere in the area around the airport. Societal risk is presented in a FN diagram. The logarithmic horizontal axis represents the number of third party victims (N) involved in a single accident. The logarithmic vertical axis represents the probability per year (F) that an accident will occur which involves more than N victims. The curve applies to the entire domain.

7.2 Calculated results

7.2.1 Individual Risk

The individual risk contours of S4S1-1990 and S5P-2010 calculated with the enhanced model described in this report are shown respectively in figure 7-1 and figure 7-2.

The early split in the long peaks in line with runway 09-27 of the lower risk contours ($1{\cdot}10^{-6}$ and $1{\cdot}10^{-7}$) of scenario S5P-2010 are caused by the 3 landing routes on runway 27. These nominal landing routes are calculated from the 95% limits (dispersal) as used in the noise calculations.

7.2.2 Societal risk

The values of societal risk of the calculated cases are presented in table 7-1. The societal risk diagrams of S5P-2010 and S4S1-1990 are shown in figure 7-3. Two societal risk diagrams are shown for S5P-2010, one which is calculated with the 1998 population files of the Survey Department (Dutch: Meetkundige Dienst), and one with the 1990 population files of ADECS.

Table 7-1: Probabilities of more than N victims per year for the S5P-2010 scenario (evaluated with two population files) and for the S4S1-1990 scenario.

Number of victims (N)	Scenario		
	S5P-2010 MD 1998	S5P-2010 ADECS 1990	S4S1-1990 ADECS 1990
1000	$9.0 \cdot 10^{-10}$	$< 1.0 \cdot 10^{-10}$	$< 1.0 \cdot 10^{-10}$
400	$9.3 \cdot 10^{-7}$	$1.2 \cdot 10^{-8}$	$2.4 \cdot 10^{-8}$
200	$1.8 \cdot 10^{-6}$	$8.3 \cdot 10^{-7}$	$1.4 \cdot 10^{-6}$
100	$4.8 \cdot 10^{-6}$	$2.0 \cdot 10^{-5}$	$1.1 \cdot 10^{-5}$
40	$3.2 \cdot 10^{-5}$	$6.4 \cdot 10^{-5}$	$6.4 \cdot 10^{-5}$
20	$1.5 \cdot 10^{-4}$	$1.8 \cdot 10^{-4}$	$1.7 \cdot 10^{-4}$
10	$5.2 \cdot 10^{-4}$	$5.3 \cdot 10^{-4}$	$3.9 \cdot 10^{-4}$
5	$1.0 \cdot 10^{-3}$	$1.1 \cdot 10^{-3}$	$6.7 \cdot 10^{-4}$
3	$1.5 \cdot 10^{-3}$	$1.6 \cdot 10^{-3}$	$8.5 \cdot 10^{-4}$
1	$2.7 \cdot 10^{-3}$	$2.9 \cdot 10^{-3}$	$1.3 \cdot 10^{-3}$

7.2.3 House counts and summed weighted risk

The individual risk gradient plays an important role in the relation between risk level changes and the associated changes in numbers of residents inside individual risk contours. If risk contours are visualised as constant elevation lines in a risk “landscape”, the individual risk gradient is the “steepness” of risk “hills”. A formal description of the risk gradient is the change in risk per unit displacement on the ground.

Close to routes and thresholds (the high risk areas) the local accident probability decreases very quickly with increasing distance from the runway threshold and the traffic route (steep gradient). In the lower risk areas, the local accident probability decreases much slower with increasing distance from routes and thresholds (shallow gradient). Consequently, a particular change in the overall risk level will generally result in a relatively small displacement of the contours in the high risk areas and a much larger displacement of the contours in lower risk areas. This means that, while the change in risk is equal for all residents in the area around the airport, the change in the number of people inside the high risk contours will be relatively small and the change in the number of people inside the lower risk contours will be relatively large.

Table 7-2 shows the results of the summed weighted risk (GGR) and the house counts carried out for a 1998 house distribution file of the Survey Department (MD) and for a 1990 house distribution file of ADECS.

The house distribution file of ADECS is based on the situation around Schiphol as it existed in 1990. The file is not corrected for the new runway layout that will exist in 2010. Evaluations with the ADECS distribution file are performed by the company ADECS b.v.

The house distribution file of the Survey Department is based on the house and company distribution around Schiphol in 1998. For the counting of number of houses in 2010 the houses on the airport perimeter of the runway layout with the fifth runway were removed. NLR has carried out the counting of houses and the calculation of GGR with the MD 1998 file.

Table 7-2: Summed weighted risk and house counts evaluated with ADECS 1990 and MD 1998 house distribution files and with the enhanced IMU model.

	House	**GGR ($*10^{-3}$)**				**Number of houses**			
Scenario	**distribution file**	**5e-5**	**1e-5**	**1e-6**	**1e-7**	**≥5e-5**	**≥1e-5**	**≥1e-6**	**≥1e-7**
S4S1-1990	MD 1998	0	0.071	1.71	4.04	0	4	1025	9713
nr. 00012103 207.000 mov.	ADECS 1990	0	0.218	1.55		0	7	774	7852
S5P-2010	MD 1998	0.273	1.44	3.25	5.18	2	58	727	8353
nr. 00012101 600.000 mov.	ADECS 1990					3	71	723	6814

To get an impression of the changes in GGR and in the counted number of houses when the number of movements increases, the 2010 traffic has been multiplied by a factor. The calculations are carried out with the house distribution file MD 1998. Table 7-3 shows the results of this movement scaling. The presented numbers are fictitious and should not be taken literally. Neither the S5P-scenario, nor (some of) the input-parameters are believed to be suited for the large amounts of traffic that were used in the evaluation.

Table 7-3: Summed weighted risk and house counts for a number of movements, based on the S5P-2010 scenario (nr. 00012101) evaluated with the MD 1998 file.

	GGR (*10^{-3})				Number of houses			
Number of movements	**5e-5**	**1e-5**	**1e-6**	**1e-7**	**≥5e-5**	**≥1e-5**	**≥1e-6**	**≥1e-7**
600,000	0.273	1.44	3.25	5.18	2	58	727	8353
800,000	0.751	2.05	4.48	7.19	9	72	922	11840
1,100,000	1.42	3.70	6.40	10.3	16	156	1275	17817
2,000,000	2.95	7.33	12.4	19.0	25	241	2652	31400

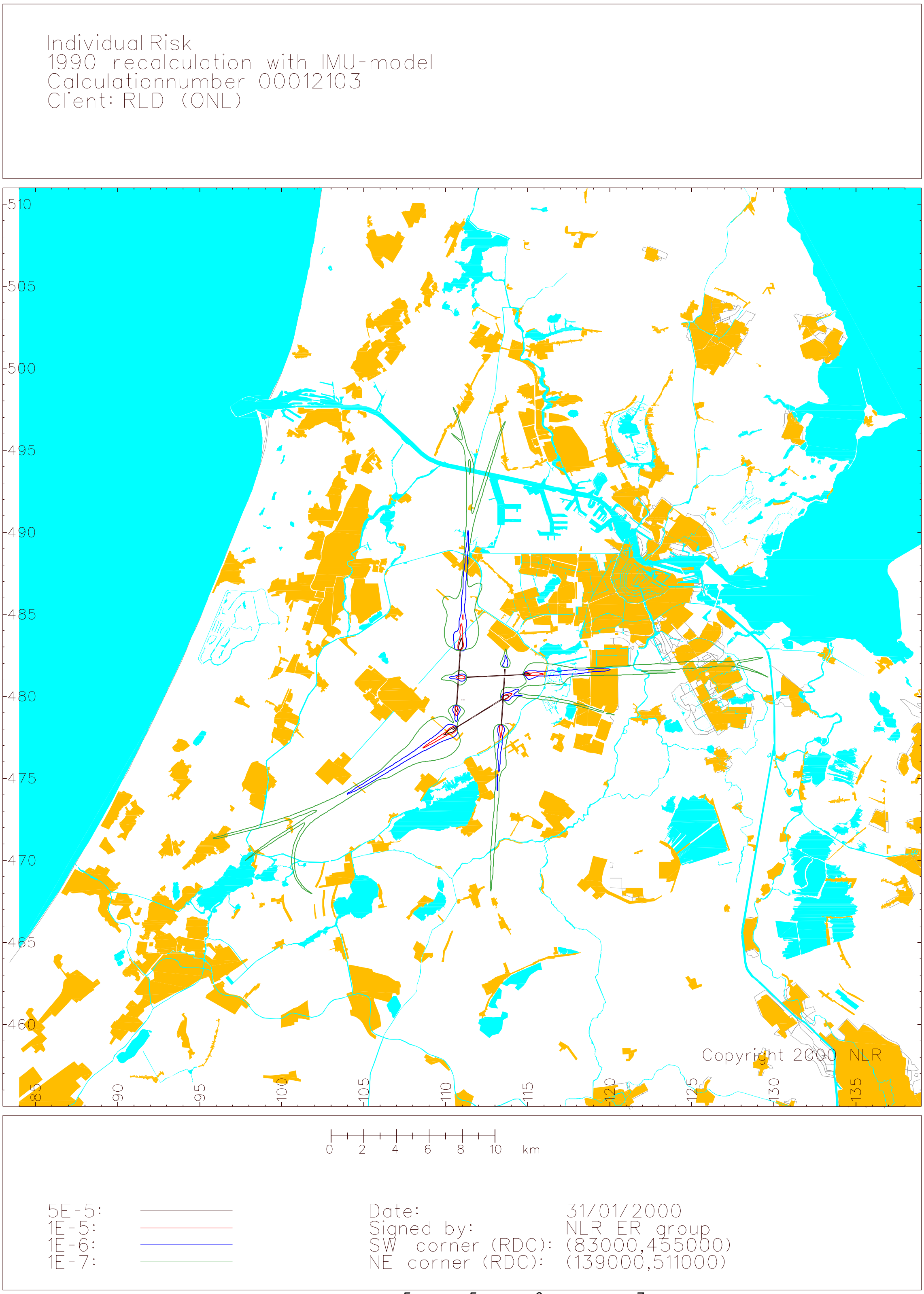

Figure 7-1a: Individual risk contours, $5{\cdot}10^{-5}$, $1{\cdot}10^{-5}$, $1{\cdot}10^{-6}$ and $1{\cdot}10^{-7}$, of the S4S1-1990 scenario.

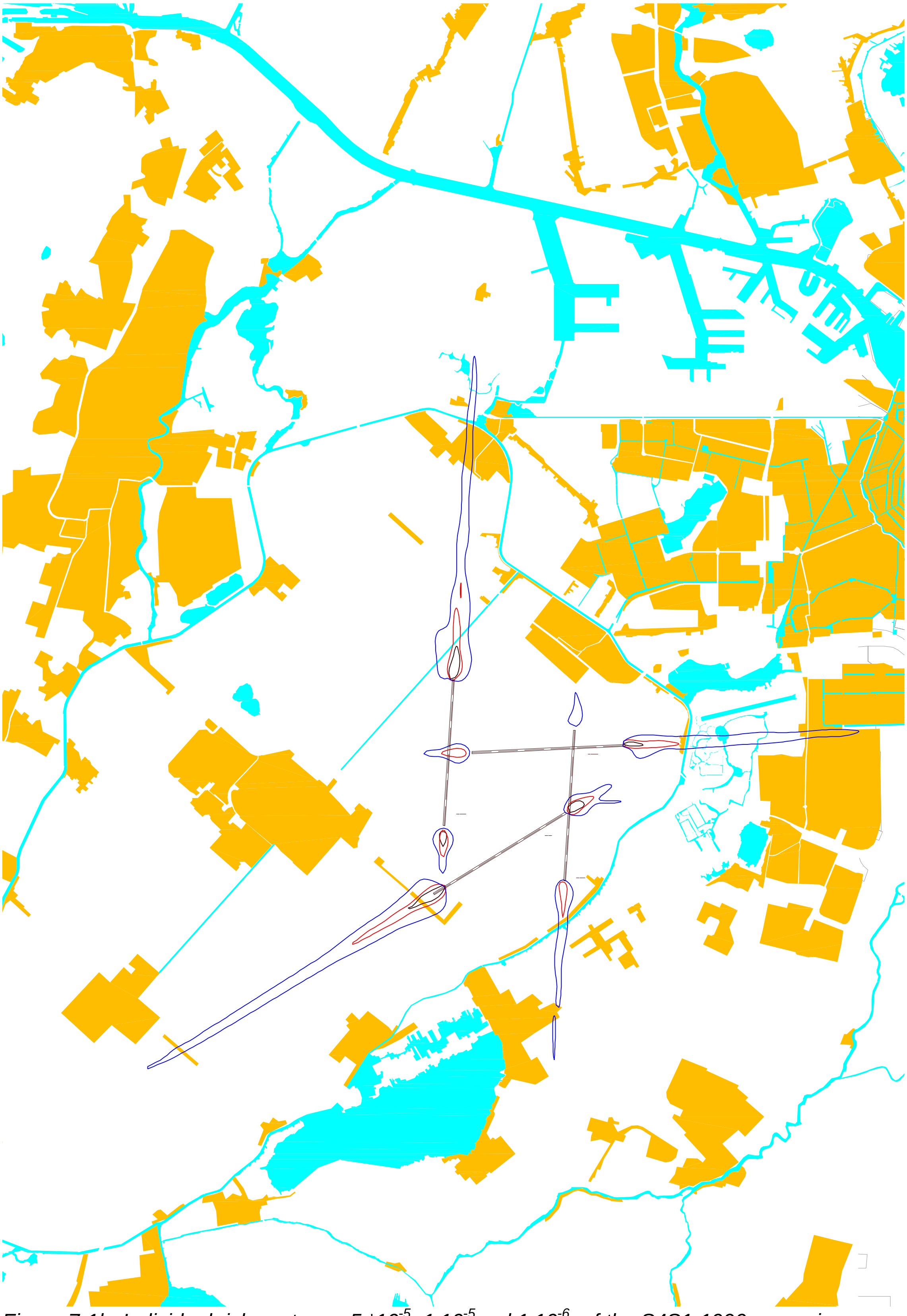

Figure 7-1b: Individual risk contours, $5\cdot{}^*10^{-5}$, $1\cdot10^{-5}$and $1\cdot10^{-6}$, of the S4S1-1990 scenario.

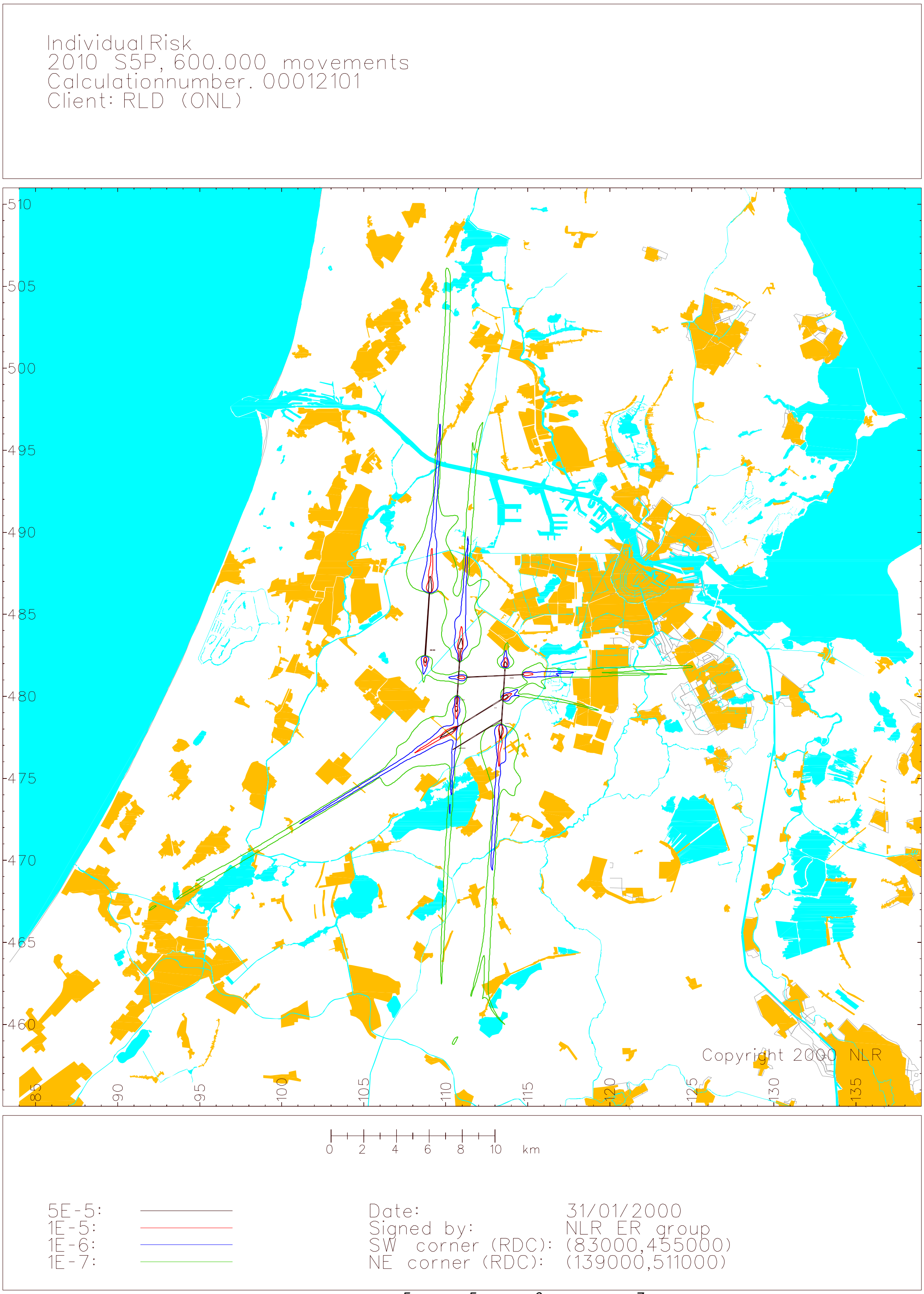

Figure 7-2a: Individual risk contours, $5{\cdot}10^{-5}$, $1{\cdot}10^{-5}$, $1{\cdot}10^{-6}$ and $1{\cdot}10^{-7}$, of the S5P-2010 scenario.

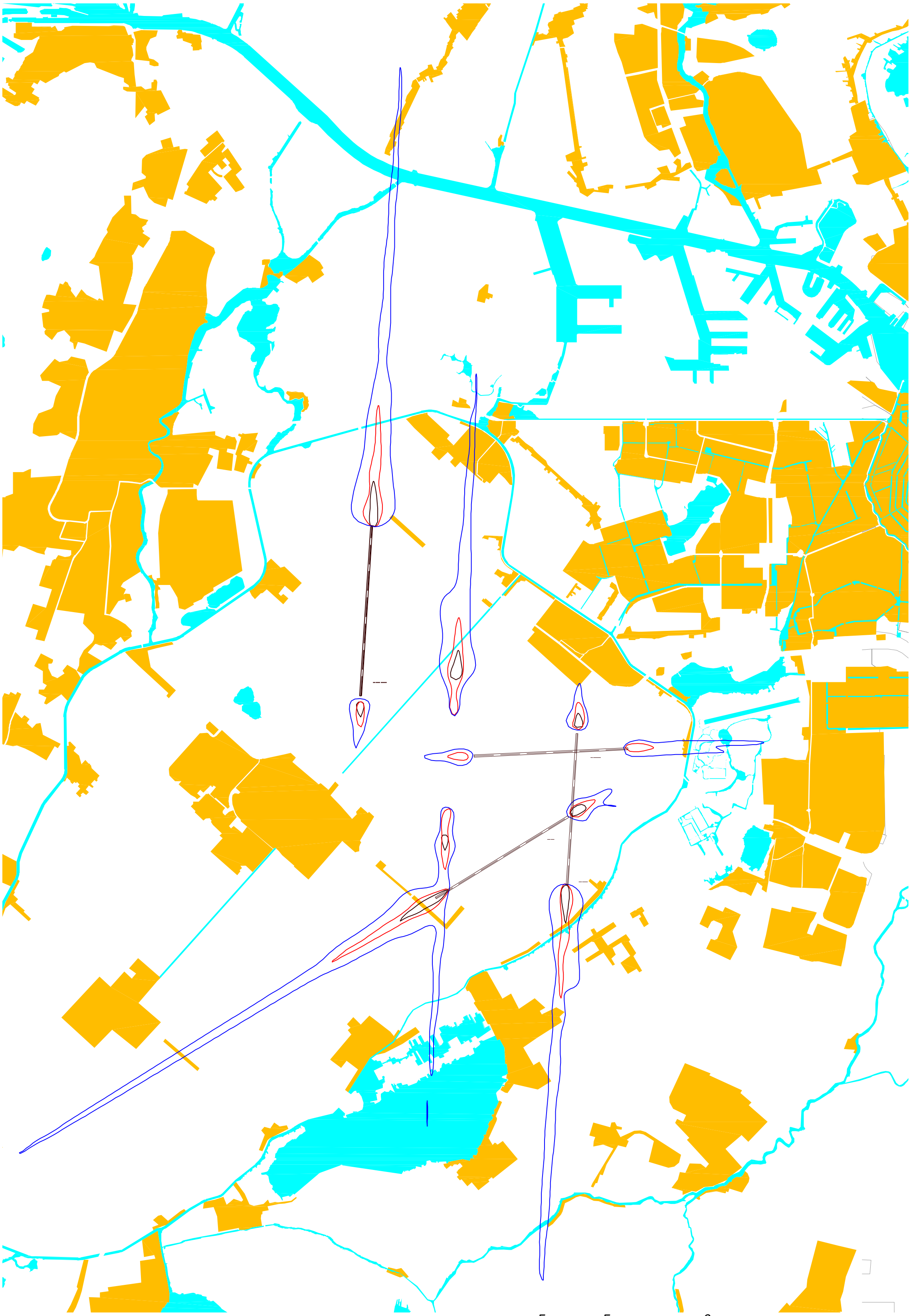

Figure 7-2b: Zoom in of the individual risk contours, $5{\cdot}10^{-5}$, $1{\cdot}10^{-5}$ and $1{\cdot}10^{-6}$, of the S5P-2010 scenario.

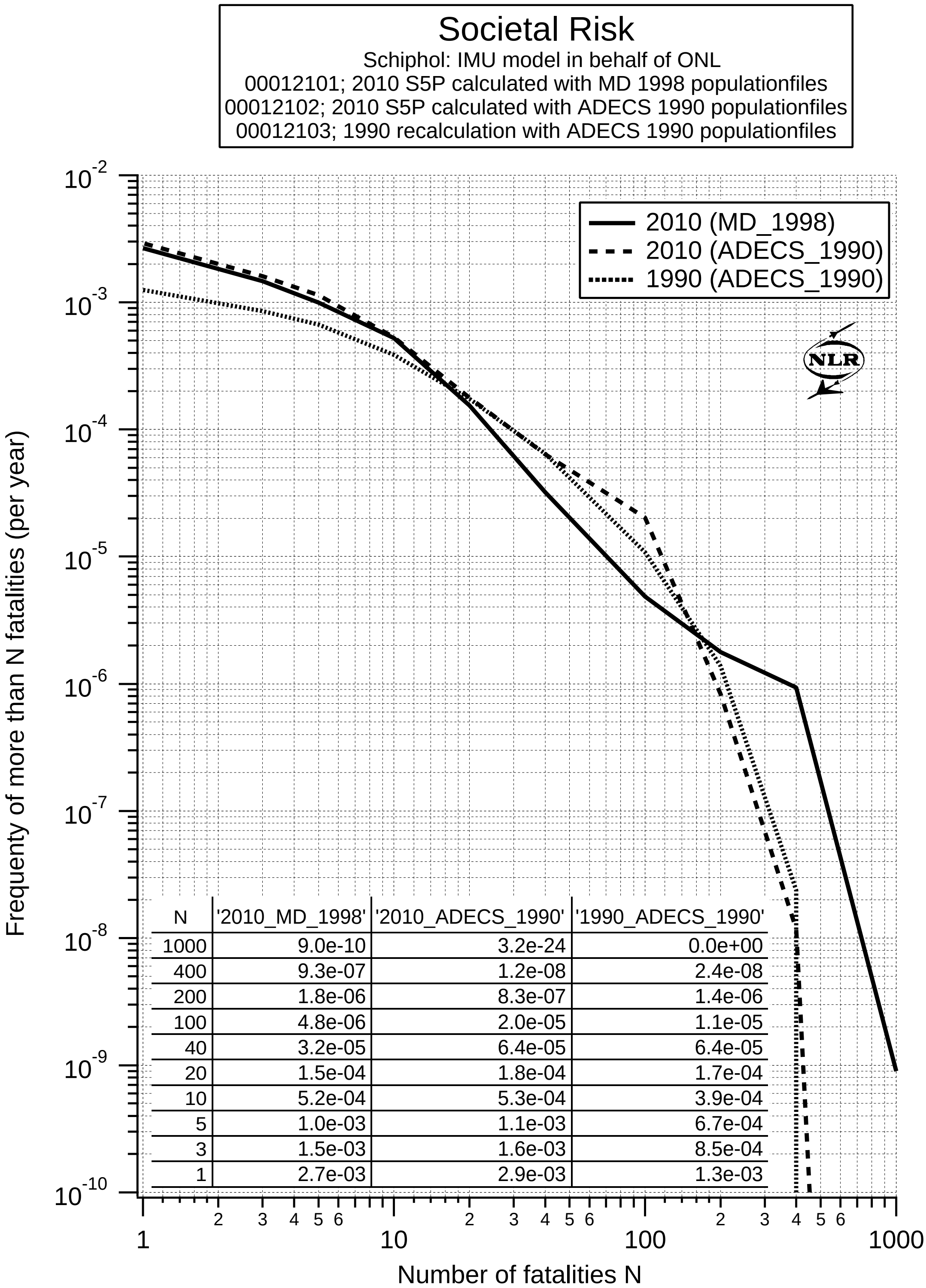

N	'2010_MD_1998'	'2010_ADECS_1990'	'1990_ADECS_1990'
1000	9.0e-10	3.2e-24	0.0e+00
400	9.3e-07	1.2e-08	2.4e-08
200	1.8e-06	8.3e-07	1.4e-06
100	4.8e-06	2.0e-05	1.1e-05
40	3.2e-05	6.4e-05	6.4e-05
20	1.5e-04	1.8e-04	1.7e-04
10	5.2e-04	5.3e-04	3.9e-04
5	1.0e-03	1.1e-03	6.7e-04
3	1.5e-03	1.6e-03	8.5e-04
1	2.7e-03	2.9e-03	1.3e-03

Figure 7-3: Societal risk for the years 1990 and 2010, using ADECS 1990 and MD 1998 population distribution files.

8 Verification and validation

Verification of the input and validation of the results of the external risk calculations as mentioned in chapter 7 have been carried out.

8.1 Verification of input

The input of the external risk calculations for the 1990 and 2010 scenarios have been checked to exclude faults as much as possible. The following checks are performed on the input data of the three risk calculations:

1. The aircraft movements, *i.e*. day, night, total, take-offs and landings, were double-checked;
2. The determination of percentages of aircraft generations in the fleet were double-checked;
3. The determination of the average MTOW of the fleet and the according consequence area and the lethality value were double-checked;
4. It has been checked in the population density files MD 1998 (day and night) if the population within the airport perimeter has been removed according to the five-runway lay-out of the airport in 2010 (S5P). The adjusted population density files MD 1998 have been compared to the source files to ensure that no population outside the five-runway airport perimeter has been removed. Furthermore, it was checked that the population density files for the 1990 risk calculations contained no population within the four-runway airport perimeter;
5. Buildings within the five-runway airport perimeter were eliminated in the building density file MD 1998, according to the perimeter of the airport in 2010 (S5P). The adjusted building density file is compared to the source file to ensure that no buildings were removed outside the five-runway airport perimeter. The house counts within the 1990 contours could not be checked, because they were carried out by ADECS;
6. The routes have been checked visually and correspond with the nominal routes as presented in appendix E. Three routes suffer a minor deficiency, which has a negligible influence on the risk: the last part of the route misses, causing the route to end within the study area. This is the case for landing route 19R W (scenario 2010 S5P), landing route 06 541 and landing route 27 641 (both scenario 1990 S4S1);
7. The probability density of each route, as well as the value of the integral of the probability density of each route has been checked;
8. The scripts have been checked on references to input files and calculation tools;
9. The summed weighted risk and house counts have been recalculated. Also it was checked whether the correct building file was used in the calculation;
10. The determination of the accident rates as well as the fact that the correct accident rates were used as input in the calculations have been checked.

No anomalies were found in the input.

8.2 Validation of risk

8.2.1 Visual inspection

A visual inspection of the calculated individual risk contours showed that the location and the shape of the contours are consistent with both the runway layout and the route structure: the (displaced) runway thresholds coincide with the ‘beginning’ of the contours; each branch in the contour can be accounted for by a specific (set of) route(s); and the area within each of the contours at a runway-end can roughly be related to the number of movements made over that runway-end.

The societal risk curve for 2010 calculated with the MD1998 population density files contains a peak at N=400. This peak is caused by a single position in the population density file of the day period. According to this population density file, 2773 people work at the flower auction in Aalsmeer. At night, only 4 persons are present at this location.

The societal risk curve for 2010 calculated with the ADECS 1990 population density files also contains a peak, although smaller and located at N=100. This peak might be caused by a concentration of population of 616 persons during the day (0 during the night) at position (475350, 113250) and 449 persons during the day (78 during the night) at position (475150, 112850). Both positions are close to the flower auction in Aalsmeer.

In order to understand the influence of individual population concentrations on the societal risk values, the contributions per square kilometre to three societal risk values are depicted in figure 8-1. The figure shows that only a small part of the study area actually contribute to societal risk. Moreover, it was found that a small set of contributing locations account for most of the risk value. For N=1, approximately 10% of the locations constitute 90% of the total risk value. The proportions are even more profound for higher values of N, *e.g.* N=100, where a single location can have a large influence on the actual societal risk value.

With a homogenous population density, one can expect an increasing decline of societal risk values with increasing values of N. A smooth FN-curve may still result in cases where the population density is not homogenous. However, when a concentration of population is combined with a high impact probability, the contribution of a single location can become disproportionately significant. This is the case with the flower auction near "Aalsmeer" and also with the student housing complex "Uilenstede" in Amstelveen. Both locations are densely populated and are located close to an air traffic route.

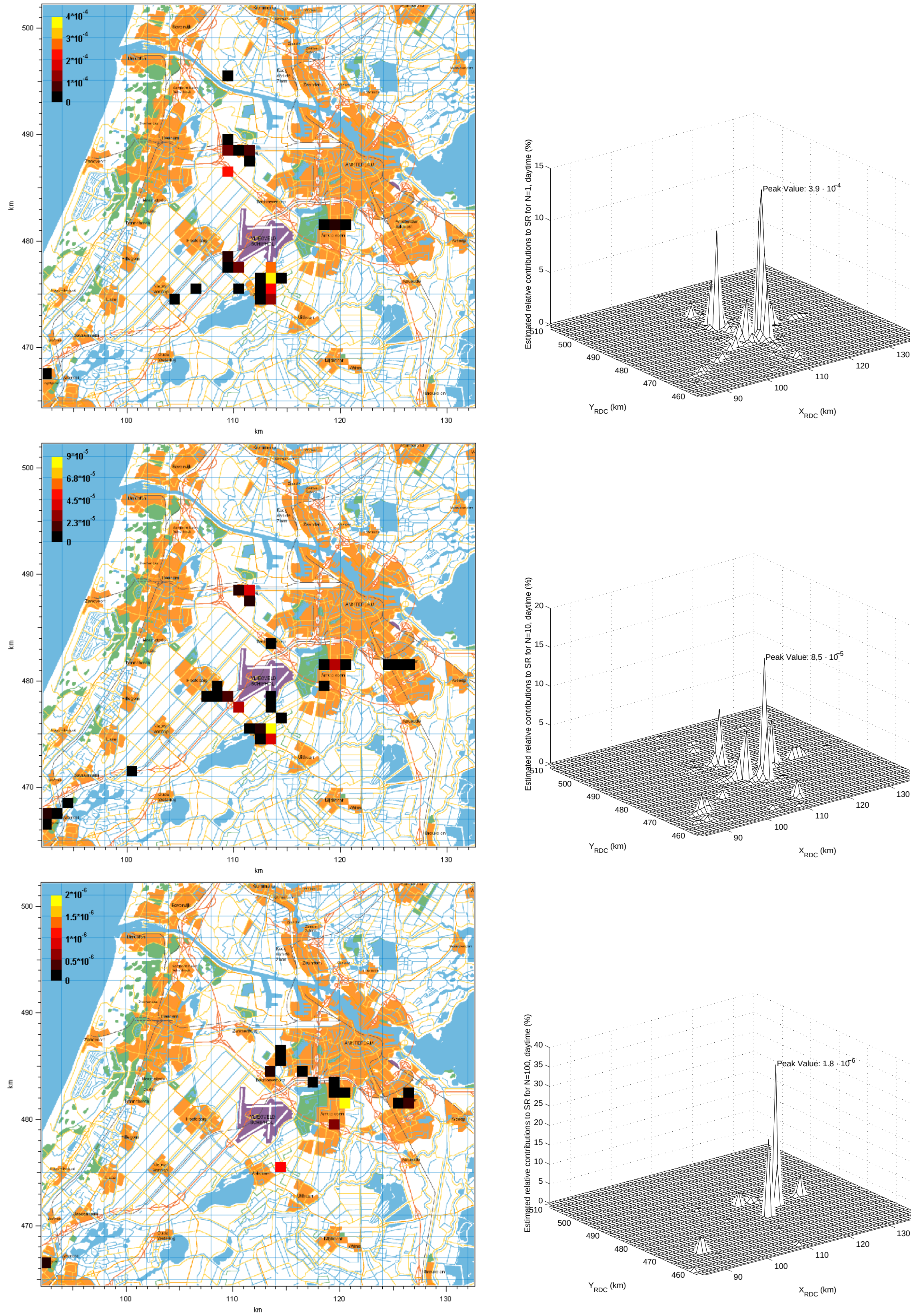

Figure 8-1: Contribution of the societal risk value to individual locations (in square kilometres) for N=1, N=10 and N=100.

8.2.2 Total risk volume

A further check is made by integrating the individual risk over the study area. It can be shown that the result should theoretically be close to the number of movements times the accident rate times the dimension of the crash area times the lethality. The values are presented in table 8-1.

Table 8-1: Volume of individual risk over the study area; theoretical and calculated values

	S5P 2010 (00012101)	**S4S1 1990 (00012103)**
Number of take-offs	300211	103577
Number of landings	300286	103433
Accident rate for take-offs	$0.108 \cdot 10^{-6}$	$0.180 \cdot 10^{-6}$
Accident rate for landing	$0.187 \cdot 10^{-6}$	$0.359 \cdot 10^{-6}$
MTOW	100.8	88.0
Dimension of crash area	8366	7304
Lethality	0.278	0.278
Theoretical integral	**206**	**113**
Calculated integral	**195**	**109**
Relative difference	-5.5 %	-3.8 %

8.2.3 Expectation of number of third party victims

The area underneath the Societal Risk curve, can be interpreted as the expectation of the number of third party fatalities per year. This value cannot be determined exactly, as the societal risk is calculated only for a limited number of values of N. An upper and lower limit of the expectation can be calculated as the area under the ‘barred curves’ as shown in figure 8-2. In order to calculate the maximum expectation, the societal risk value at N=0 ($F_{N=0}$) needs to be estimated and a maximum to the possible number of fatalities must be chosen.

Societal Risk value at N=0

The probability of one or more fatalities given a crash is complementary to the probability of no fatalities. The latter is for each grid cell equal to

$$(1 - \text{lethality factor})^{\text{residing population}}$$

where ‘residing population’ is the number of people in the crash area. The size of a crash area is in rough order of magnitude equal to the size of a grid cell (1 hectare) and the population in the grid cell is therefore considered to be in the crash area (given a crash in the grid cell).

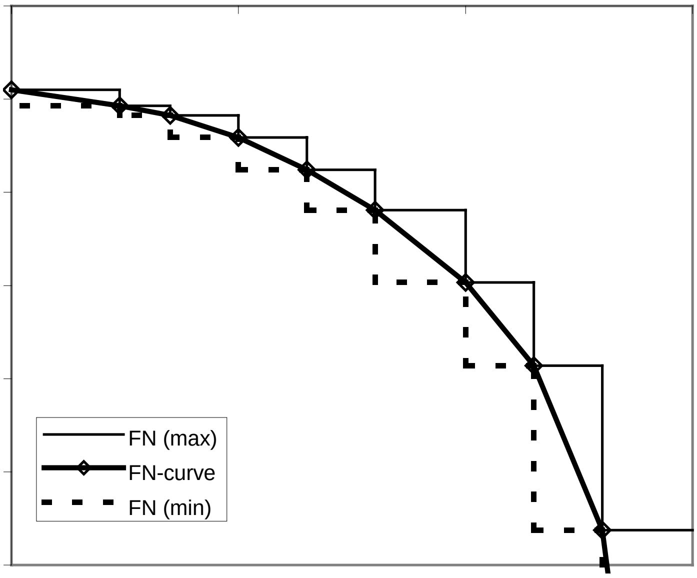

Figure 8-2: Maximum and minimum area underneath the FN-curve

The societal risk value at N=0, $F_{N=0}$, can thus be estimated using:

$$F_{N=0} = 1 - (1 - \text{lethality factor})^{\text{population in grid cell}}$$

Since different population densities are available (daytime and nighttime), the largest estimates for $F_{N=0}$ have been used. Table 8-2 gives the estimated values of $F_{N=0}$.

Table 8-2: Estimated societal risk values for N=0.

Scenario	$F_{N=0}$
S5P 2010, MD 1998, 00012101	4.06E-03
S5P 2010, ADECS 1990, 00012102	4.68E-03
S4S1 1990, ADECS 1990, 00012103	2.08E-03

Maximum number of fatalities

The upper limit to the number of fatalities has been taken to be 9999, being the largest possible input value to the calculation software. It is considered a reasonable assumption that the probability of 10000 or more third party fatalities in one aircraft accident equals zero.

Given the estimated societal risk values at N=0 and the maximum number of fatalities, the minimum and maximum expectations can be calculated as listed in table 8-3.

Table 8-3: Maximum and minimum expectation of third party fatalities per year

	Expectation	
Scenario	maximum	Minimum
S5P 2010, MD 1998, 00012101	2.9E-02	1.3E-02
S5P 2010, ADECS 1990, 00012102	3.4E-02	1.5E-02
S4S1 1990, ADECS 1990, 00012103	2.2E-02	1.0E-02

8.3 Upper limits

An upper limit of individual risk is calculated from the upper limits for the accident rates, for the crash area dimensions and for lethality. All other values are equivalent to the input described in chapter 6.

The upper limits for the accident rates are taken from the 95% confidence limits as given in table 2-2. The upper limit for the crash area dimensions are read from the confidence lines in figure 4-1. This resulted in 99 m^2 per ton. The value used for lethality is the upper bound derived from the ADREP database. The values of the input parameters that were changed compared to chapter 6 are given in the following table.

Table 8-4: Upper limit of adapted input parameters for the S4S1-1990 and the S5P-2010 scenarios.

	S4S1-1990 (00022902)	**S5P-2010 (00022901 & 00022903)**
take-off overrun	$0.346 \cdot 10^{-6}$	$0.224 \cdot 10^{-6}$
take-off overshoot	$0.195 \cdot 10^{-6}$	$0.117 \cdot 10^{-6}$
landing overrun	$0.369 \cdot 10^{-6}$	$0.226 \cdot 10^{-6}$
landing undershoot	$0.481 \cdot 10^{-6}$	$0.318 \cdot 10^{-6}$
Lethality	0.612	0.612
CA radius [m]	52.66	56.36

The results of the upper limit calculations are presented in figure 8-3, figure 8-4 and figure 8-5. The calculated maximum societal risk values are given in the following table.

Table 8-5: Upper limit values of societal risk for the S4S1-1990 scenario and for the S5P-2010 scenarios; between brackets are the values as given in figure 7-3.

N	**2010 MD 1998**		**2010 ADECS 1990**		**1990 ADECS 1990**	
1000	$1.0 \cdot 10^{-6}$	$(< 1.0 \cdot 10^{-10})$	$1.6 \cdot 10^{-8}$	$(< 1.0 \cdot 10^{-10})$	$3.6 \cdot 10^{-8}$	$(< 1.0 \cdot 10^{-10})$
400	$4.3 \cdot 10^{-6}$	$(9.3 \cdot 10^{-7})$	$2.3 \cdot 10^{-6}$	$(1.2 \cdot 10^{-8})$	$3.3 \cdot 10^{-6}$	$(2.4 \cdot 10^{-8})$
200	$9.4 \cdot 10^{-6}$	$(1.8 \cdot 10^{-6})$	$3.6 \cdot 10^{-5}$	$(8.3 \cdot 10^{-7})$	$2.1 \cdot 10^{-5}$	$(1.4 \cdot 10^{-6})$
100	$4.3 \cdot 10^{-5}$	$(4.8 \cdot 10^{-6})$	$9.1 \cdot 10^{-5}$	$(2.0 \cdot 10^{-5})$	$8.3 \cdot 10^{-5}$	$(1.1 \cdot 10^{-5})$
40	$3.4 \cdot 10^{-4}$	$(3.2 \cdot 10^{-5})$	$3.9 \cdot 10^{-4}$	$(6.4 \cdot 10^{-5})$	$3.0 \cdot 10^{-4}$	$(6.4 \cdot 10^{-5})$
20	$9.4 \cdot 10^{-4}$	$(1.5 \cdot 10^{-4})$	$1.0 \cdot 10^{-3}$	$(1.8 \cdot 10^{-4})$	$6.2 \cdot 10^{-4}$	$(1.7 \cdot 10^{-4})$
10	$1.7 \cdot 10^{-3}$	$(5.2 \cdot 10^{-4})$	$2.0 \cdot 10^{-3}$	$(5.3 \cdot 10^{-4})$	$1.0 \cdot 10^{-3}$	$(3.9 \cdot 10^{-4})$
5	$2.7 \cdot 10^{-3}$	$(1.0 \cdot 10^{-3})$	$2.8 \cdot 10^{-3}$	$(1.1 \cdot 10^{-3})$	$1.2 \cdot 10^{-3}$	$(6.7 \cdot 10^{-4})$
3	$3.5 \cdot 10^{-3}$	$(1.5 \cdot 10^{-3})$	$3.8 \cdot 10^{-3}$	$(1.6 \cdot 10^{-3})$	$1.5 \cdot 10^{-3}$	$(8.5 \cdot 10^{-4})$
1	$5.6 \cdot 10^{-3}$	$(2.7 \cdot 10^{-3})$	$6.3 \cdot 10^{-3}$	$(2.9 \cdot 10^{-3})$	$2.3 \cdot 10^{-3}$	$(1.3 \cdot 10^{-3})$

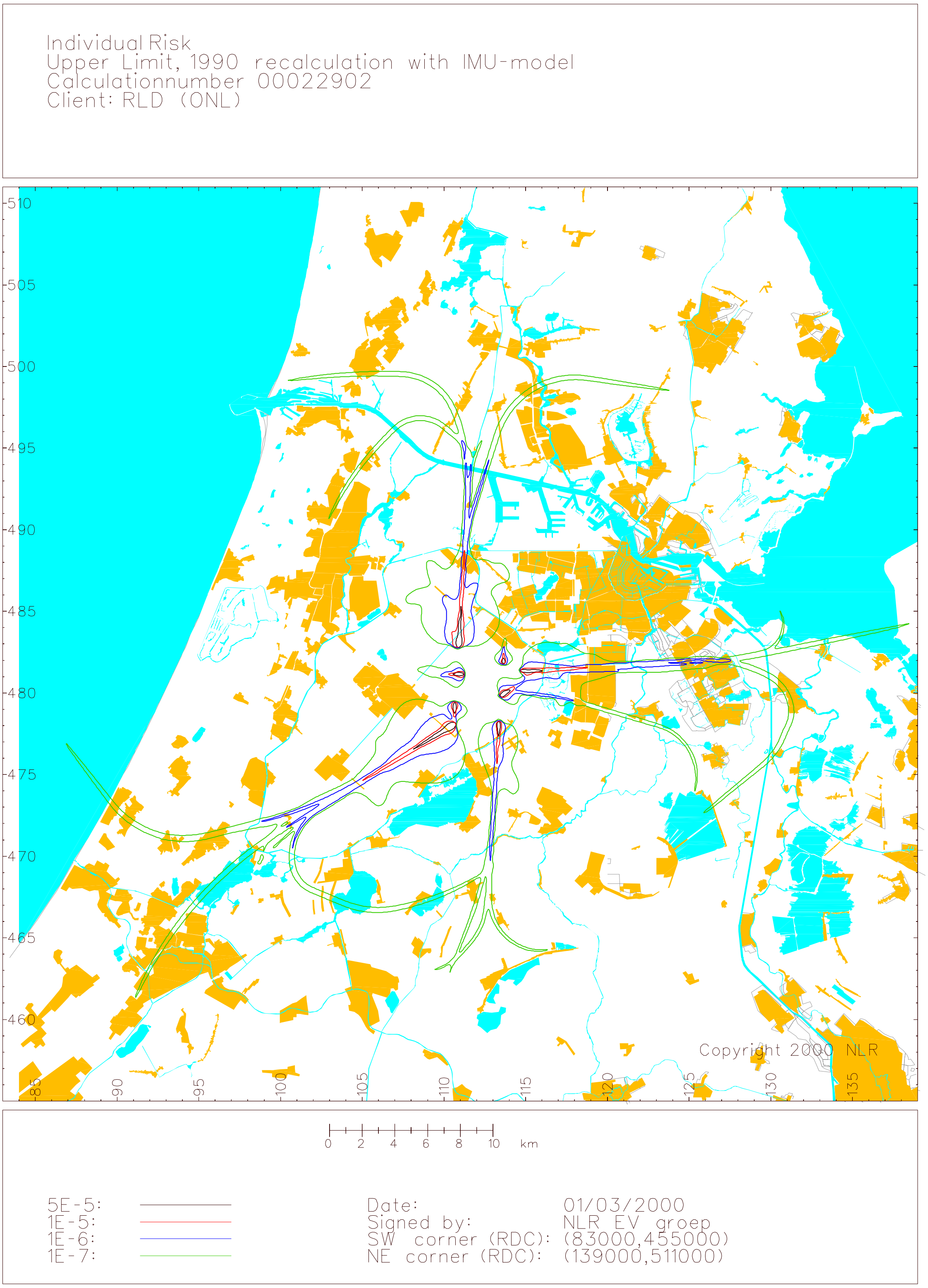

Figure 8-3: Upper limit of individual risk for the S4S1-1990 scenario.

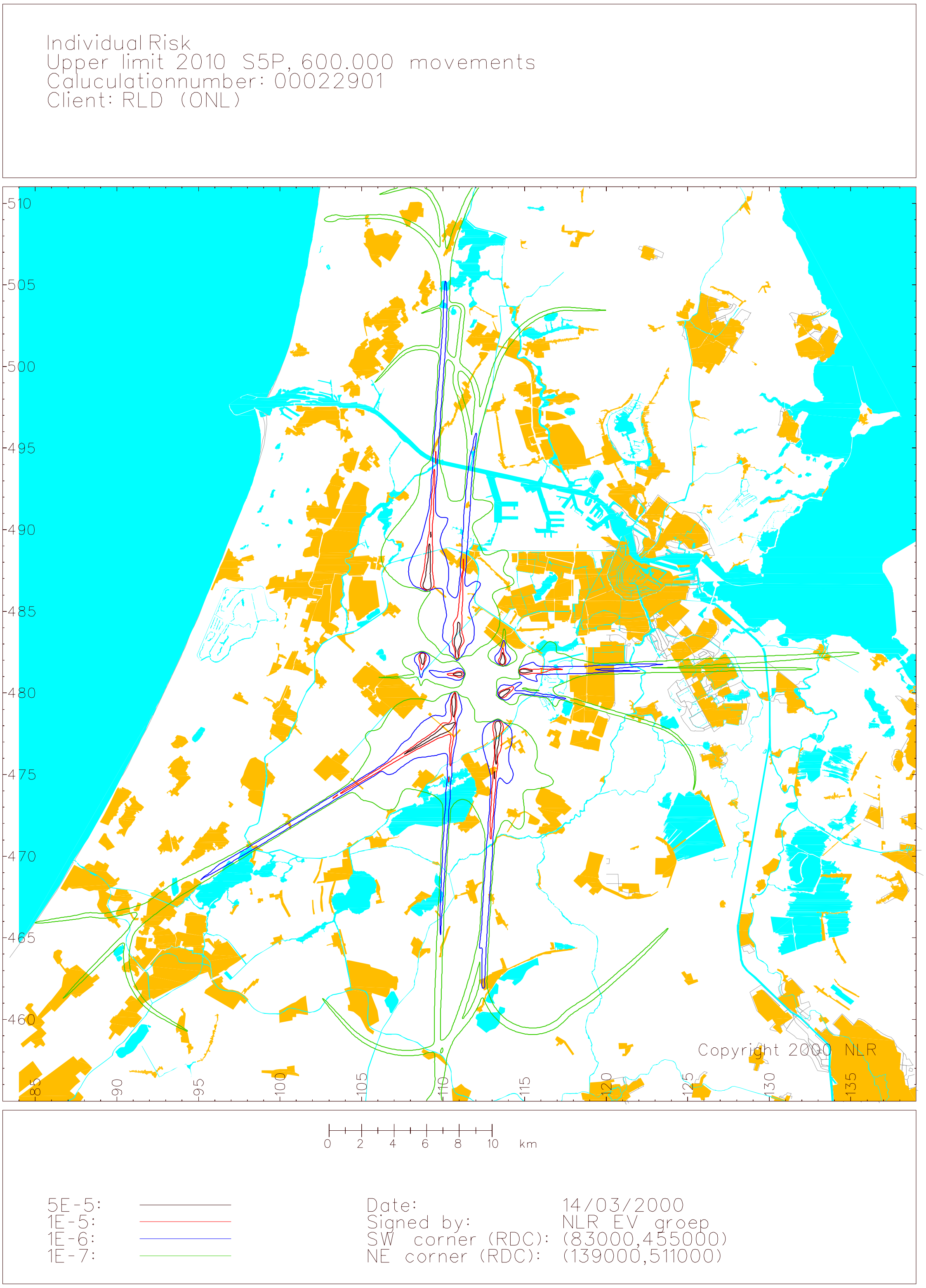

Figure 8-4: Upper limit of individual risk for the S5P-2010 scenario.

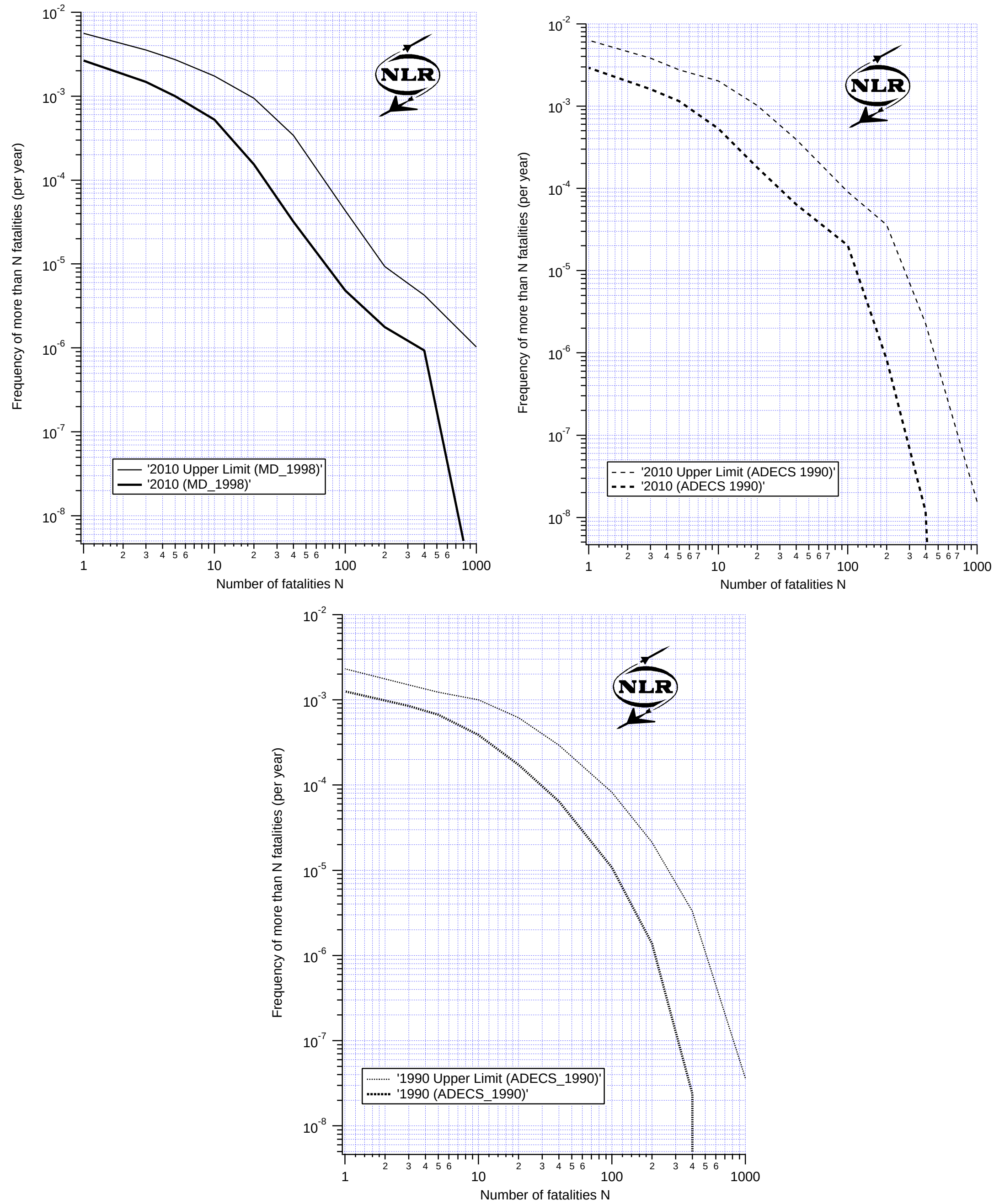

Figure 8-5: Estimates and upper limits of societal risk for:
(top left) the S5P-2010 scenario evaluated with the MD 1998 population density file,
(top right) the S5P-2010 scenario evaluated with the ADECS 1990 population density file, and (bottom) the S4S1-1990 scenario evaluated with the ADECS 1990 population density file.

9 Concluding remarks

This report presents a revision of the method for calculating third party risk around airports. Calculations with the revised model have been performed for two scenarios: one representing Schiphol in 1990 for reference, and one predicting risk around Schiphol in 2010. The results supported the government in its decision of 17 December 1999 that Schiphol can grow within limits on its current location.

The three models (aircraft accident model, accident location model and consequence model) that constitute the method are discussed separately.

New accident ratios are derived for three aircraft generations and for six flight phases (take-off veer-off, take-off overrun, take-off overshoot, landing undershoot, landing overrun and landing veer-off). The ratios are lower than determined in the original model, which was foreseen in a study for TNLI ([2]). The reduction is nevertheless more than expected in that study: the new ratio for 1990 is less than 50% of the former value for 1990 (a reduction of 15% was estimated); the new value for 1997 is only 30% of the former 1990 ratio (a reduction of 70% where 50% was estimated).

A number of changes are applied to the accident location model. Separate distributions are determined for four of the six flight phases mentioned before. Distribution for veer-offs are not yet determined. The distributions for overshoot and undershoot are modelled as being partially route independent, whereas in the former model these distributions were entirely route dependent. The route dependent distributions in the revised model are derived from data on the distribution of operational traffic.

The dimensions of the consequence areas are determined again based on more accurate data. This has resulted in crash areas that are 45 to 65% smaller than in the former model. The terrain type does not appear to contribute much to the size of the consequence area. The dimension of the consequence areas are therefore taken independent of the terrain type. Lethality is determined to be about 7% less than in the former model.

Calculations made with the improved model show that individual risk levels and societal risk values are considerably lower than predicted with the original model.

10 References

[1] M.A. Piers, M.P. Loog, M.K.H. Giesberts, G. Moek, M.J.H. Couwenberg and M.C.J. Smeets;
The Development of a Method for the Analysis of Societal and Individual Risk due to Aircraft Accidents in the Vicinity of Airports;
NLR CR 93372 L, Amsterdam, 1993.

[2] C.J.M. de Jong, B. van Deenen, A.J. Pikaar, M.A. Piers, G.W.H. van Es and M.P. Loog;
Verwachting ten aanzien van de ontwikkeling van de externe veiligheid rond de TNLI locaties tussen 1990 en 2020;
NLR-CR-98491, herziene versie, Amsterdam, March 1999.

[3] J.H. Enders, R. Dodd, R. Tarrel, R. Khatwa, A.L.C. Roelen and A.K. Karwal;
Airport Safety: A Study of Accidents and Available Approach-and-landing Aids;
Flight Safety Digest, Vol. 15 No. 3, March 1996.

[4] Anon.;
Manual on the use of the collision risk model (CRM) for ILS operations;
ICAO, Doc 9274-AN/904, first edition 1980.

This page intentionally left blank

Appendix A Aircraft generation

This appendix lists the aircraft in three generations. There are no quantitative criteria to classify aircraft into one of the three generations. It is, however, possible to describe the rules of thumb that were considered. The rules in this report are also used by for instance Boeing and Airbus.

First generation

These aircraft were typically designed in the fifties, when there was limited knowledge of for example fatigue of metal constructions. The certification was often before 1965, based on old British Civil Airworthiness Requirements (BCAR) or other certification bases. The engines applied on the jets were first production versions. Furthermore, the aircraft had very limited cockpit automation, simple navigational aids, and no or limited approach equipment. Examples of this generation are the Fokker 27 and the Boeing 707.

Second generation

Designed in the sixties and seventies, these aircraft had better and more reliable engines. Certification was between 1965 and 1980, not yet based on common JAR25/FAR25 rules. The cockpit was better and more reliably equipped, for instance with better auto pilots, auto throttles, flight directors, and better navigational aids. Electronic Flight Instrument Systems (EFIS) were not yet used. Examples of second generation aircraft are the Fokker 28, the Boeing 737-200 and the Airbus A300.

Third generation

The aircraft design of the eighties and nineties typically showed consideration for the human factors in the cockpit. The cockpits contain EFIS, and improved auto pilots. Furthermore, the aircraft is equipped with modern high-by-pass engines (which require higher certification standards), and aircraft performance monitoring systems. The Fokker 50, Airbus 320 and Boeing 737-700 are examples of this generation aircraft.

Some people refer to fourth generation aircraft as those using fly-by-wire systems. These systems essentially reduce the weight of the aircraft. The flight envelope is protected by software which is sometimes seen as an improvement in safety. However, a mechanical protection of the flight envelope can also be found in non-fly-by-wire aircraft. Statistics show that there is yet no significant difference in relative safety between fly-by-wire and non-fly-by-wire third generation aircraft. Therefore, fly-by-wire aircraft are considered third generation.

Every aircraft can be equipped with systems such as TCAS, GWPS, EGWPS and GPS/NAV. The presence of these systems have no influence on the division into generations.

Table A-1: List of aircraft generations.

Aircraft type	Generation
Aerospatiale N262/Mohawk 298	1
Aerospatiale SE-210 Caravelle 10/11/12	1
Aerospatiale SE-210 Caravelle 10B	1
Aerospatiale SE-210 Caravelle 10R	1
Aerospatiale SE-210 Caravelle 3	1
Aerospatiale SE-210 Caravelle 6N/6R	1
Aerospatiale SE-210 Carvelle 12	1
Aerospatiale SE-219 Caravelle 11R	1
Aerospatiale SN601 Corvette	1
Antonov An-12	1
Antonov An-22	1
Antonov An-24	1
Antonov An-26	1
Beechcraft King Air 200	1
Belfast-Short	1
Boeing 377 Stratocruiser Freighter	1
Boeing 707 Freighter	1
Boeing 707 Mixed configuration	1
Boeing 707-120	1
Boeing 707-220	1
Boeing 707-320	1
Boeing 707-320 Freighter	1
Boeing 707-320 Mixed configuration	1
Boeing 707-320C Mixed configuration	1
Boeing 707-420	1
Boeing 720	1
Boeing 720B	1
Boeing 720H	1
Bristol Britannia	1
Bristol Britannia Freighter	1
Convair 240	1
Convair 340	1
Convair 440	1
Convair 580	1
Convair 600	1
Convair 600/640	1
Convair 880	1

Aircraft type	Generation
Convair 990	1
Curtiss C-46 Commando	1
Dassault Falcon 20	1
Dassault Mercure	1
De Havilland Canada DHC-4 Caribou	1
De Havilland Comet 4	1
De Havilland Heron	1
Douglas DC-3	1
Douglas DC-3 Freighter	1
Douglas DC-3 Mixed configuration	1
Douglas DC-4	1
Douglas DC-6	1
Douglas DC-6A Freighter	1
Douglas DC-6B	1
Fairchild FH-227	1
Fairchild Metro	1
Fokker/Fairchild F-27-100	1
Fokker/Fairchild F-27-200	1
Fokker/Fairchild F-27-500	1
Fokker/Fairchild F-27-600	1
Grumman AA-5 Tiger	1
Grumman G-111 Albatross	1
Gulfstream 1/1-C	1
Gulfstream 1/2/2B	1
Handley Page Herald	1
Handley Page Jetstream	1
Hawker Siddeley Argosy Freighter	1
Hawker Siddeley Argosy Mixed configuration	1
Hawker Siddeley HS748	1
HFB-320 Hansa Jet	1
IAI 1124 Westwind	1
IAI 1124 Westwind Freighter	1
IAI Arava	1
Ilysuhin Il-14	1
Ilyushin Il-18	1
Ilyushin Il-62	1
Lockheed L-100 Hercules	1
Lockheed L-1049 Super Constellation	1

Aircraft type	Generation
Lockheed L-188 Electra	1
Lockheed L-188 Electra Freighter	1
Lockheed L-188 Electra Mixed configuration	1
Lockheed L-749 Constellation	1
McDonnell Douglas DC-8 Freighter	1
McDonnell Douglas DC-8 Mixed configuration	1
McDonnell Douglas DC-8-30	1
McDonnell Douglas DC-8-50	1
McDonnell Douglas DC-8-50/61/62/63 Freighter	1
McDonnell Douglas DC-8-60/70	1
McDonnell Douglas DC-8-61/61CF/71/71CF	1
McDonnell Douglas DC-8-62/62CF/72/72CF	1
McDonnell Douglas DC-8-62AF/62CF Freighter	1
McDonnell Douglas DC-8-62CF Mixed configuration	1
McDonnell Douglas DC-8-63/63CF/73/73CF	1
McDonnell Douglas DC-8-63AF/63CF/73AF/73CF Freighter	1
McDonnell Douglas DC-8-63CF/73CF Mixed configuration	1
McDonnell Douglas DC-8-71/72/73 Freighter	1
Merchantman	1
Mooney M20A	1
Mystere 10/2	1
NAMC YS-11	1
Sabreliner	1
Shorts 330	1
Shorts 360	1
Shorts Skyliner	1
Shorts Skyvan	1
Super Guppy	1
Tupolev Tu-104	1
Tupolev Tu-114	1
Tupolev Tu-124	1
Tupolev Tu-144	1
Vickers Vanguard	1
Vickers Vanguard Freighter	1
Vickers Viscount 700	1

Aircraft type	Generation
Vickers Viscount 800	1
Xian Yun-7	1
Yakovlev Yak-40	1
Aerospatiale/British Aerospace Concorde	2
Airbus Industrie A300	2
Airbus Industrie A300 Freighter	2
Airbus Industrie A300B2	2
Airbus Industrie A300B4	2
Airbus Industrie A300C4 Mixed configuration	2
Antonov An-26/32	2
BAC One Eleven 200	2
BAC One Eleven 300	2
BAC One Eleven 400	2
BAC One Eleven 500	2
Beechcraft 1900/C	2
Beechcraft 1900D	2
Beechcraft B200 Super King Air	2
Boeing 727 Freighter	2
Boeing 727 Mixed configuration	2
Boeing 727-100	2
Boeing 727-100C Mixed configuration	2
Boeing 727-100C/100QC Mixed configuration	2
Boeing 727-100QC/100F Freighter	2
Boeing 727-200	2
Boeing 727-200 Advanced	2
Boeing 737-100	2
Boeing 737-200	2
Boeing 737-200 Advanced	2
Boeing 737-200C Mixed configuration	2
Boeing 737-200C/QC Freighter	2
Boeing 737-200C/QC Mixed configuration	2
Boeing 747-100	2
Boeing 747-100F/200C/F Freighter	2
Boeing 747-200	2
Boeing 747-200B	2
Boeing 747-200B/C Mixed configuration	2

Aircraft type	Generation
Boeing 747-200C Mixed configuration	2
Boeing 747-300	2
Boeing 747-300 Mixed configuration	2
Boeing 747SP	2
Boeing 747SR	2
British Aerospace Jetstream 31	2
British Aerospace Jetstream 31 Freighter	2
Canadair CL-44	2
Casa/IPTN CN-235	2
Casa/IPTN NC-212	2
De Havilland Canada DHC-6 Twin Otter	2
De Havilland Canada DHC-7	2
De havilland Canada DHC-7 Freighter	2
De Havilland Canada DHC-7 Mixed configuration	2
Dornier 228-100	2
Dornier 228-200	2
Embraer EMB-110 Bandeirante	2
Embraer EMB-120 Brasilia	2
Fokker F-28-1000	2
Fokker F-28-2000	2
Fokker F-28-3000	2
Fokker F-28-4000	2
Fokker F-28-6000	2
Gulfstream III	2
Hawker Siddeley HS121 Trident 1/1C	2
Hawker Siddeley HS121 Trident 1E	2
Hawker Siddeley HS121 Trident 2E	2
Hawker Siddeley HS121 Trident 3/3B/Super 3B	2
Ilyushin Il-76	2
Ilyushin Il-86	2
Ilyushin Il-96	2
Learjet 35/36	2
Let 410 Turbolet	2
Lockheed L-1011 TriStar 1	2
Lockheed L-1011 TriStar 100	2
Lockheed L-1011 TriStar 200	2

Aircraft type	Generation
Lockheed L-1011 TriStar 500	2
Lockheed L-1011 TriStar Freighter	2
McDonnell Douglas DC-10	2
McDonnell Douglas DC-10 Freighter	2
McDonnell Douglas DC-10 Mixed configuration	2
McDonnell Douglas DC-10/15	2
McDonnell Douglas DC-10-30	2
McDonnell Douglas DC-10-40	2
McDonnell Douglas DC-10CF Freighter	2
McDonnell Douglas DC-9 Freighter	2
McDonnell Douglas DC-9-10	2
McDonnell Douglas DC-9-10F/10CF Freighter	2
McDonnell Douglas DC-9-20	2
McDonnell Douglas DC-9-30	2
McDonnell Douglas DC-9-30/40/50	2
McDonnell Douglas DC-9-30F/30CF Freighter	2
McDonnell Douglas DC-9-40	2
McDonnell Douglas DC-9-50	2
Tupolev Tu-134	2
Tupolev Tu-154	2
VFW-614	2
Vickers Super VC-10	2
Vickers VC-10	2
Yakovlev Yak-42	2
Airbus Industrie A300-600	3
Airbus Industrie A310 Freighter	3
Airbus Industrie A310-200	3
Airbus Industrie A310-300	3
Airbus Industrie A319	3
Airbus Industrie A319/A320/A321	3
Airbus Industrie A320	3
Airbus Industrie A320-200	3
Airbus Industrie A321	3
Airbus Industrie A330	3
Airbus Industrie A330-300	3
Airbus Industrie A340-200	3
Airbus Industrie A340-300	3

Aircraft type	Generation
Antonov An-124	3
ATR-42	3
ATR-72	3
Avro International RJ100	3
Avro International RJ70	3
Avro International RJ85	3
Boeing 737-300	3
Boeing 737-300QC Freighter	3
Boeing 737-400	3
Boeing 737-500	3
Boeing 747-400	3
Boeing 747-400 Freighter	3
Boeing 747-400 Mixed configuration	3
Boeing 757-200	3
Boeing 757-200 Freighter	3
Boeing 767 Freighter	3
Boeing 767-100	3
Boeing 767-200	3
Boeing 767-300	3
Boeing 777	3
Boeing 777-200	3
British Aerospace 146-100	3
British Aerospace 146-200	3
British Aerospace 146-200 Freighter	3

Aircraft type	Generation
British Aerospace 146-300	3
British Aerospace ATP	3
British Aerospace Jetstream 41	3
Canadair Regional Jet	3
De Havilland Canada DHC-8-100	3
De Havilland Canada DHC-8-300	3
Dornier 328	3
Embraer RJ-145	3
Fokker 100	3
Fokker 50	3
Fokker 70	3
McDonnell Douglas MD-11	3
McDonnell Douglas MD-11 Freighter	3
McDonnell Douglas MD-11 Mixed configuration	3
McDonnell Douglas MD-81	3
McDonnell Douglas MD-82	3
McDonnell Douglas MD-83	3
McDonnell Douglas MD-87	3
McDonnell Douglas MD-88	3
McDonnell Douglas MD-90	3
Saab 2000	3
Saab 340	3
Saab 340 Freighter	3

Appendix B Airport list

ICAO Region	Airport	City	Country
Europe	Schwechat	Vienna	Austria
Europe	Brussels National	Brussels	Belgium
Europe	Kastrup	Copenhagen	Denmark
Europe	Orly	Paris	France
Europe	Charles de Gaulle	Paris	France
Europe	Munich	Munich	Germany
Europe	Dusseldorf	Dusseldorf	Germany
Europe	Frankfurt-Rhein	Frankfurt	Germany
Europe	Fiumicino	Rome	Italy
Europe	Schiphol	Amsterdam	Netherlands
Europe	Barajas	Madrid	Spain
Europe	Heathrow	London	UK
Europe	Gatwick	London	UK
North America	Pearson INTL	Toronto	Canada
North America	SKY HARBOR INTL	Phoenix	USA
North America	San Fransisco INTL	San Fransisco	USA, CA
North America	Los Angeles INTL	Los Angeles	USA, CA
North America	Tampa INTL	Tampa	USA, FL
North America	Miami INTL	Miami	USA, FL
North America	Orlando INTL	Orlando	USA, FL
North America	Hartsfield	Atlanta	USA, GA
North America	O’Hara INTL	Chicago	USA, IL
North America	Cincinnati Greater	Cincinnati	USA, KY
North America	Logan INTL	Boston	USA, MA
North America	Baltimore-Washington DC INTL	Baltimore	USA, MD
North America	Wayne County MET	Detroit	USA, MI
North America	Lambert INTL	St Louis	USA, MO
North America	Kansas City INTL	Kansas City	USA, MO
North America	Charlotte Douglas INTL	Charlotte	USA, NC
North America	Newark INTL	Newark	USA, NJ
North America	La Guardia	New York	USA, NY
North America	J.F. Kennedy INTL	New York	USA, NY
North America	Hopkins INTL	Cleveland	USA, OH
North America	Portland INTL	Portland	USA, OR
North America	Philadelphia INTL	Philadelphia	USA, PA
North America	Memphis INTL	Memphis	USA, TN
North America	Houston Intercontinental	Houston	USA, TX
North America	Dallas Fort Worth INTL	Dallas	USA, TX
North America	Dulles INTL	Washington DC	USA, VA
North America	Tacoma INTL	Seattle	USA, WA

Appendix C Aircraft accident list

Date (d-m-y)	19-Jun-80
Source	Airclaims
Aircraft type	Aerospatiale SE-210 Caravelle
Operator name	Airborn Express
Airport, City,	Hartsfield, Atlanta, USA, GA
Flight phase	Landing
Accident type	Veer-off
Narrative	Aircraft landed hard due to turbulence of the wake of another aircraft. Landing gear collapsed and aircraft veer-off the runway.

Date (d-m-y)	25-Jun-80
Source	ALPA
Aircraft type	Boeing 727-100
Operator name	Eastern
Airport, City,	Tampa INTL, Tampa, USA, FL
Flight phase	Landing
Accident type	Undershoot
Narrative	Landed short of the runway.

Date (d-m-y)	16-Dec-80
Source	ICAO
Aircraft type	BAC One Eleven 200
Operator name	-
Airport, City,	Schiphol, Amsterdam, Netherlands
Flight phase	Landing
Accident type	Veer-off
Narrative	The a/c landed normally, spoilers were deployed and reverse thrust selected. The a/c swung to the right and ran over grass, coming to rest in a ploughed field. Cause of the accident not determined.

Date (d-m-y)	13-Sep-81
Source	ALPA
Aircraft type	McDonnell Douglas DC-10
Operator name	AA
Airport, City,	Logan INTL, Boston, USA, MA
Flight phase	Landing
Accident type	Overrun
Narrative	Overran on a wet runway.

Date (d-m-y)	16-Sep-81
Source	ALPA
Aircraft type	McDonnell Douglas DC-9-10
Operator name	Rep.
Airport, City,	Tampa INTL, Tampa, USA, FL
Flight phase	Landing
Accident type	Veer-off
Narrative	Veered off the runway during landing.

Date (d-m-y)	04-Oct-81
Source	ALPA
Aircraft type	Lockheed L-1011 TriStar 1
Operator name	DELTA
Airport, City,	Tampa INTL, Tampa, USA, FL
Flight phase	Landing
Accident type	Overrun
Narrative	Overran runway. Hydroplaning was a factor.

Date (d-m-y)	24-Jan-82
Source	Airclaims
Aircraft type	McDonnell Douglas DC-10-30
Operator name	World Airways
Airport, City,	Logan INTL, Boston, USA, MA
Flight phase	Landing
Accident type	Overrun
Narrative	The aircraft landed on a contaminated runway and could not be stop due to low braking action. The aircraft overran the runway end and went into the Boston Harbor.

Date (d-m-y)	03-Feb-82
Source	ICAO
Aircraft type	McDonnell Douglas DC-10-30
Operator name	United
Airport, City,	Philadelphia INTL, Philadelphia, USA, PA
Flight phase	Take-off
Accident type	Overrun
Narrative	Take-off on a wet runway was aborted. Aircraft could not be stopped and overran the runway end.

Date (d-m-y)	24-Feb-82
Source	ICAO
Aircraft type	Fairchild Metro
Operator name	Midstate
Airport, City,	O'Hara INTL, Chicago, USA, IL
Flight phase	Landing
Accident type	Veer-off
Narrative	During ground roll the aircraft veered off the runway. Cause unknown.

Date (d-m-y)	11-Jan-83
Source	Airclaims
Aircraft type	McDonnell Douglas DC-8-30
Operator name	United Airlines
Airport, City,	Wayne County MET, Detroit, USA, MI
Flight phase	Take-off
Accident type	Overshoot (plof)
Narrative	Aircraft crashed during climb 1000 ft from the threshold. The aircraft stabilizer was mistrimmed.

Date (d-m-y)	20-Jul-83
Source	ICAO
Aircraft type	McDonnell Douglas DC-8-30
Operator name	UNITED
Airport, City,	O'Hara INTL, Chicago, USA, IL
Flight phase	Landing
Accident type	Overrun
Narrative	Aircraft overran runway end.

Date (d-m-y)	11-Oct-83
Source	Airclaims
Aircraft type	Boeing 747-200
Operator name	Flying Tigers
Airport, City,	Frankfurt-Rhein, Frankfurt, Germany
Flight phase	Take-off
Accident type	Veer-off
Narrative	Aircraft went off the runway during take-off roll at about 60 kt. ground speed. A CG shift due to loose cargo caused the loss of control.

Date (d-m-y)	11-Nov-83
Source	Airclaims
Aircraft type	Boeing 727-200
Operator name	Eastern Airlines
Airport, City,	Miami INTL, Miami, USA, FL
Flight phase	Landing
Accident type	Veer-off
Narrative	Aircraft went off the runway after landing with right main gear up.

Date (d-m-y)	27-Nov-83
Source	Airclaims
Aircraft type	Boeing 747-200
Operator name	Avianca
Airport, City,	Barajas, Madrid, Spain
Flight phase	Landing
Accident type	Undershoot
Narrative	PIC intercepted the ILS on an incorrect track. Aircraft struck the ground 10 km from the threshold.

Date (d-m-y)	05-Jan-84
Source	ALPA
Aircraft type	Boeing 727-100
Operator name	ALASKA
Airport, City,	Tacoma INTL, Seattle, USA, WA
Flight phase	Landing
Accident type	Undershoot
Narrative	Undershot runway and hit approach lights.

Date (d-m-y)	28-Mar-84
Source	Airclaims
Aircraft type	McDonnell Douglas DC-10
Operator name	SAS
Airport, City,	J.F. Kennedy INTL, New York, USA, NY
Flight phase	Landing
Accident type	Overrun
Narrative	Aircraft landed long on a wet runway and could not be stopped on the remaining runway. The aircraft overran and ended in the Thurston Basin

Date (d-m-y)	13-Jun-84
Source	Airclaims
Aircraft type	McDonnell Douglas dc-9-30
Operator name	US Airways
Airport, City,	Wayne County MET, Detroit, USA, MI
Flight phase	Landing
Accident type	Veer-off
Narrative	During landing the PIC elected to conduct a missed approach however the aircraft would not climb. Therefore the PIC elected to land the aircraft. The aircraft veered off the runway after skidding for about 3000 ft. on it

Date (d-m-y)	23-Jul-84
Source	ICAO
Aircraft type	Boeing 707-120
Operator name	Tradewinds
Airport, City,	O'Hara INTL, Chicago, USA, IL
Flight phase	Landing
Accident type	Overrun
Narrative	Aircraft landed on a very wet runway and could not be stopped.

Date (d-m-y)	18-Sep-84
Source	Airclaims
Aircraft type	Fairchild Metro
Operator name	Austrian Air Services
Airport, City,	Schwechat, Vienna, Austria
Flight phase	Landing
Accident type	Veer-off
Narrative	Aircraft veered off the runway during landing roll. Cause unknown.

Date (d-m-y)	02-Aug-85
Source	Airclaims
Aircraft type	Lockheed L-1011 TriStar 1
Operator name	Delta
Airport, City,	Dallas Fort Worth INTL, Dallas, USA, TX
Flight phase	Landing
Accident type	Undershoot
Narrative	The aircraft encountered a windshear and undershot the runway. The aircraft struck two cars and was destroyed.

Date (d-m-y)	10-Nov-85
Source	ICAO
Aircraft type	McDonnell Douglas DC-9-30
Operator name	IBERIA
Airport, City,	Munich, Munich, Germany
Flight phase	Take-off
Accident type	Overrun
Narrative	The tread of inner tire was torn off and ingested into the NO 1 engine. The take-off was aborted and the aircraft overran due to aquaplaning.

Date (d-m-y)	20-Dec-85
Source	Airclaims
Aircraft type	Fairchild Metro
Operator name	Britt Airways
Airport, City,	Hopkins INTL, Cleveland, USA, OH
Flight phase	Landing
Accident type	Veer-off
Narrative	The aircraft landed on a snow covered runway in strong winds. The aircraft could not be kept on the runway and veered off the side of it.

Date (d-m-y)	02-Jan-86
Source	ALPA
Aircraft type	McDonnell Douglas DC-10
Operator name	AA
Airport, City,	Wayne County MET, Detroit, USA, MI
Flight phase	Landing
Accident type	Overrun
Narrative	Brakes lost effectiveness and aircraft overran.

Date (d-m-y)	06-Feb-86
Source	ICAO
Aircraft type	Boeing 727-100
Operator name	-
Airport, City,	O'Hara INTL, Chicago, USA, IL
Flight phase	Landing
Accident type	Overrun
Narrative	The aircraft landed on a contaminated runway and overran it.

Date (d-m-y)	10-Mar-86
Source	ICAO
Aircraft type	Boeing 727-200
Operator name	Eastern
Airport, City,	Pearson INTL, Toronto, Canada
Flight phase	Landing
Accident type	Veer-off
Narrative	On landing the aircraft veered off the runway.

Date (d-m-y)	31-Aug-86
Source	Airclaims
Aircraft type	McDonnell Douglas DC-9-30
Operator name	Aeromexico
Airport, City,	Los Angeles INTL, Los Angeles, USA, CA
Flight phase	Landing
Accident type	Undershoot
Narrative	Aircraft collided with a small GA aircraft while on approach for LAX. Aircraft crashed into several buildings on the ground

Date (d-m-y)	19-Oct-86
Source	Airclaims
Aircraft type	McDonnell Douglas DC-9-30/40/50
Operator name	SAS
Airport, City,	Kastrup, Copenhagen, Denmark
Flight phase	Landing
Accident type	Veer-off
Narrative	The aircraft landed with a rudder malfunction. During the ground roll the control was lost and the aircraft veered off the runway.

Date (d-m-y)	25-Oct-86
Source	Airclaims
Aircraft type	Boeing 737-200
Operator name	Piedmont
Airport, City,	Charlotte Douglas INTL, Charlotte, USA, NC
Flight phase	Landing
Accident type	Overrun
Narrative	Aircraft landed on a wet runway and could not be stopped. Aircraft overran and was damaged.

Date (d-m-y)	29-Jan-87
Source	ALPA
Aircraft type	McDonnell Douglas DC-9-10
Operator name	northwest
Airport, City,	O'Hara INTL, Chicago, USA, IL
Flight phase	Landing
Accident type	Overrun
Narrative	Overran wet runway.

Date (d-m-y)	23-Mar-87
Source	Airclaims
Aircraft type	Convair 580
Operator name	Metroflights
Airport, City,	Dallas Fort Worth INTL, Dallas, USA, TX
Flight phase	Take-off
Accident type	Veer-off
Narrative	During take-off ground roll control was lost and the aircraft veered off the runway. Strong crosswind conditions.

Date (d-m-y)	13-Apr-87
Source	Airclaims
Aircraft type	Boeing 707-320
Operator name	Buffalo Air
Airport, City,	Kansas City INTL, Kansas City, USA, MO
Flight phase	Landing
Accident type	Undershoot
Narrative	During the an ILS approach the aircraft undershot the runway.

Date (d-m-y)	16-Aug-87
Source	Airclaims
Aircraft type	McDonnell Douglas MD-81
Operator name	North west
Airport, City,	Wayne County MET, Detroit, USA, MI
Flight phase	Take-off
Accident type	Overshoot (plof)
Narrative	Aircraft took off without flaps selected. After lift-off the wing struck a light standard after which the aircraft crashed.

Date (d-m-y)	18-Dec-87
Source	Airclaims
Aircraft type	Fairchild Metro
Operator name	AV air
Airport, City,	Dulles INTL, Washington DC, USA, VA
Flight phase	Landing
Accident type	Undershoot
Narrative	During the approach all power was lost. A forced landing was made. Aircraft undershot the runway.

Date (d-m-y)	08-Feb-88
Source	Airclaims
Aircraft type	Fairchild Metro
Operator name	NFD
Airport, City,	Dusseldorf, Dusseldorf, Germany
Flight phase	Landing
Accident type	Undershoot
Narrative	During the ILS approach the aircraft entered an uncontrolled descent and crashed.

Date (d-m-y)	04-Mar-88
Source	Airclaims
Aircraft type	Fairchild FH-227
Operator name	TAT
Airport, City,	Orly, Paris, France
Flight phase	Landing
Accident type	Undershoot
Narrative	During approach the aircraft struck a powerline and crashed.

Date (d-m-y)	13-Apr-88
Source	Airclaims
Aircraft type	McDonnell Douglas DC-8-30
Operator name	Gabon
Airport, City,	Frankfurt-Rhein, Frankfurt, Germany
Flight phase	Take-off
Accident type	Overrun
Narrative	Take-off was aborted and the aircraft overran the runway.

Date (d-m-y)	15-Apr-88
Source	Airclaims
Aircraft type	De Havilland Canada DHC-8-100
Operator name	Horizon
Airport, City,	Tacoma INTL, Seattle, USA, WA
Flight phase	Landing
Accident type	Veer-off
Narrative	During an emergency landing control was lost during the landing roll and the aircraft veer-off the runway.

Date (d-m-y)	21-May-88
Source	Airclaims
Aircraft type	McDonnell Douglas DC-10-30
Operator name	AA
Airport, City,	Dallas Fort Worth INTL, Dallas, USA, TX
Flight phase	Take-off
Accident type	Overrun
Narrative	The aircraft overran after the take-off was aborted.

Date (d-m-y)	12-Jun-88
Source	ICAO
Aircraft type	Boeing 727-100
Operator name	ALASKA
Airport, City,	Tacoma INTL, Seattle, USA, WA
Flight phase	Landing
Accident type	Veer-off
Narrative	The aircraft veered off the runway during landing.

Date (d-m-y)	31-Aug-88
Source	Airclaims
Aircraft type	Boeing 727-200
Operator name	Delta Airlines
Airport, City,	Dallas Fort Worth INTL, Dallas, USA, TX
Flight phase	Take-off
Accident type	Overshoot (plof)
Narrative	Aircraft crashed after take-off some 300 meters beyond the threshold.

Date (d-m-y)	14-Oct-88
Source	ALPA
Aircraft type	Boeing 727-200
Operator name	DELTA
Airport, City,	Tacoma INTL, Seattle, USA, WA
Flight phase	Landing
Accident type	Overrun
Narrative	Overran the runway due to aquaplaning.

Date (d-m-y)	17-Oct-88
Source	Airclaims
Aircraft type	Boeing 707-320
Operator name	Uganda Airlines
Airport, City,	Fiumicino, Rome, Italy
Flight phase	Landing
Accident type	Undershoot
Narrative	The aircraft undershot the runway and was destroyed.

Date (d-m-y)	23-Jan-89
Source	ICAO
Aircraft type	Fairchild FH-227
Operator name	Horizon
Airport, City,	Tacoma INTL, Seattle, USA, WA
Flight phase	Take-off
Accident type	Overrun
Narrative	During the take-off ground roll there was a malfunction in the nose gear steering. The aircraft went out off control and overran.

Date (d-m-y)	17-Jun-89
Source	ICAO
Aircraft type	Lockheed L-1011 TriStar 1
Operator name	Delta
Airport, City,	Frankfurt-Rhein, Frankfurt, Germany
Flight phase	Take-off
Accident type	Overrun
Narrative	Overran after aborted take-off.

Date (d-m-y)	11-Sep-89
Source	ICAO
Aircraft type	Fokker/Fairchild F-27-100
Operator name	KLM
Airport, City,	Dusseldorf, Dusseldorf, Germany
Flight phase	Landing
Accident type	Veer-off
Narrative	Landed with locked brakes and veered off the runway during ground roll.

Date (d-m-y)	12-Sep-89
Source	Airclaims
Aircraft type	McDonnell Douglas MD-82
Operator name	AA
Airport, City,	O'Hara INTL, Chicago, USA, IL
Flight phase	Landing
Accident type	Veer-off
Narrative	Control was lost during ground roll in strong crosswind. The aircraft veered off the runway.

Date (d-m-y)	20-Sep-89
Source	Airclaims
Aircraft type	Boeing 737-400
Operator name	US airways
Airport, City,	La Guardia, New York, USA, NY
Flight phase	Take-off
Accident type	Overrun
Narrative	Aircraft overran the runway after an aborted take-off.

Date (d-m-y)	25-Jan-90
Source	Airclaims
Aircraft type	Boeing 707-320
Operator name	Avianca
Airport, City,	J.F. Kennedy INTL, New York, USA, NY
Flight phase	Landing
Accident type	Undershoot
Narrative	On approach power on all four engines was lost. The aircraft undershot the runway and was destroyed.

Date (d-m-y)	24-Apr-90
Source	ICAO
Aircraft type	Boeing 707
Operator name	Operada
Airport, City,	Miami INTL, Miami, USA, FL
Flight phase	Take-off
Accident type	Veer-off
Narrative	The aircraft veered off the runway. Aft cargo limit has been exceeded.

Date (d-m-y)	07-Jan-91
Source	ICAO
Aircraft type	Boeing 737-300
Operator name	United
Airport, City,	Kansas City INTL, Kansas City, USA, MO
Flight phase	Take-off
Accident type	Veer-off
Narrative	On a ice-covered runway the control was lost and the aircraft veered off the runway.

Date (d-m-y)	01-Feb-91
Source	Airclaims
Aircraft type	Boeing 737-300
Operator name	US airways
Airport, City,	Los Angeles INTL, Los Angeles, USA, CA
Flight phase	Landing
Accident type	Veer-off
Narrative	During the landing roll the aircraft collided with another aircraft on the runway. The 737-300 veered off the runway and was destroyed by fire.

Date (d-m-y)	12-Mar-91
Source	ICAO
Aircraft type	McDonnell Douglas DC-8
Operator name	ATI
Airport, City,	J.F. Kennedy INTL, New York, USA, NY
Flight phase	Take-off
Accident type	Overrun
Narrative	Take-off was aborted. Aircraft could not be stopped on the runway and overran.

Date (d-m-y)	22-Mar-92
Source	Airclaims
Aircraft type	Fokker F-28-4000
Operator name	US airways
Airport, City,	La Guardia, New York, USA, NY
Flight phase	Take-off
Accident type	Overshoot (plof)
Narrative	Just after rotation the aircraft experienced heavy buffeting and rolled to the left. Aircraft impacted the ground just eyond the threshold. Wing icing caused the accident.

Date (d-m-y)	15-Apr-92
Source	ICAO
Aircraft type	Fokker F-28-4000
Operator name	US AIR
Airport, City,	Charlotte Douglas INTL, Charlotte, USA, NC
Flight phase	Take-off
Accident type	Overrun
Narrative	The crew reported a loss in acceleration during ground roll and aborted the take-off at or above V1. The aircraft overran the runway.

Date (d-m-y)	25-Jun-92
Source	ICAO
Aircraft type	Fairchild FH-227
Operator name	NER
Airport, City,	Logan INTL, Boston, USA, MA
Flight phase	Landing
Accident type	Veer-off
Narrative	Due to a 21 kt. crosswind the aircraft could not be put correctly on the runway. After touchdown the aircraft veered off the runway.

Date (d-m-y)	30-Jul-92
Source	ICAO
Aircraft type	Lockheed L-1011 TriStar 1
Operator name	TWA
Airport, City,	J.F. Kennedy INTL, New York, USA, NY
Flight phase	Take-off
Accident type	Overshoot (plof)
Narrative	After VR the stick shaker came in and the PIC landed the aircraft fast and hard beyond the runway end.

Date (d-m-y)	02-Oct-92
Source	ICAO
Aircraft type	Boeing 737-200
Operator name	Sultan Air
Airport, City,	Munich, Munich, Germany
Flight phase	Landing
Accident type	Overrun
Narrative	During the landing roll there was only little barking. The aircraft could not be stopped and overran.

Date (d-m-y)	04-Oct-92
Source	Airclaims
Aircraft type	Boeing 747-100F/200C/F
Operator name	EL AL
Airport, City,	Schiphol, Amsterdam, Netherlands
Flight phase	Landing
Accident type	Undershoot
Narrative	After take-off the aircraft lost two engines. During the emergency landing the control was lost and the aircraft impacted an apartment building.

Date (d-m-y)	06-Jan-93
Source	Airclaims
Aircraft type	De Havilland Canada DHC-8-300
Operator name	Lufthansa Cityline
Airport, City,	Orly, Paris, France
Flight phase	Landing
Accident type	Undershoot
Narrative	The aircraft undershot the runway during an ILS approach.

Date (d-m-y)	13-Mar-93
Source	ALPA
Aircraft type	Boeing 737-100
Operator name	USAIR
Airport, City,	Charlotte Douglas INTL, Charlotte, USA, NC
Flight phase	Landing
Accident type	Overrun
Narrative	Overran the snow covered runway.

Date (d-m-y)	20-Mar-93
Source	Airclaims
Aircraft type	Boeing 747-100F/200C/F
Operator name	Lufhthansa
Airport, City,	Frankfurt-Rhein, Frankfurt, Germany
Flight phase	Take-off
Accident type	Overrun
Narrative	Close to VR there was a loud bang. After that the PIC elected to abort the take-off and the aircraft overran.

Date (d-m-y)	14-Apr-93
Source	Airclaims
Aircraft type	McDonnell Douglas DC-10-30
Operator name	AA
Airport, City,	Dallas Fort Worth INTL, Dallas, USA, TX
Flight phase	Landing
Accident type	Veer-off
Narrative	The aircraft landed long. During the ground roll the PIC had difficulties in controlling the aircraft. The aircraft veered off the runway.

Date (d-m-y)	08-Dec-93
Source	ICAO
Aircraft type	Boeing 737-300
Operator name	AWE
Airport, City,	Dallas Fort Worth INTL, Dallas, USA, TX
Flight phase	Landing
Accident type	Undershoot
Narrative	PIC failed to attain glide slope and undershot the runway.

Date (d-m-y)	02-Mar-94
Source	Airclaims
Aircraft type	McDonnell Douglas MD-81
Operator name	Continental
Airport, City,	La Guardia, New York, USA, NY
Flight phase	Take-off
Accident type	Overrun
Narrative	The acceleration was low and the PIC elected to abort the take-off. The runway was slippery and the aircraft could not be stopped on the runway. The aircraft overran and ended in the East river.

Date (d-m-y)	04-Apr-94
Source	Airclaims
Aircraft type	Saab 340
Operator name	KLM
Airport, City,	Schiphol, Amsterdam, Netherlands
Flight phase	Landing
Accident type	Undershoot
Narrative	During a landing with OEI, the control was lost and the aircraft crashed.

Date (d-m-y)	09-Apr-94
Source	ICAO
Aircraft type	McDonnell Douglas DC-8
Operator name	ICX
Airport, City,	Frankfurt-Rhein, Frankfurt, Germany
Flight phase	Landing
Accident type	Veer-off
Narrative	Aircraft veered off the runway after touchdown.

Date (d-m-y)	02-Jul-94
Source	Airclaims
Aircraft type	McDonnell Douglas DC-9-30
Operator name	US airways
Airport, City,	Charlotte Douglas INTL, Charlotte, USA, NC
Flight phase	Landing
Accident type	Undershoot
Narrative	During an ILS approach the crew decided to carry out a go-around. However, before the go-around was started the aircraft undershot the runway and was destroyed.

Date (d-m-y)	20-Dec-95
Source	Airclaims
Aircraft type	Boeing 747-100
Operator name	Tower Air
Airport, City,	J.F. Kennedy INTL, New York, USA, NY
Flight phase	Take-off
Accident type	Veer-off
Narrative	During the ground roll the control was lost and the aircraft veered off the runway.

Date (d-m-y)	19-Feb-96
Source	ICAO
Aircraft type	McDonnell Douglas DC-9-30
Operator name	Continental
Airport, City,	Houston Intercontinental, Houston, USA, TX
Flight phase	Landing
Accident type	Veer-off
Narrative	Aircraft made a wheels up landing and veered off the runway.

Date (d-m-y)	19-Oct-96
Source	Airclaims
Aircraft type	McDonnell Douglas MD-88
Operator name	Delta
Airport, City,	La Guardia, New York, USA, NY
Flight phase	Landing
Accident type	Undershoot
Narrative	Aircraft undershot the runway during a landing in poor weather.

Date (d-m-y)	12-Dec-96
Source	Airclaims
Aircraft type	McDonnell Douglas MD-87
Operator name	Iberia
Airport, City,	Barajas, Madrid, Spain
Flight phase	Landing
Accident type	Overrun
Narrative	During the landing roll the aircraft the aquaplaned and could not be stopped on the runway. The aircraft overran the runway.

Date (d-m-y)	30-Dec-96
Source	ICAO
Aircraft type	McDonnell Douglas DC-8
Operator name	ABX
Airport, City,	Orlando INTL, Orlando, USA, FL
Flight phase	Take-off
Accident type	Veer-off
Narrative	During ground run control was lost and the aircraft veered off the runway.

Date (d-m-y)	09-Jan-97
Source	ICAO
Aircraft type	Embraer EMB-120 Brasilia
Operator name	Comair
Airport, City,	Wayne County MET, Detroit, USA, MI
Flight phase	Landing
Accident type	Undershoot
Narrative	Aircraft crashed during approach.

Date (d-m-y)	29-Jan-97
Source	Airclaims
Aircraft type	Boeing 747-200
Operator name	China Airlines
Airport, City,	J.F. Kennedy INTL, New York, USA, NY
Flight phase	Landing
Accident type	Veer-off
Narrative	After a normal landing the control was lost during the ground roll. The aircraft veered off the runway.

Date (d-m-y)	02-Mar-97
Source	Airclaims
Aircraft type	McDonnell Douglas MD-82
Operator name	AA
Airport, City,	Hopkins INTL, Cleveland, USA, OH
Flight phase	Landing
Accident type	Overrun
Narrative	The aircraft landed on a runway covered with wet snow. During the ground roll, control was lost and the aircraft veer-off the side of the runway.

Appendix D Lethality

The following table contains the data points used for the determination of the lethality.

Table D-1: NLR data points used for the determination of lethality.

Date	Location	Third party fatalities	Population (NLR estimate)
5-1-69	Gatwick	2	3
3-3-72	Albany	1	2
8-12-72	Chicago	2	4
3-6-73	Goussainville	8	68
23-7-73	St Louis	0	4
15-12-73	Miami	6	17
27-4-76	St.Thomas	0	6
4-6-76	Agana Naval Air Station	1	7
23-6-76	Philadelphia	0	1
6-8-76	Chicago	1	12
4-4-77	New Hope	8	16
28-4-77	Mclean - Virginia	0	8
25-9-78	San Diego	7	22
25-5-79	Chicago	2	8
31-10-79	Mexico City	1	1
13-1-82	Washington	4	8
9-7-82	New Orleans	8	24
10-11-85	Fairview	1	3
31-8-86	Cerritos	15	23
26-5-87	Kenner	0	2
16-8-87	Detroit	2	7
14-12-88	Luxor	1	8
21-12-88	Lockerbie	11	42
4-10-92	Amsterdam	43[6]	150
26-5-93	Southampton	0	3
2-7-94	Charlotte	0	2
14-12-94	Fresno	0	21
21-12-94	Willenhall	0	1
8-10-96	Turin	2	4
6-12-97	Irkutsk	47	147
7-3-99	New Delhi	3	10
	Total	**95**	**634**

Some typical examples for the determination of the population in a crash area are given:

- July 23, 1973; a Fairchild Hiller-227B at Missouri, U.S.A.; source: NTSB/AAR 74/05.
  At 17.43 hours (local time) the aeroplane crashed while trying to land and slightly damaged two houses. Assuming 4 persons were present in the houses at the time of the accident. There were no fatalities.
- June 4, 1976; a Lockheed L-188A Electra at Guam; source: NTSB/AAR 77/06.
  On take-off, the aeroplane crashed between 6 houses injuring 2 people and skidded on an

[6] The official accident report of the Amsterdam accident indicates 39 third party victims. The number of 43 victims that is used in the determination of lethality in this report is an unofficial number that dates from before the release of the accident report.

highway killing a driver. Assuming 7 people were present in the crash area: the driver and 6 people in the houses.

In some cases, the population in the crash area could not be determined satisfactory. For instance, it is not possible to make a good estimate of the number of people that were on the market place during the crash of an Antonov-32 in Kinshasa, Zaire, on January 7, 1996.

The data points of the ADREP source are given in the following table.

Table D-2: ADREP data points used for determination of lethality.

Date	Location	Third party fatalities	Population (ADREP limit)	Population NLR
12-2-70	Enroute	2	2	
30-5-70	Atlanta	5	5	
30-11-70	Tel Aviv	3	4	
1-12-70	Dacca	4	4	
30-7-71	Jet Route J11l	0	1	
2-10-71	Aarsele	0	1	
3-3-72	Albany	1	6	2
8-12-72	Chicago	2	4	4
26-2-73	Atlanta	0	1	
10-5-73	Kathmandu	1	1	
30-6-73	Amman	7	7	
5-7-73	Bucaramanga	2	7	
15-12-73	Miami	6	8	17
19-12-73	Detroit	0	2	
20-12-73	Delhi	0	1	
14-1-74	Jolo Airport	2	2	
17-6-75	Pedro Afonso	3	7	
24-9-75	Palembang	1	1	
27-9-75	Miami	0	1	
20-11-75	Dumsfold Aerodrom	6	6	
8-2-76	Van Nuys	0	13	
27-4-76	St.Thomas	0	1	6
23-6-76	Philadelphia	0	1	1
2-8-76	Mehrabad	2	2	
13-10-76	Santa Cruz	77	155	
25-12-76	Bangkok	19	42	
4-4-77	New Hope	8	9	16
27-4-77	Wheeling	0	1	
18-10-77	Manila Airport	3	3	
1-3-78	Los Angeles	0	10	
25-9-78	San Diego	7	23	22
17-12-78	Hyderabad	3	3	
15-5-79	Mesa	0	1	
25-5-79	Chicago	2	4	8
31-10-79	Mexico City	1	1	1
10-12-79	Forli	2	4	
3-3-80	Port Au Prince	3	4	
19-11-80	Seoul	1	1	
8-1-81	Guatemala City	0	6	
13-9-82	Malaga A/P	0	1	
9-10-82	Graskop	0	7	

Date	Location	Third party fatalities	Population (ADREP limit)	Population NLR
12-12-82	Mariquita	1	1	
16-4-83	Khartoum	9	9	
14-12-83	Medellin	22	22	
20-12-83	Sioux Falls	1	1	
4-9-84	Farnborough	0	1	
10-9-84	Kandale	1	1	
18-9-84	Quito A/P	49	79	
10-11-85	Fairview	1	3	3
31-8-86	Cerritos	15	23	23
4-3-87	Romulus	0	3	
30-7-87	Ciudad De Mexico	44	44	
16-8-87	Detroit	2	7	7
14-12-88	Karmomran-Kena	1	6	8
21-12-88	Lockerbie	11	16	42
8-1-89	East Midlands	0	2	
3-2-89	Rangoon	1	3	
21-3-89	Guarulhos	22	70	
12-2-90	Bauru	2	2	
22-4-90	Luang Nam Tha	1	1	
7-8-90	Gatwick	0	2	
20-7-92	Tbilisi A/P	4	4	
4-10-92	Amsterdam	43	69	150
26-5-93	Southampton	0	3	3
3-1-94	Irkutsk	1	1	
14-12-94	Fresno	0	20	21
28-4-95	La Aurora	6	6	
15-9-95	Tawau	0	9	
7-1-96	Kinshasa	237	298	
4-2-96	Asuncion	18	18	
22-2-96	Baia Mare	2	2	
	Total	**667**	**1089**	**334**

There are 17 aircraft accidents that occur in both the NLR and the ADREP database. The following table compares the similar data points. It is noted that NLR estimated the population in two cases lower than the limit given by the ADREP database. The values were deliberately not corrected in order to stay consistent.

Appendix E Route structure of the scenarios S4S1-1990 and S5P-2010

Figures E-1 to E-5 show the route structure of the 1990 S4S1 scenario for runways 01L-19R, 01R-19L, 06-24 and 09-27.

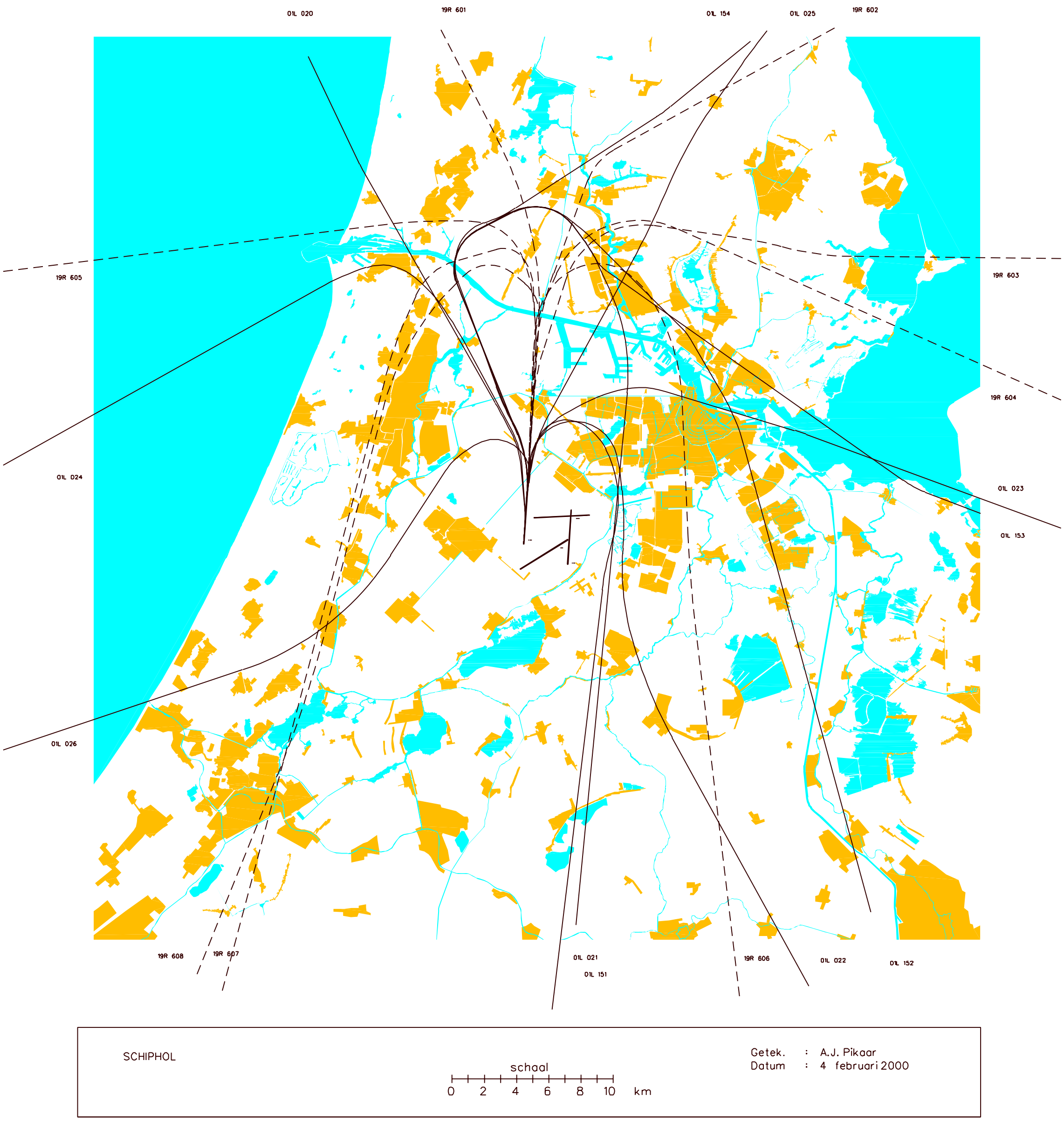

Figure E-1: Arrival and departure routes of runway 01L-19R.

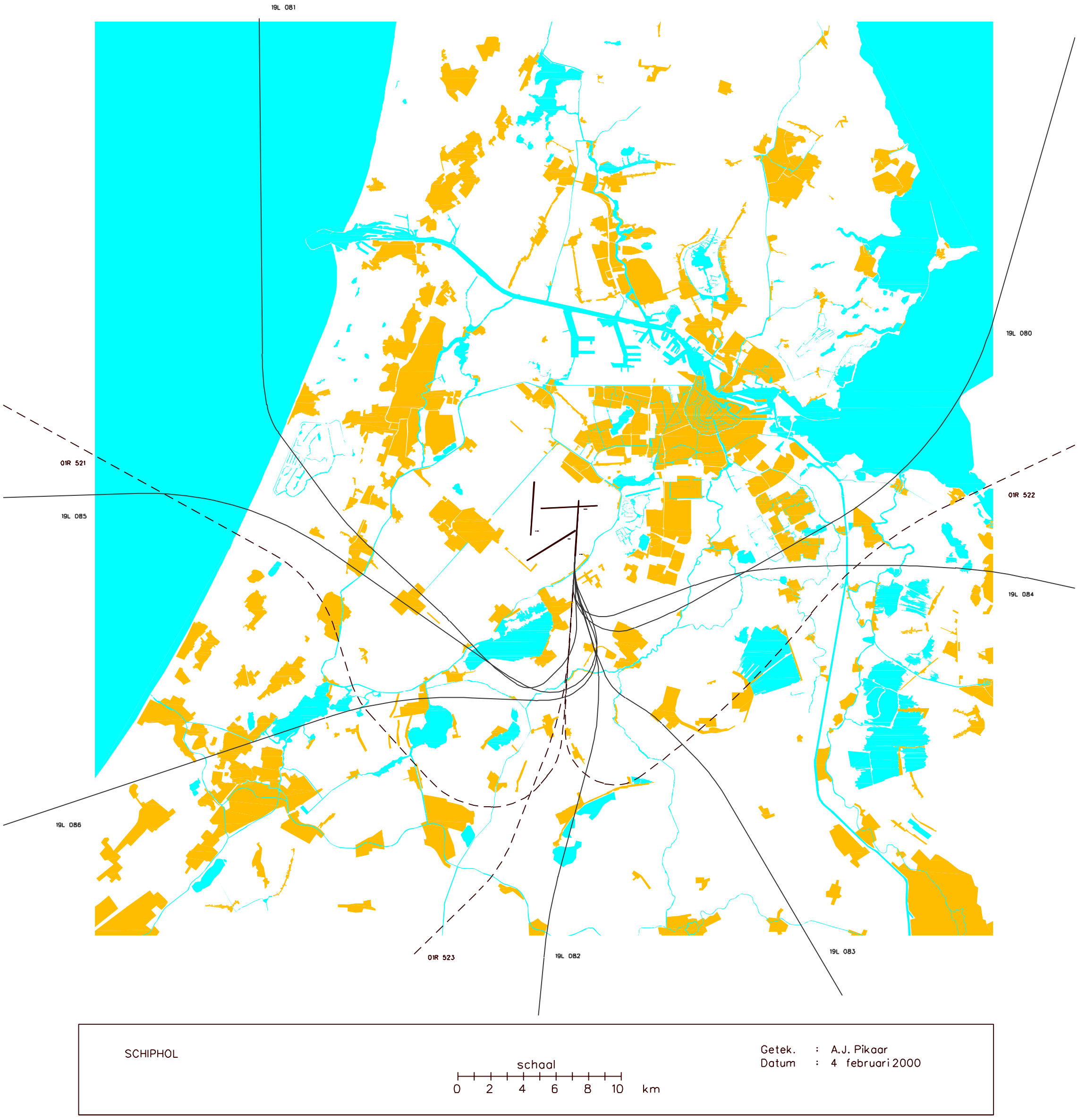

Figure E-2: Arrival and departure routes of runway 01R-19L.

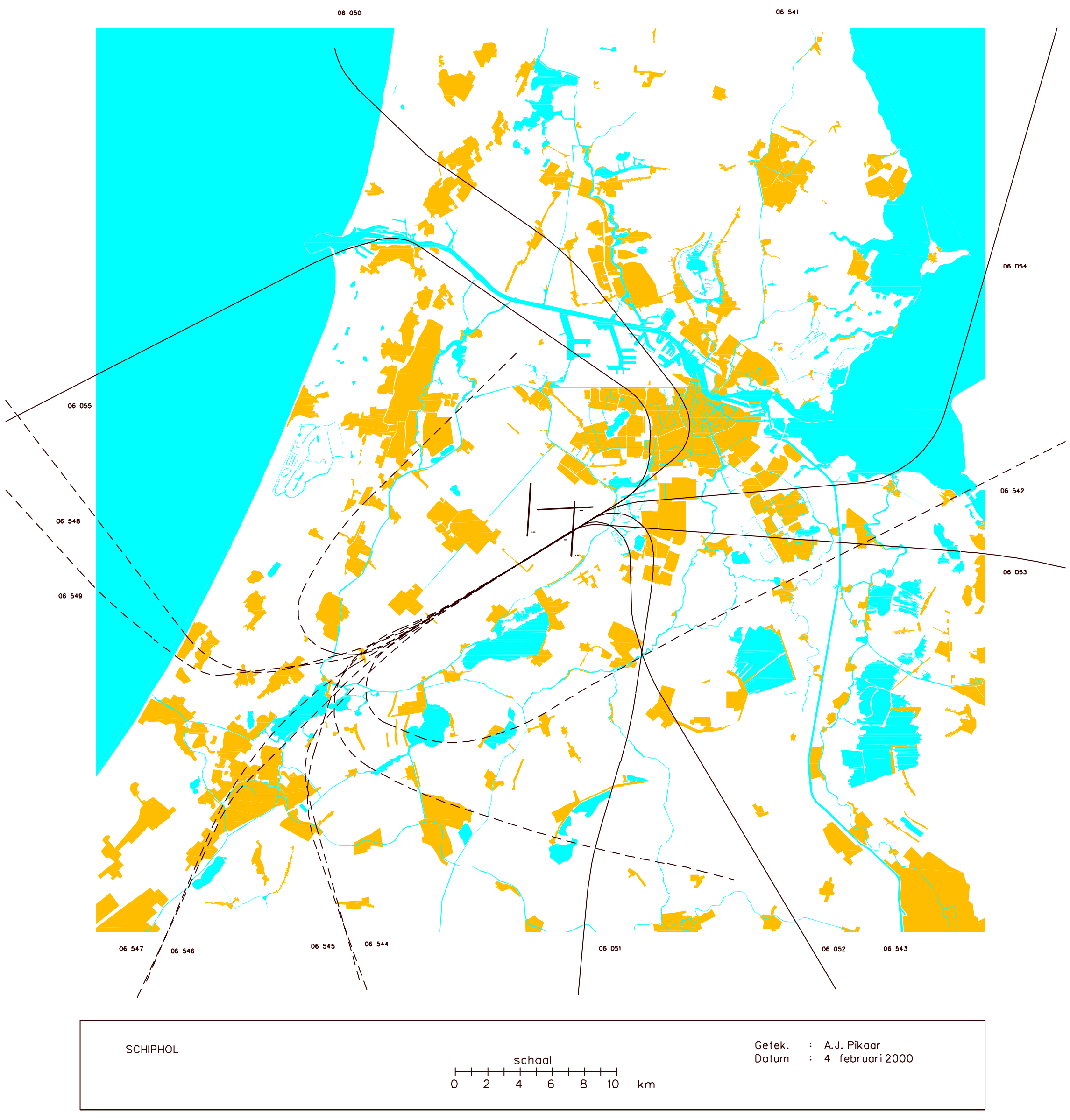

Figure E-3: Arrival and departure routes of runway 06.

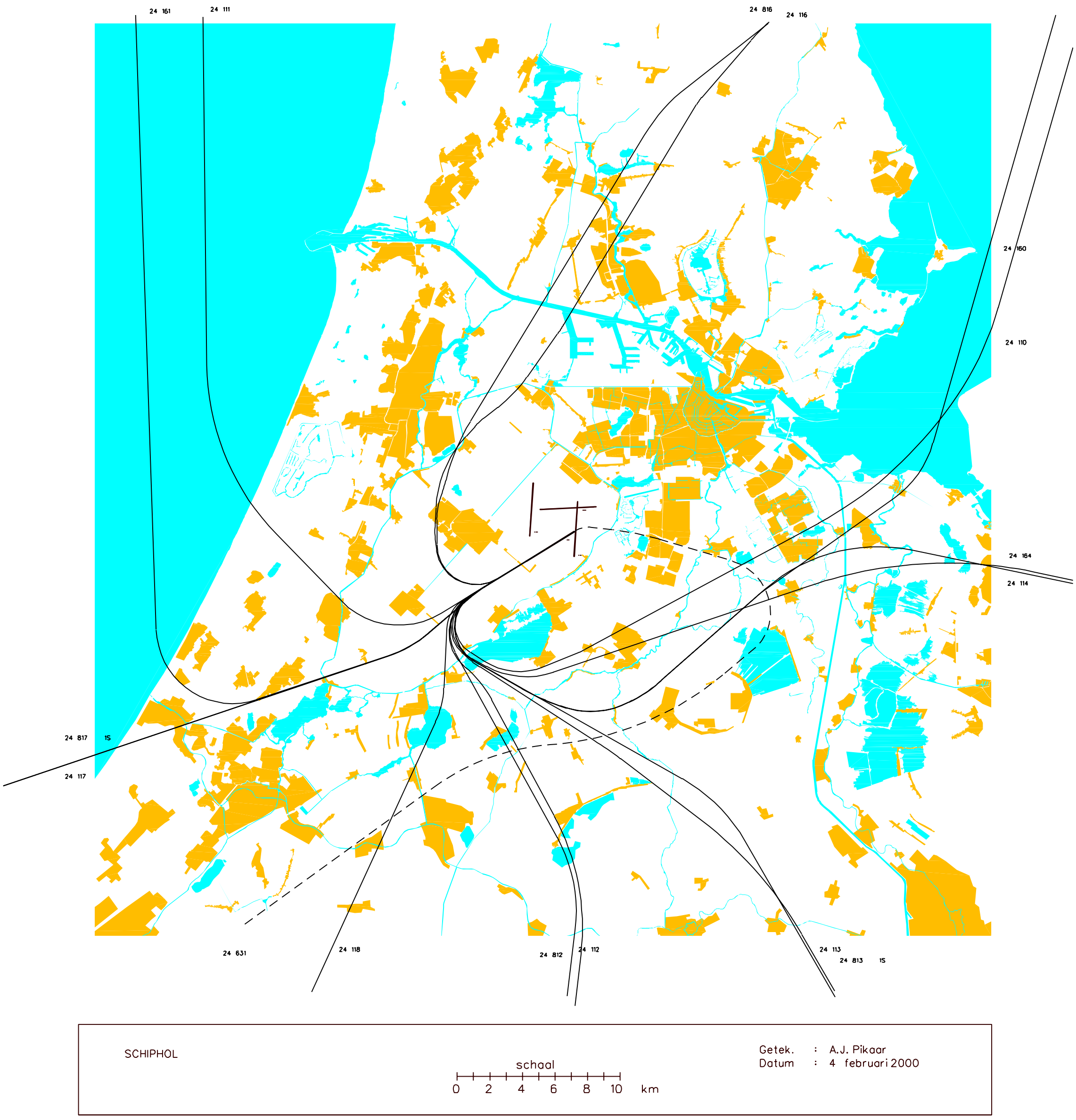

Figure E-4: Arrival and departure routes of runway 24.

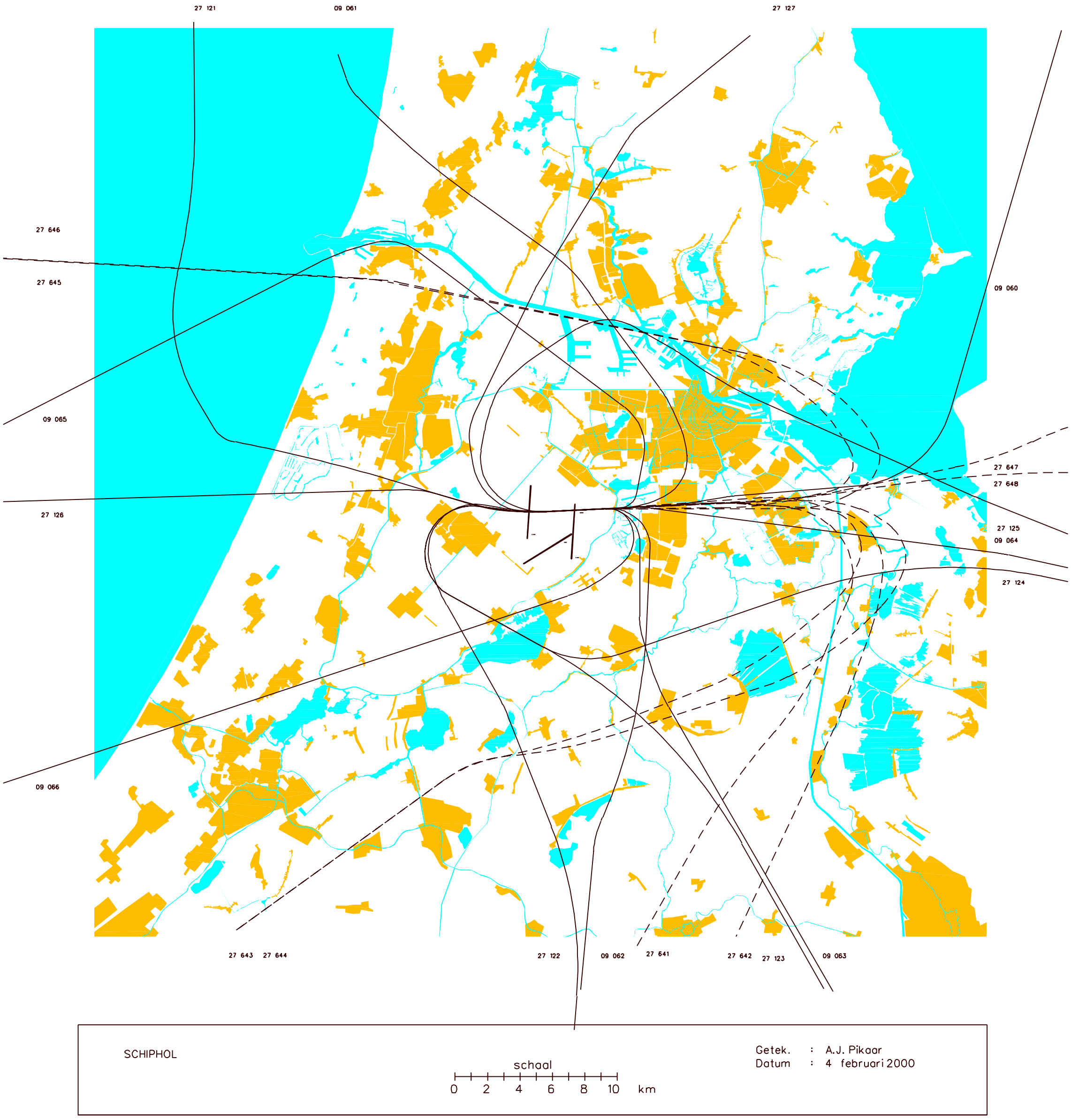

Figure E-5: Arrival and departure routes of runway 09-27.

Figures E-6 to E-10 show the route structure of the 2010 S5P scenario for runways 01L-19R, 01R-19L, 06-24, 09-27 and 18-36.

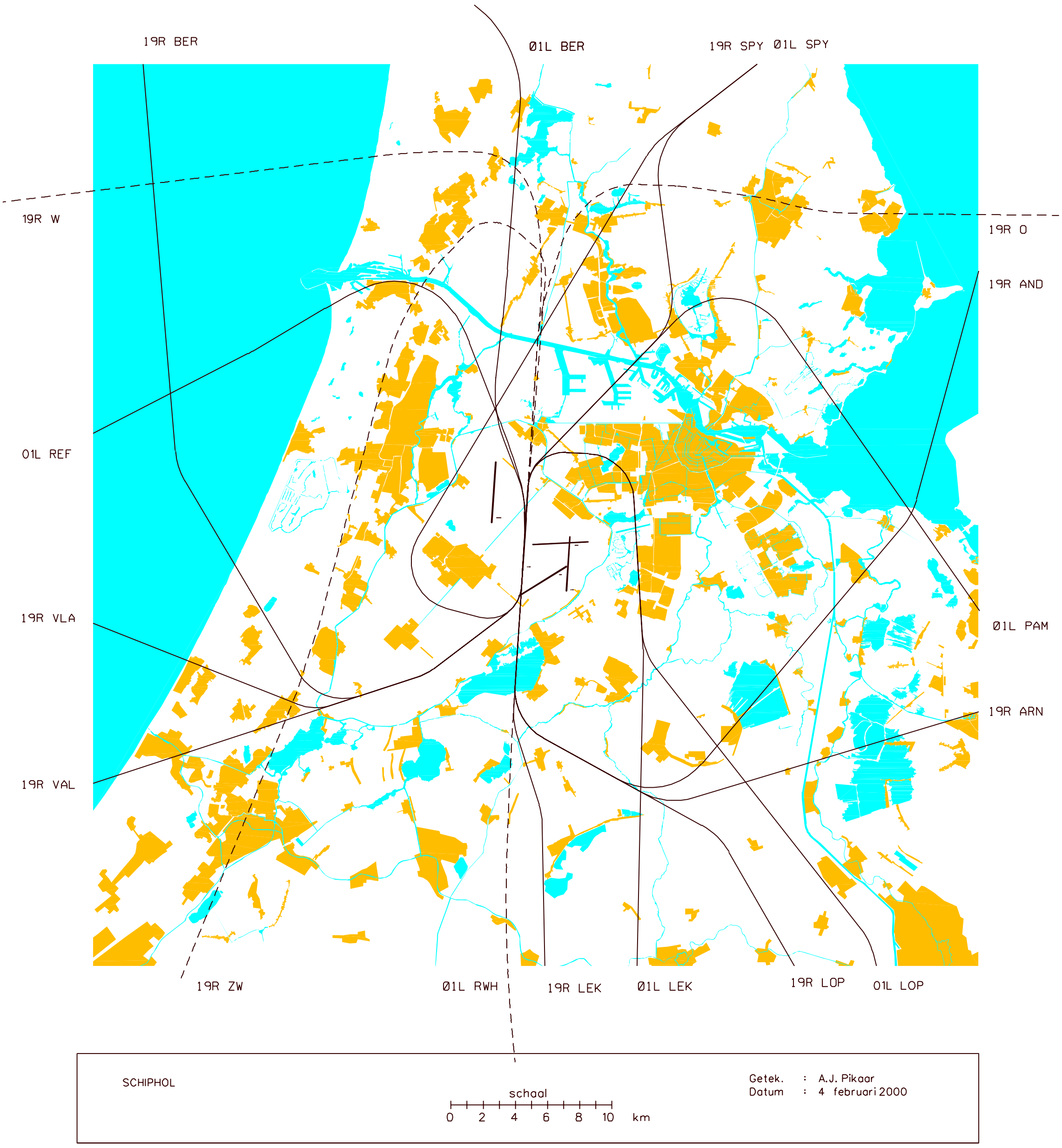

Figure E-6: Arrival and departure routes of runway 01L-19R.

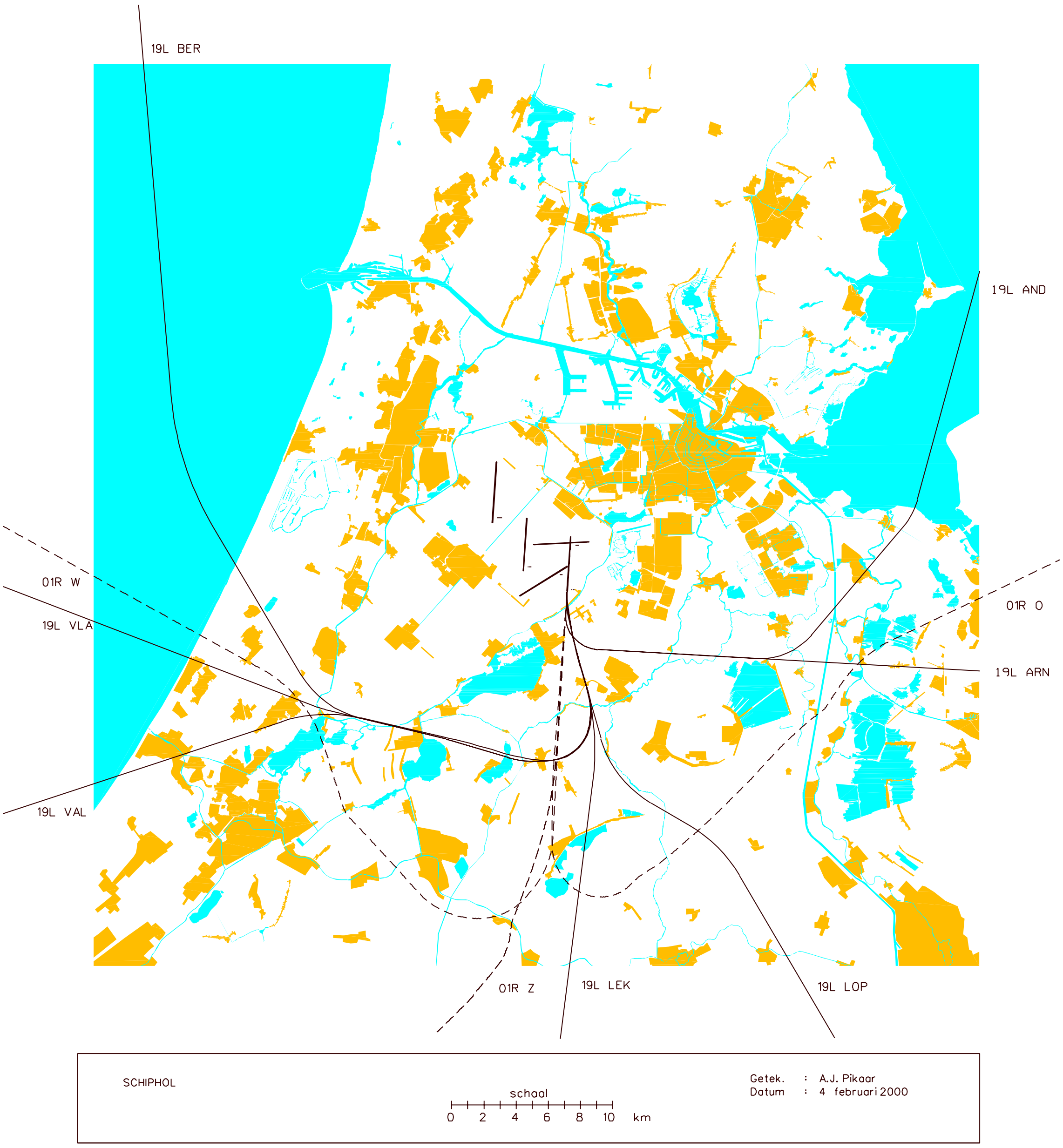

Figure E-7: Arrival and departure routes of runway 01R-19L.

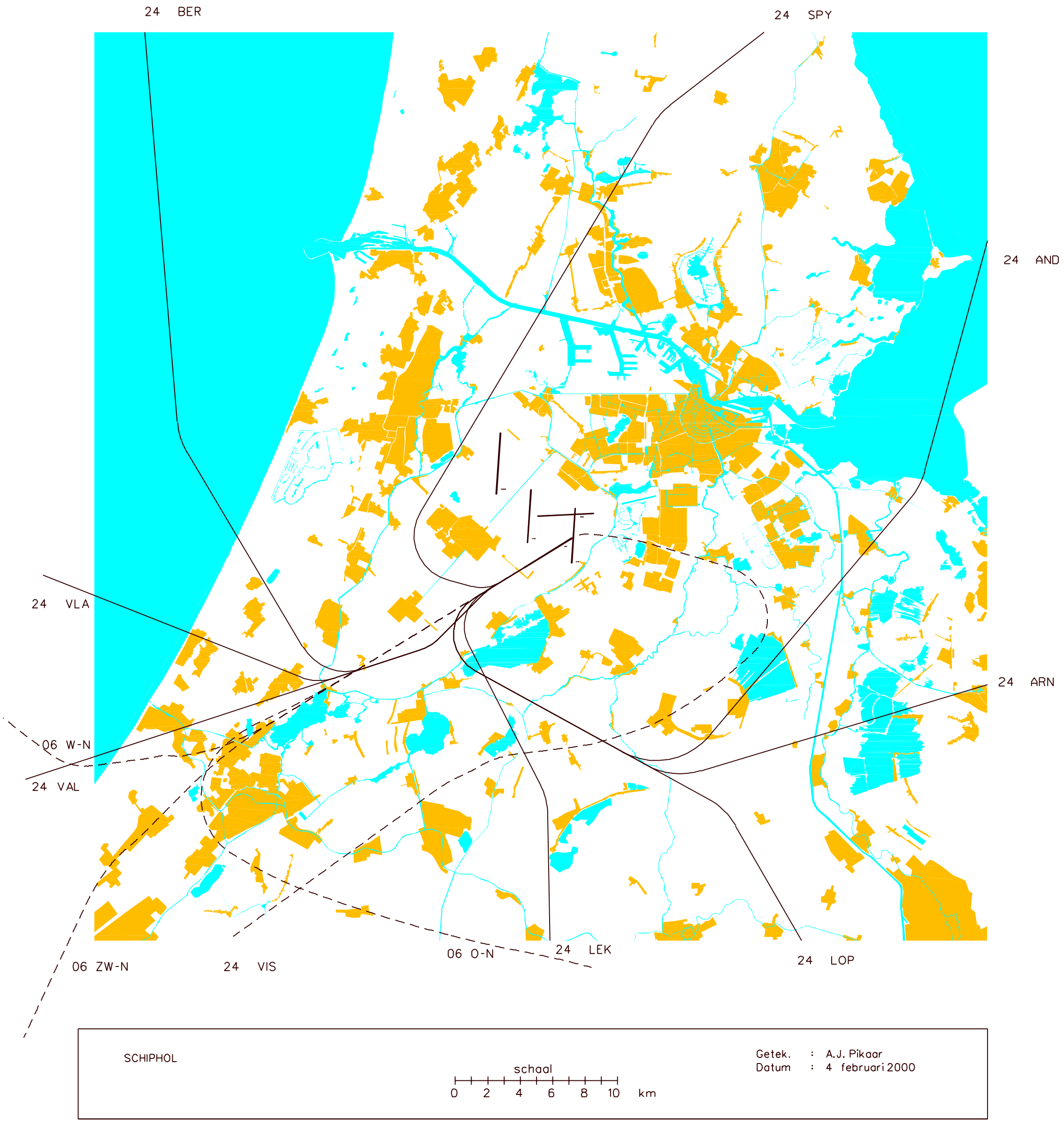

Figure E-8: Arrival and departure routes of runway 06-24.

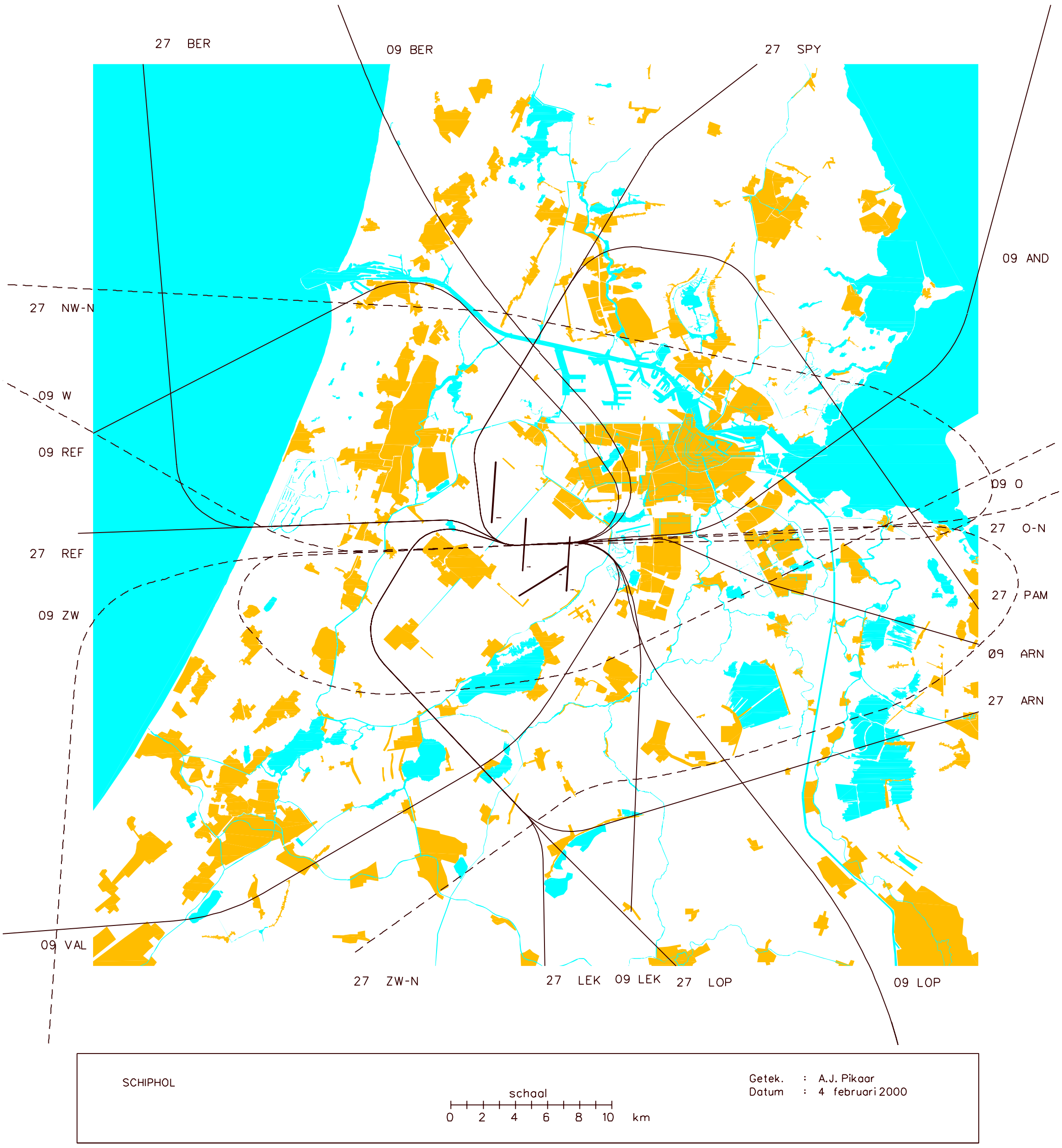

Figure E-9: Arrival and departure routes of runway 09-27.

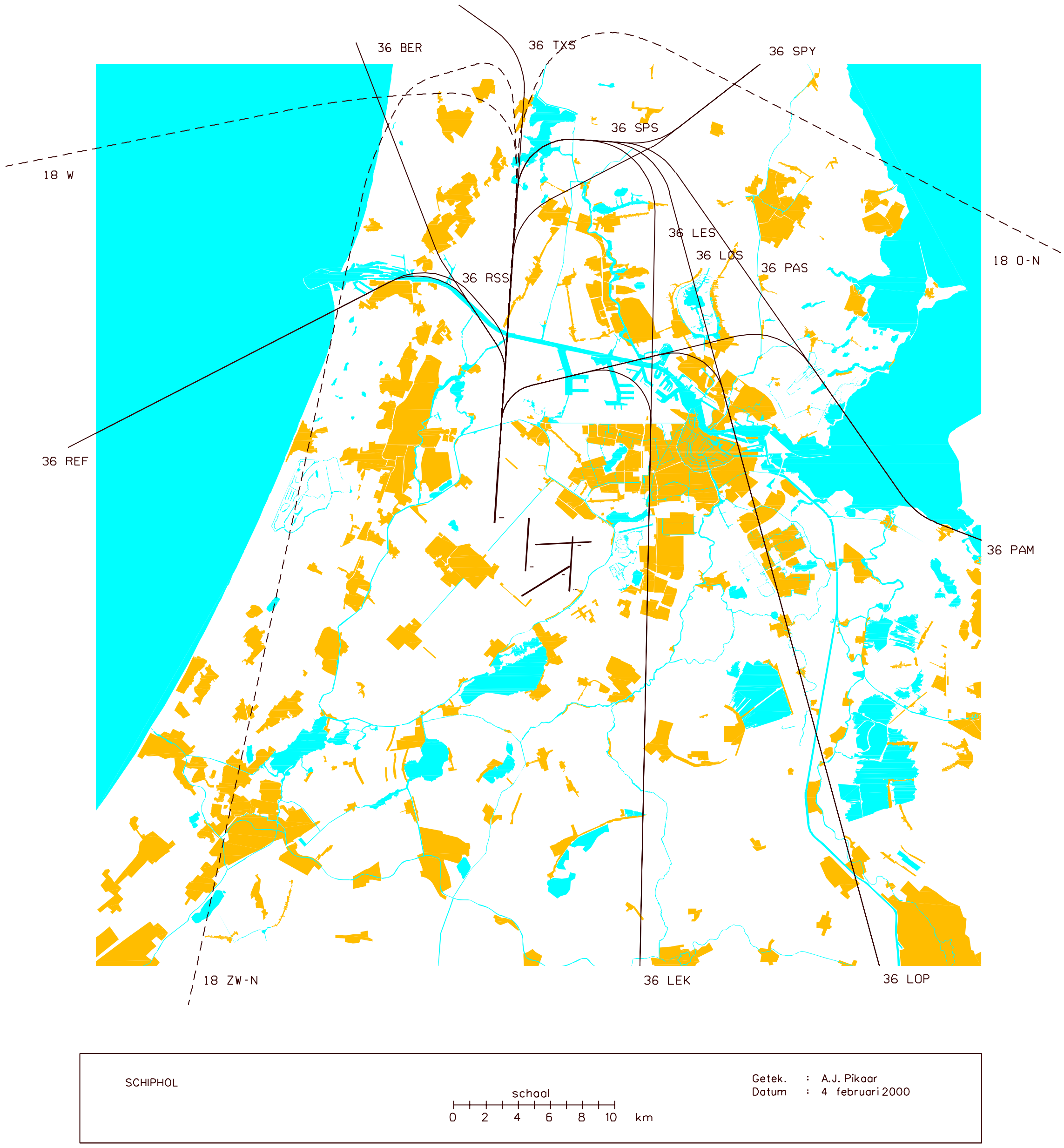

Figure E-10: Arrival and departure routes of runway 18-36.

Appendix F Aircraft movements

Table F-1: Aircraft movements per generation for the year 1990 (source: Amsterdam Airport Schiphol, statistical annual review 1990).

	Generation		
Aircraft type	**1**	**2**	**3**
Antonov 124			6
Boeing 747-400			4194
Boeing 747-300		5993	
Boeing 747-200		4973	
Boeing 747-100		674	
Boeing 747-SP		40	
DC-10-30/40		5208	
Tristar L-1011-500		1284	
Tristar L-1011-100		775	
Ilyushin 76		16	
Ilyushin 62	210		
Boeing 767			2518
Airbus A-300		522	
DC-8-60/70	1054		
DC-8-30/50	184		
Airbus A-310			12789
Boeing 707	1665		
Boeing 757			4985
Belfast-Short	82		
Tupolev 154		1434	
Boeing 727		5423	
Canadair CL-44		4	
Super Guppy	12		
Airbus A-320			2910
MD 80			5824
DC-9-50		344	
DC-9-40		3534	
DC-9-30		8969	
DC-9-10		934	
Hercules	970		
Boeing 737-500			60
Boeing 737-400			3846
Boeing 737-300			32569
Boeing 737-200		18698	
Boeing 737-100		152	
Merchantman	934		
Ilyushin 18	16		
Antonov 12	26		
Caravelle	80		

Aircraft type	Generation 1	2	3
Electra L188	34		
Tupolev 134		894	
BAE 1-11-500		2110	
BAE 1-11-300		1232	
BAE 1-11-200		706	
Douglas DC-6	2		
Fokker 100			1209
BAE 146			7994
Fokker 28		6028	
Gulfstream III		2	
Viscount 800	78		
BAE ATP			1128
BAE 748 (HS748)	1072		
Fokker F50			1753
Fokker F27	16211		
Herald	32		
DHC - 07		1864	
DHC 6 - Twin Otter		2780	
Gulfstream I	17		
ATR 42			1266
YAK 40	2		
Mystere 10/2	2		
Short-SD360	1306		
Short-SD330	418		
SAAB SF340			10095
Embraer 121 (120-100?)		4573	
Sabreliner	1		
Learjet 35/36		12	
Metro/Merlin	1620		
HP Jetstream	732		
Dornier 228		982	
Embraer 110		1068	
TOTAL	**26,760**	**81,228**	**93,146**
	13.3%	40.4%	46.3%
Average MTOW=88 ton			

Two errors have been noted in the source file:

- In the calculation of the subtotals of the A-310 a total of 76+1=76 is noted. In the list above a subtotal of 76 is used.
- The total number of movements of the DC-9 is larger (338) than the sum of all subtotals. In the list above the sum of all subtotals is used.

The aircraft movements of the Beechcraft, Cessna and Piper are not used in the table above, because these aircraft are lighter than 5700 kg.

Table F-2: Aircraft movements per generation for the year 2010 (Source: KLM).

	Generations		
Aircraft type	**2**	**3**	**MTOW**
747-300	2190		377.8
DC-10-30	3285		263.1
757-200		14235	115.7
757-300		1460	122.5
757-300		6205	122.5
737-300		32587.2	62.8
737-400		28513.8	68
737-600		5110	65.5
737-700		2190	70.1
737-700		27740	70.1
737-700 (all M)		8146.8	70.1
737-700 (all M)		15695	70.1
737-800		12045	79
737-800		43435	79
737-800		57027.6	79
737-800 (all M)		8146.8	79
737-800 (all M)		14125.5	79
737-900		18250	79
737-900		22403.7	79
747-400		2190	396.9
747-400 Combi		19710	396.9
747-400 Pax		11169	396.9
757-200 (all M)		4708.5	115.7
757-200 (all M)(HV/MP)		730	115.7
767-300ER		365	186.9
767-300ER		1460	186.9
767-300ER		1569.5	186.9
767-300ER		8961.48	186.9
767-300ER		11563.2	186.9
767-300ER (all M)		1460	186.9
767-300ER (all M)		1971	186.9
A-330		1460	233
ATR-42/72		2920	21.5
F100		20367	45.8
Fokker 70		2920	39.9
J105		14256.9	48
J35		24440.4	20
J50		52954.2	24
J75		50917.5	39.9

Aircraft type	Generations 2	Generations 3	MTOW
MD-11		730	286
MD-11		5840	286
MD-11 (all M)		657	286
MD-11 (all M)		730	286
MD-11 (all M)		6570	286
X250		5256	233
X300		5256	297.6
X300 (all M)		1098.65	297.6
X300 (all M)		1460	297.6
X300 (all M)		1971	297.6
TOTAL	**5,475**	**582,979**	
	0.93%	99.07%	
Average MTOW=100.8 ton			

Remark:

- In the determination of the average MTOW and the percentages of generation of the aircraft movements of the 2010 scenario 14,053 movements of freighter aircraft are not taken into account, because of lack of information about the aircraft type.
- Classics of the Boeing 747 of KLM are upgraded with an Electronic Flight Instrumentation System (EFIS), which makes them third generation aircraft.

Appendix G Distribution of traffic over the routes

The table below records for all routes (runway + route name) the number of aircraft movements during the day, the night and total for the year 1990. Also mentioned is the utilisation of the route as a take-off route or a landing route.

Table G-1: Aircraft movements for the S4S1-1990 scenario.

Runway	Route name	Day	Night	Total	Take-off/ Landing
01L	020	3028	2242	5270	Take-off
01L	021	4023	4470	8492	Take-off
01L	022	1051	998	2049	Take-off
01L	023	4531	3656	8187	Take-off
01L	024	460	479	938	Take-off
01L	025	2306	2417	4724	Take-off
01L	026	3076	3359	6435	Take-off
01L	151		286	286	Take-off
01L	152		48	48	Take-off
01L	153		194	194	Take-off
01L	154		142	142	Take-off
01R	521	1568	967	2535	Landing
01R	522	1784	751	2535	Landing
01R	523	1399	725	2124	Landing
06	050	19	10	29	Take-off
06	051	29	21	50	Take-off
06	052	7	5	11	Take-off
06	053	29	18	46	Take-off
06	054	14	12	26	Take-off
06	055	23	18	40	Take-off
06	541	245	759	1004	Landing
06	542	6342	5485	11827	Landing
06	543		1404	1404	Landing
06	544	95	97	192	Landing
06	545		268	268	Landing
06	546	5069	5422	10491	Landing
06	547		1298	1298	Landing
06	548	5790	7457	13248	Landing
06	549		1487	1487	Landing
09	060	463	488	951	Take-off
09	061	578	422	1000	Take-off
09	062	1433	903	2336	Take-off
09	063	201	202	402	Take-off
09	064	865	738	1603	Take-off
09	065	172	186	358	Take-off

Runway	Route name	Day	Night	Total	Take-off/ Landing
09	066	515	558	1073	Take-off
19L	080	1012	233	1246	Take-off
19L	081	547	212	758	Take-off
19L	082	826	439	1265	Take-off
19L	083	190	93	282	Take-off
19L	084	818	346	1164	Take-off
19L	085	62	33	95	Take-off
19L	086	651	302	953	Take-off
19R	601	246	551	797	Landing
19R	602	254	358	612	Landing
19R	603	6562	3001	9563	Landing
19R	604		630	630	Landing
19R	605	5746	4196	9942	Landing
19R	606	98	174	272	Landing
19R	607	5245	2966	8211	Landing
19R	608		583	583	Landing
24	110	2254	1331	3585	Take-off
24	111	5701	1648	7349	Take-off
24	112	5740	2349	8089	Take-off
24	113	1978	787	2765	Take-off
24	114	8530	2883	11413	Take-off
24	116	1169	575	1743	Take-off
24	117	6775	2904	9678	Take-off
24	118	2870	1175	4045	Take-off
24	160		318	318	Take-off
24	161		525	525	Take-off
24	164		667	667	Take-off
24	631	1340	669	2008	Landing
24	812		984	984	Take-off
24	813		164	164	Take-off
24	816		171	171	Take-off
24	817		534	534	Take-off
27	121	98	30	128	Take-off
27	122	148	64	213	Take-off
27	123	34	14	48	Take-off
27	124	143	51	194	Take-off
27	125	4	1	5	Take-off
27	126	117	53	170	Take-off
27	127	301	35	336	Take-off
27	641	516	129	645	Landing
27	642		160	160	Landing
27	643	8064	2039	10104	Landing
27	644		72	72	Landing

Runway	Route name	Day	Night	Total	Take-off/ Landing
27	645	2374	858	3232	Landing
27	646		79	79	Landing
27	647	6587	1319	7907	Landing
27	648		203	203	Landing
	Total	**122,115**	**84,900**	**207,010**	

Remark:
The sum of movements of the day plus the night is not equal to the total movements due to rounding off of the values in an earlier stage.

The table below records for all routes (runway + route name) the number of aircraft movements during the day, the night and total for the year 2010. Also mentioned is the utilisation of the route as a take-off route or a landing route.

Table G-2: Aircraft movements for the S5P-2010 scenario.

Runway	Route name	Day	Night	Total	Take-off/ Landing
01L	RWH	21178	4766	25944	Landing
01L	BER	6915	1805	8720	Take-off
01L	LEK	11424	2786	14210	Take-off
01L	LOP	5211	1226	6437	Take-off
01L	PAM	13670	3426	17096	Take-off
01L	REF	10053	2384	12437	Take-off
01L	SPY	8332	1958	10290	Take-off
01R	O	23423	6259	29682	Landing
01R	W	17995	4609	22604	Landing
01R	Z	17710	4897	22607	Landing
06	O-N	21676	8084	29760	Landing
06	W-N	16652	6035	22687	Landing
06	ZW-N	16389	5989	22378	Landing
09	AND	476	128	604	Take-off
09	ARN	785	221	1006	Take-off
09	BER	397	114	511	Take-off
09	LEK	654	177	831	Take-off
09	LOP	298	78	376	Take-off
09	O	87		87	Landing
09	REF	396	105	501	Take-off
09	VAL	176	47	223	Take-off
09	W	67		67	Landing
09	ZW	65		65	Landing
18	O-N	15075	11704	26779	Landing

Runway	Route name	Day	Night	Total	Take-off/ Landing
18	W	11418	8895	20313	Landing
18	ZW-N	10926	8046	18972	Landing
19L	AND	4814	854	5668	Take-off
19L	ARN	7900	1492	9392	Take-off
19L	BER	3995	784	4779	Take-off
19L	LEK	6601	1211	7812	Take-off
19L	LOP	3012	534	3546	Take-off
19L	VAL	5749	1026	6775	Take-off
19L	VLA	55	8	63	Take-off
19R	O	13332	2476	15808	Landing
19R	W	10405	1824	12229	Landing
19R	ZW	10548	1934	12482	Landing
19R	AND	1		1	Take-off
19R	ARN	392	227	619	Take-off
19R	BER	195	92	287	Take-off
19R	LEK	328	161	489	Take-off
19R	LOP	150	59	209	Take-off
19R	SPY	237	84	321	Take-off
19R	VAL	275		275	Take-off
19R	VLA	10	110	120	Take-off
24	AND	2370	1963	4333	Take-off
24	ARN	12157	7459	19616	Take-off
24	BER	6147	3362	9509	Take-off
24	LEK	10159	5537	15696	Take-off
24	LOP	4636	2208	6844	Take-off
24	SPY	5039	1367	6406	Take-off
24	VAL	8759	1869	10628	Take-off
24	VIS	2426	315	2741	Landing
24	VLA	176	2315	2491	Take-off
27	ARN		31	31	Take-off
27	BER	566	75	641	Take-off
27	LEK	937	115	1052	Take-off
27	LOP	424	50	474	Take-off
27	NW-N	3424	1175	4599	Landing
27	O-N	4458	1553	6011	Landing
27	PAM	1119	108	1227	Take-off
27	REF	823	99	922	Take-off
27	SPY	683	80	763	Take-off
27	ZW-N	3370	1101	4471	Landing
36	BER	10112	2639	12751	Take-off
36	LEK	16714	4070	20784	Take-off
36	LES		1037	1037	Take-off
36	LOP	7624	1794	9418	Take-off

Runway	Route name	Day	Night	Total	Take-off/ Landing
36	LOS		385	385	Take-off
36	PAM	19999	5009	25008	Take-off
36	PAS		1477	1477	Take-off
36	REF	14706	3484	18190	Take-off
36	RSS		715	715	Take-off
36	SPS		553	553	Take-off
36	SPY	12192	2863	15055	Take-off
36	TXS		607	607	Take-off
	Total	**448,467**	**152,030**	**600,497**	